PROJECT SCANNAR

Satellite Communications and Aircraft Navigation for the North Atlantic Region

Cover drawn by Stanley R. Nunn, Sr.

A Student Design Project
Department of Aerospace Engineering
The University of Michigan
Winter Term 1970

ABSTRACT

Project SCANNAR is a preliminary design feasibility study of an experimental navigation and communication satellite capable of handling all air traffic over the North Atlantic. The navigation system will provide accurate position fixes to the traffic control center and thus safely allow closer spacing in the increasingly crowded Atlantic air corridor. The communications ability will be used for traffic control, emergencies, and weather information.

Launch will take place in early 1975 from the Eastern Test Range using a three stage thrust augmented Delta launch vehicle (McDonnell Douglas DSV-603 with six Castor II's and a TE 364-3 third stage). The satellite will be placed in an earth synchronous orbit at 27.5° west longitude, and will have a projected life of two years with an on-station weight of 521 pounds.

Once on-station SCANNAR will deploy two 2.5 ft by 8 ft solar panels, a 4.38 diameter communications antenna with a steerable feed, and four 2.92 ft diameter interferometric antennas, each on the end of a 45 ft boom. A position fix within approximately two nm will be accomplished with two sets of interferometers and a ranging signal. The data will be transmitted to a ground station where the position will be determined. Communications will be on five narrow band FM channels plus one channel for the communication request and initiation. In both functions, SCANNAR will essentially act as a repeater in the L-band frequency spectrum.

Two hundred thirty-eight watts of power will be provided by solar cells, or by silver-cadmium batteries when the satellite is eclipsed by the earth. The thermal system is passive and consists of heat pipes, radiating surfaces, and power shunts. The power shunts dissipate unused power as heat. Attitude is controlled by reaction wheels which are activated, through an on board computer, by five sun sensors, one planar scanner, and three position gyros. Hydrazine thrusters are used to unload the reaction wheels and to provide velocity increments for stationkeeping.

TABLE OF CONTENTS

1
GENERAL INTRODUCTION

1.1 THE NEED FOR A COMMUNICATIONS AND AIR NAVIGATION SATELLITE

In the past twenty years, air travel has increased enormously. In the near future, the air corridors will become more crowded with the advent of the supersonic transports and the increased use of cargo planes.

Airways above the North Atlantic Ocean in particular are becoming increasingly crowded. Projected figures for the late 1970's indicate that up to 200 aircraft will be in the North Atlantic Region at peak periods (Reference 1.1). Because of present loose surveillance of aircraft in the North Atlantic (aircraft now report their position each time they cross ten degrees of longitude), safety factors dictate separation minimums for aircraft of twenty minutes flying time along the flight path, 120 nautical miles laterally, and 2000 feet in altitude (Reference 1.2). Since this allows relatively few aircraft in one preferred air corridor at any one time, some aircraft must fly on non-optimum flight paths and at undesirable times. Because of future increased traffic needs, resulting in more non-optimum flight conditions, a surveillance system and traffic control system is desired so that the minimum separation distances can be decreased. A navigation satellite has one tremendous advantage over other systems for air traffic control-the satellite is geometrically situated in direct line-of-sight with aircraft and ground stations.

One synchronous satellite could serve two main purposes. First it would provide a direct communication link between the ground station and any aircraft. Presently, VHF communication is used for aircraft within 300 miles of any shore; but HF radio frequencies, which are propagated by ionospheric reflection, are used when an aircraft is outside this limit. Since HF frequencies are unreliable and of poor quality, the air traffic over the North Atlantic would be better served in the future by a satellite using a higher frequency band on direct line-of-sight. This direct communication link could provide aircraft with meteorological or emergency information besides voice communication. Especially valuable would be solar flare radiation information for high altitude supersonic transports.

Secondly, the satellite would provide position fixing of aircraft. This would serve as a check for the aircraft navigator, thus eliminating possible gross navigational errors. Also, since a control station on ground would know the positions of all aircraft to a greater accuracy than the present surveillance system, separation minimums could be reduced. This would enable a larger number of aircraft to fly on optimum paths and at times best suited for passengers and freight handlers. In addition, accurate navigational information could reduce travel time for aircraft, thus lowering fuel and operating costs and reducing cargo deterioration.

1.2 PROJECT DEFINITION

This project is a preliminary design feasibility study for an earth synchronous communications and navigation satellite for aircraft in the North Atlantic Region. The satellite is to be experimental with the primary purpose of testing the position fixing technique. The following constraints have been placed on the system:

1. State of the art technology with very limited technical developments.
2. Simplicity
3. Reliability
4. Two year lifetime
5. Compatibility with ground equipment
6. Limited aircraft requirements
7. Voice and data communications
8. Position fix within five nautical miles

1.3 GENERAL PROJECT DESCRIPTION

Project SCANNAR complements a navigational system consisting of a ground control station, calibration stations, and aircraft (see Figure 1.1). The ground control station receives position fixing data of North Atlantic aircraft from SCANNAR. After processing this data, the control station can then provide the positions of aircraft in the North Atlantic Region to any desired terminal or aircraft. Calibration stations are needed to monitor

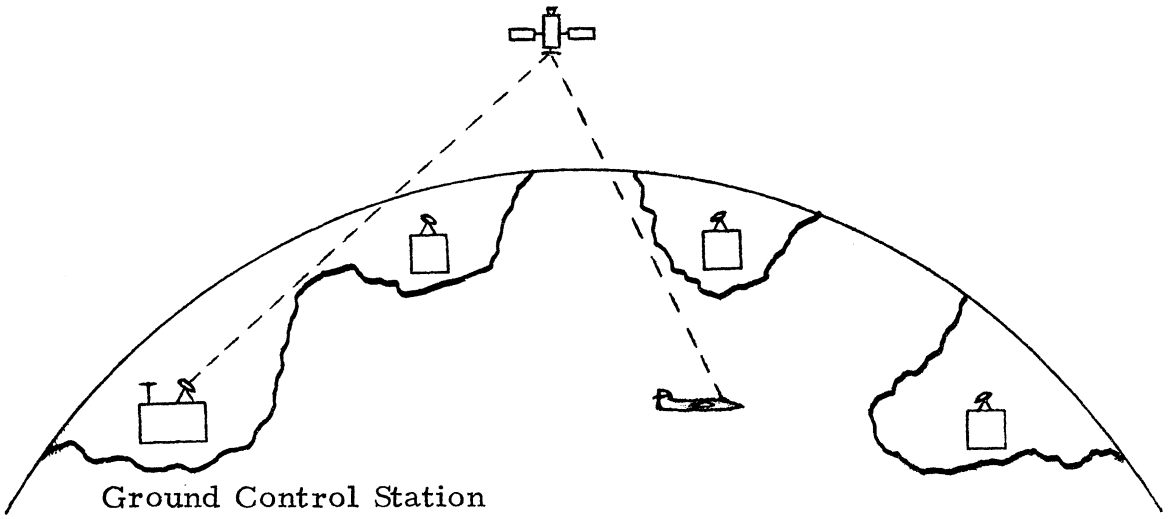

Figure 1.1 System Configuration

the positions of the boom antennas on SCANNAR so that the position fixing technique is kept accurate. Because of the position fixing technique used, this system is unique in that only one satellite is needed to provide enough data for the location of an aircraft.

SCANNAR uses two interferometers plus ranging for position fixing of aircraft. Both interferometers consist of two 2.92 ft diameter mesh antennas, each of which is placed on a forty-five foot boom. The two interferometers provide data for two angle measurements while the range data is supplied by a 4.38 ft diameter mesh communications antenna at the base of the satellite. Voice and data communications are also handled by this antenna. For telemetry, tracking, and command there are four cavity backed spiral antennas, one wire antenna and one helical antenna.

The attitude of the satellite on-station is determined by a planar scanner and sun sensors; the attitude of the satellite before it is on-station is obtained by the sun sensors and three position gyroscopes. While on-station small attitude corrections are accomplished by three reaction wheels and thrusters.

On-station power is supplied by two solar panels each 8 ft by 2.5 ft. To receive maximum solar energy, these panels must rotate once each day. When SCANNAR is in the earth's shadow, silver-cadmium batteries supply the needed power. Prior to the on-station condition, power is supplied by body cells and part of the folded solar panels.

The body of the satellite is a cylinder with a hexagonal cross-section. Inside are the fuel tanks, electronics, reaction wheels, gyroscopes, batteries and apogee motor. Outside are the four booms, solar panels, small thrusters and antennas. Thermal control is passive with heat pipes, power shunts and radiating surfaces used to control temperatures of components.

SCANNAR will be launched in early 1975 from the Eastern Test Range by a Douglas DSV-603 with six Castor II's and a TE 364-3 third stage. After the apogee motor burn at approximately synchronous altitude, two ten pound thrusters will be used to trim the orbit to the desired circular synchronous orbit, and to place the satellite at approximately 27.5° west longitude. Terminal phase rendezvous will be initiated so that SCANNAR can acquire this location. Since SCANNAR will tend to drift eastward during its two-year lifetime, occasional firings of 0.05 pound thrusters will be needed to bring it back to its desired position. It is from this position that SCANNAR will "scan" the North Atlantic for aircraft.

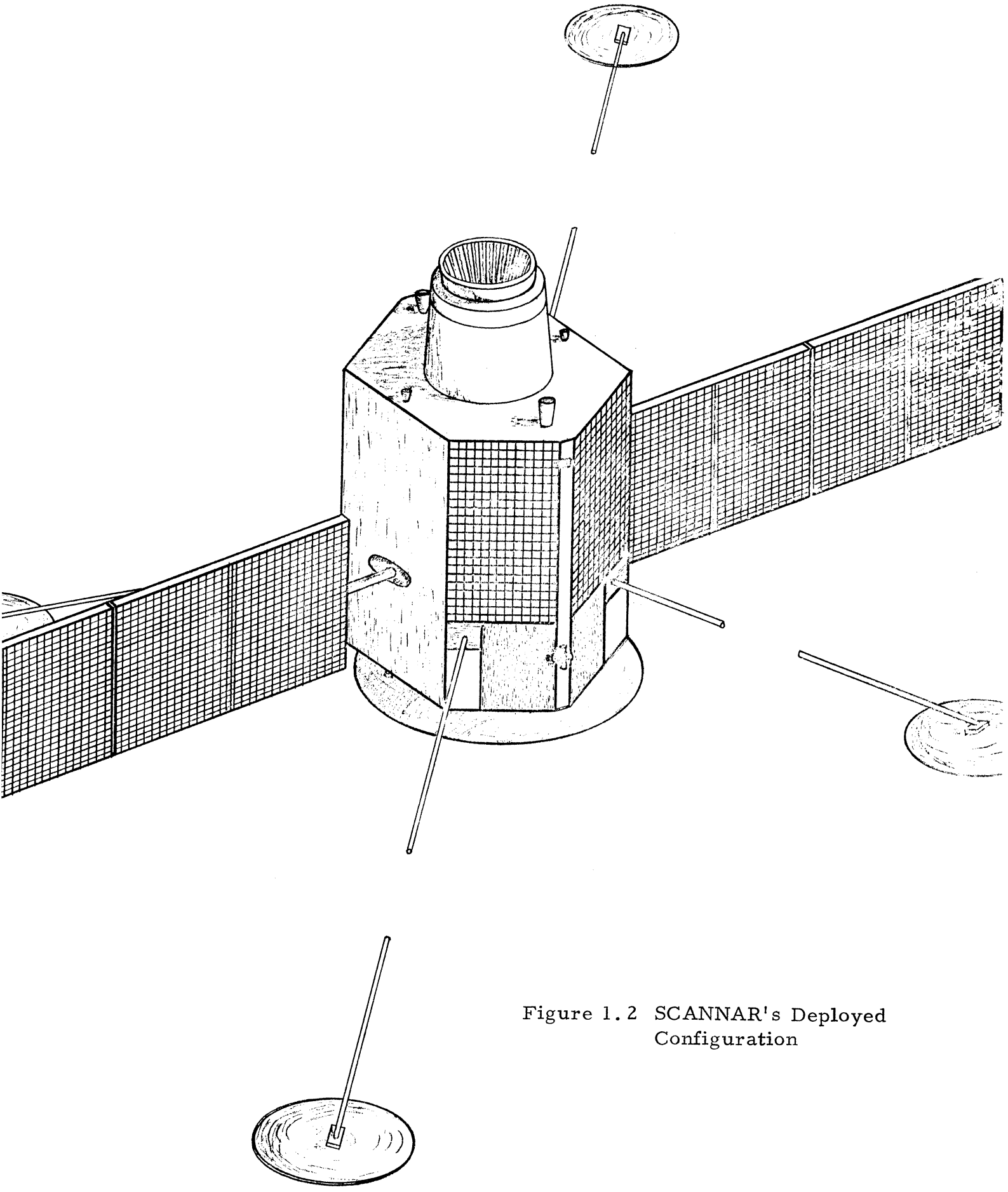

Figure 1.2 SCANNAR's Deployed Configuration

REFERENCES

1.1 Jorasch, R. E. and Murphy, C. L., Synthesis of an Aeronautical Service Satellite System, Philco-Ford Corporation, October 1969.

1.2 Useful Applications of Earth-Oriented Satellites-Navigation and Traffic Control, Summer Study on Space Applications, Division of Engineering National Research Council, 1969.

* * *

Ehrlich, Eugene, "Navigation Satellites for Worldwide Traffic Control", Astronautics and Aeronautics, December 1965.

2
NAVIGATION

2.1 INTRODUCTION

The primary purpose of this experimental navigational satellite is to show the feasibility of determining the position of an aircraft flying over the North Atlantic within such an accuracy as to give traffic controllers a reasonable fix on the aircraft's position.

The technique chosen for SCANNAR's navigation system uses the L-Band frequency range (1540-1660 MHz) and involves the measurement of two angles and a range between the user vehicle and the satellite. The angles are measured by two crossed interferometers whose antennas are located on the ends of forty-five foot booms. Each interferometer determines a cone. The intersection of the two cones determines 2 lines, one of which is the line between the satellite and the user vehicle. The ranging signal determines the location of the user along this line (Figure 2.1). The interferometric system with ranging requires only one earth-synchronous satellite to determine the position of an aircraft.

Having the aircraft transpond its altitude along with the range signal allows for some redundancy in the navigation system. If one of the interferometers fails or the range measurement capability is lost, it is still possible to determine the user vehicle's position by utilizing its absolute altitude (determined by a radar altimeter on the aircraft) as the third parameter for calculating its position.

The initiation of position fixing is controlled by the ground station. The ground station transmits a coded signal which is received by the satellite. The satellite then transmits a sidetone modulated carrier wave which has the code of the aircraft to be located. The interrogated aircraft transponder, along with the calibration stations, transponds the appropriate signals back to the satellite. At the satellite the signals are combined and then sent to the main ground station where the position of the aircraft is determined. Position fixes will be initiated once every two seconds, since the ranging signal is required to be continuous for approximately one half second. SCANNAR's ranging method uses a carrier wave and thus takes longer than a ranging method using a pulse. In an operational traffic control system, the aircraft's position would be hardlined to the appropriate traffic control center. The aircraft can determine its position, along with weather and radiation information, from the control center using the voice link.

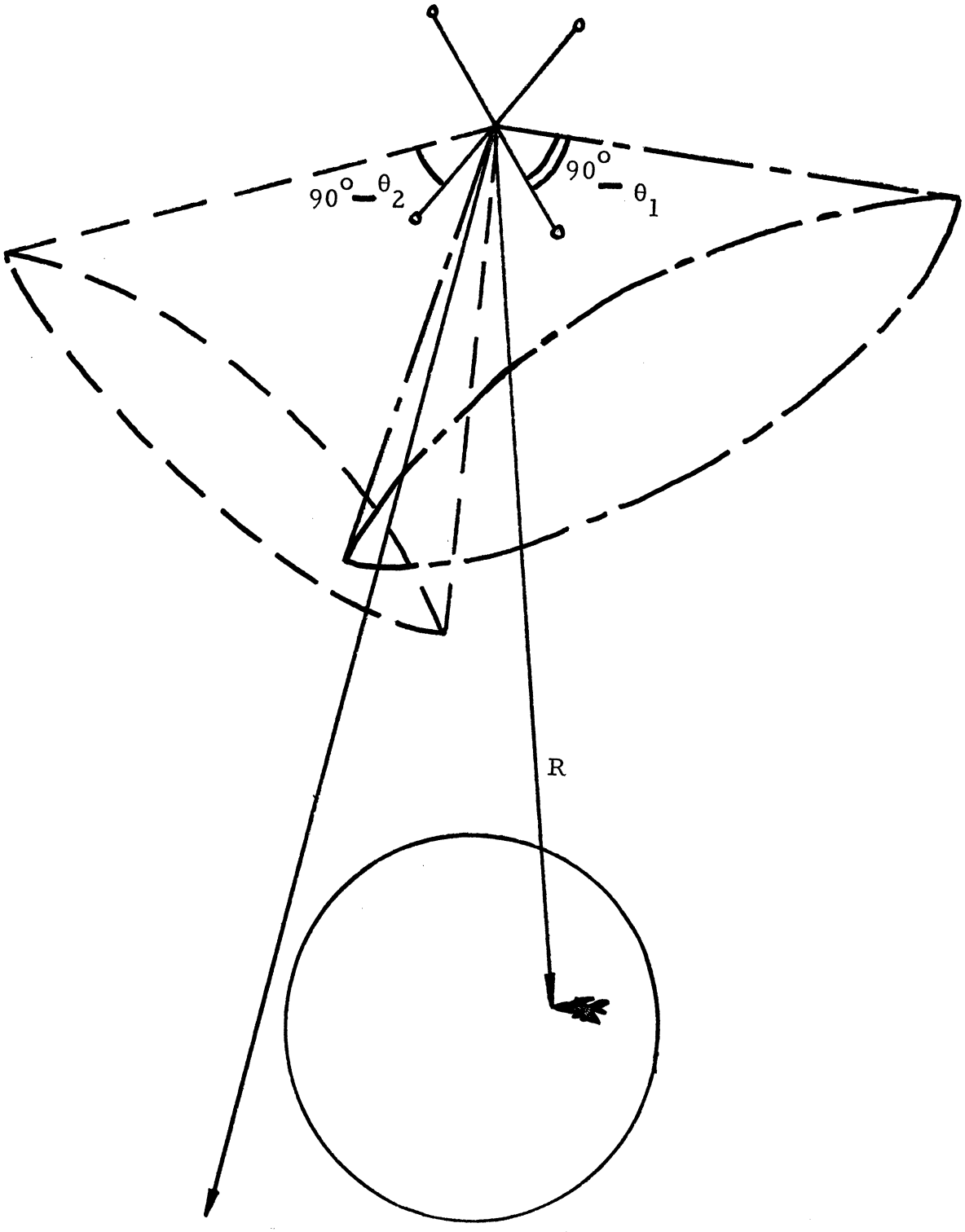

Figure 2.1 Interferometric Navigation System (not to scale)

2.2 INTERFEROMETRIC SYSTEM

2.2.1 Principle

For an interferometer system located at synchronous altitude, it is reasonably justified to assume that the wavefront, originated at the aircraft, is planar. Thus, if the source of the radiation is not directly below the baseline center, the arriving wavefront makes an angle, θ, with the antenna baseline (Figure 2.2). Since the wavefront arrives at each of the antennas at a different time, the signals received by the two antennas will be out of phase with each other. This electrical phase difference, ϕ, has the geometric equivalence of:

$$\phi = \frac{2\pi D}{\lambda} \sin \theta$$

where D = baseline length
λ = wavelength
θ = angle of arrival of signal, or space angle to the source

The space angle, θ, describes the surface of a cone with apex at the center of the interferometer baseline, axis along the baseline, and vertex angle given by (90-θ) degrees. The two interferometers define two cones which intersect along two straight lines. One line points toward the aircraft in the North Atlantic and the other points away from the earth (Reference 2.1).

The sensitivity of the interferometers is given by:

$$\frac{d\phi}{d\theta} = \frac{2\pi D}{\lambda} \cos \theta$$

which is the slope of the phase versus space angle function. With a satellite at synchronous altitude and a coverage area (including pointing errors) of ten degrees, cos θ is nearly equal to one. With a small variation in the value of cos θ, the sensitivity of the interferometers will not change significantly by assuming that cos θ is unity.

It is a reasonable assumption that the phase can be measured to approximately one degree (Appendix A.2). For a North-South accuracy of two nautical miles on the earth (at approximately 70° north latitude--10° elevation angle), a space angle accuracy of 20 microradians is necessary at synchronous altitude. For this sensitivity, $2\pi D/\lambda$ is approximately 938, resulting in an antenna separation of 149 wavelengths at 1640 MHz.

The space angles are measured relative to the orientation of the satellite based interferometer system. Therefore, it is necessary to know the orientation of the interferometer axes relative to some known reference coordinate system. Because SCANNAR is in a dynamic environment, many

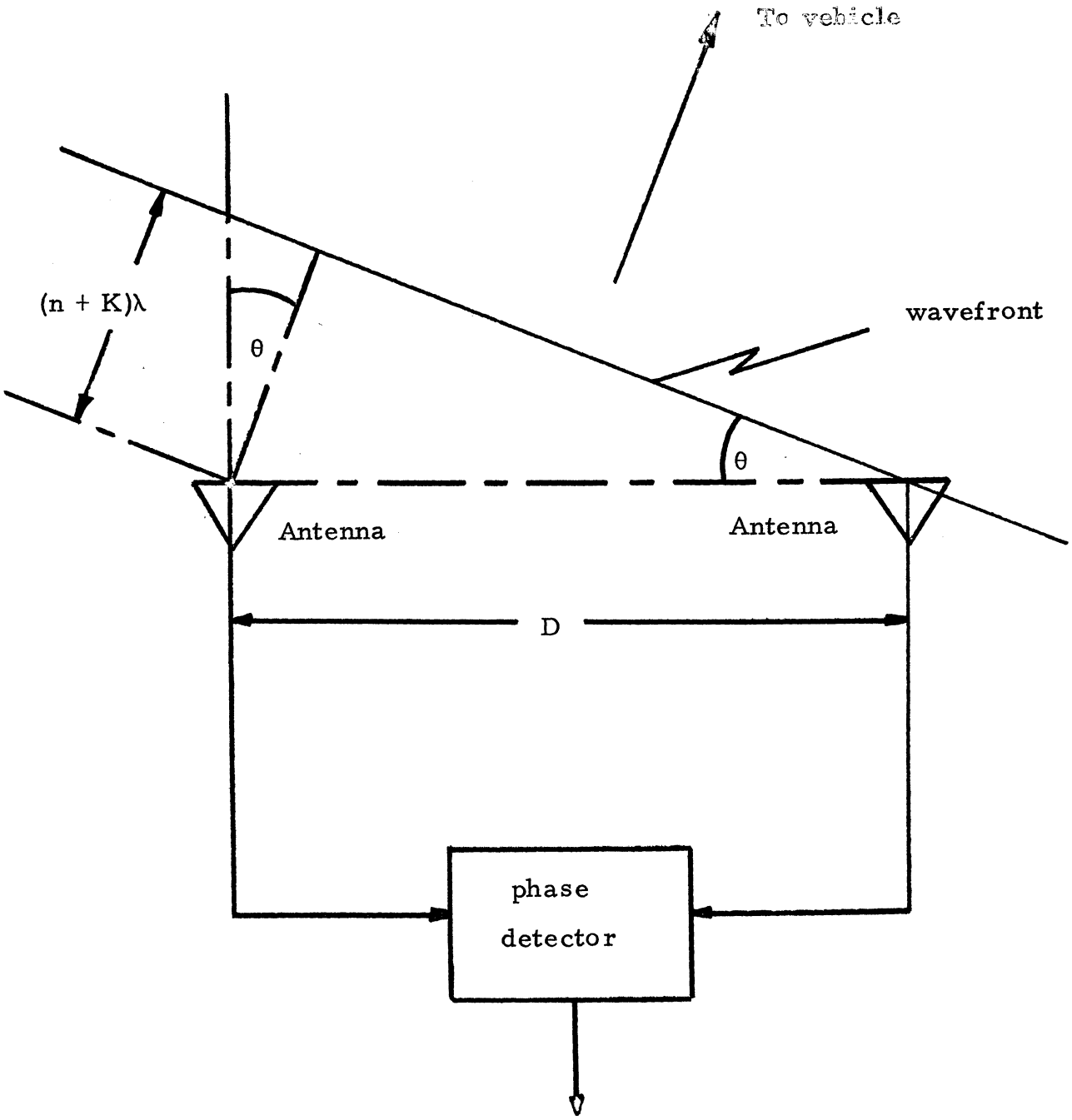

$$\phi = \frac{2\pi D}{\lambda} \sin \theta$$

Figure 2.2 Interferometer (Reference 2.1)

critical system parameters will vary with time. Among these are satellite attitude, varying lengths of the interferometer booms, and unknown phase delays between the antenna and phase measuring equipment. By determining the position of known, fixed reference stations on the earth, it is possible to solve for the unknown constants in the navigation equations.

To determine the orientation of the interferometer axes, eight quantities must be known. Two direction cosines are needed to locate each of the two interferometer axes (relative to some coordinate system), since the sum of the squares of the direction cosines of each interferometer equals unity. Therefore, measurement of four other independent quantities will determine the interferometer orientation relative to some coordinate system. These four quantities are the angles, relative to each of the two interferometers, of two of the fixed ground reference stations. By knowing the true positions of these two stations, their positions relative to the interferometer axes, and the position of the satellite, the orientation of the interferometer axes can be computed.

The interferometer scale factor, $2\pi D/\lambda$, which includes the physical separation of the interferometer antennas, requires an additional independent measurement for each interferometer. These two pieces of data are obtained by measuring the angular position of a third reference station.

In a similar fashion, the unknown differential phase delay in each of the interferometer booms can be determined by measuring the angular position of an additional station. These eight angular measurements of four fixed, ground reference stations give sufficient data to determine the necessary interferometer constants (Reference 2.2).

2.2.2 Angle Ambiguity Resolution

The crossing of one wavefront must be measured at the two antennas for a determination of the correct phase. Since the antenna baseline, D, is greater than 2λ (approximately 1.2 feet), the determination of the correct space angle is ambiguous. This is because the integral number of wavefronts, n, and therefore $(n + K)\lambda$, where K is not an integer, is unknown (Figure 2.2). This ambiguity can be resolved by using a second frequency that is slightly offset from the first.

SCANNAR will use navigation frequencies in the upper portion of the L-Band spectrum, since a higher frequency has a shorter wavelength, a greater D/λ, and therefore better accuracy. Within the L-Band frequency spectrum (Figure B.2), a nominal frequency of 1640 MHz will be used. This results (Appendix A.1) in a frequency separation of 36 MHz, and resolves all but one ambiguity with two points approximately 5500 nautical miles apart at the equator. Therefore, the second frequency used for SCANNAR's navigation requirement will be 1600 MHz.

Since ϕ is bounded by 2π, the function $\phi = 2\pi D/\lambda \sin\theta$ is repeatable as shown in Figure 2.3. Figure 2.4 shows that if two phase difference measurements are made with two frequencies, a space angle of θ_1 can be found. The other space angle, θ_2, is determined similarly using the other interferometer. These two space angles are used to determine a straight line to the aircraft or ground station as described in Section 2.2.1.

2.3 RANGE MEASUREMENT TECHNIQUE

Accurate range measurements are accomplished by using a carrier wave that is frequency modulated with ranging sidetones. This technique is based on the fact that the range between the satellite and the aircraft is directly proportional to the phase shift between the satellite-transmitted sidetones and the aircraft transponder-returned sidetones.

Assuming that the phase shift of the ranging signals can be measured as accurately as the interferometer signals ($\Delta\phi = 1^o$), a sidetone frequency of 100 Hz provides for a ranging ambiguity every c/f feet = 9.84×10^6 feet = 1620 nautical miles (where c is the velocity of light). The range error is given by $\frac{\pm\Delta\phi}{360^o}\lambda$. So, for 100 Hz, the range error is approximately $\pm$ 27,300 ft. Therefore, a higher frequency must also be used to improve the range accuracy, since the wavelength and the error will decrease.

For a sidetone frequency of 10 KHz, the range error is $\pm$ 273 feet or $\pm$ 0.045 nautical miles. This is equivalent to $3\sigma_{rms} = 0.105$ nautical miles (Appendix A.2).

In summary, SCANNAR's range measurement technique will employ a carrier wave that is frequency modulated with two ranging sidetones: one for accuracy, and the other to resolve ambiguities to an acceptable value. A 100 Hz sidetone will resolve ambiguities to the acceptable value of 1620 nautical miles; and a 10 KHz sidetone will locate the aircraft with a ranging error of $\pm$ 0.045 nautical miles. If aircraft doppler data is desired, a phase modulated carrier wave can be used.

Since ranging techniques have been fairly well developed and tested, the major purpose of SCANNAR is to test the interferometric technique of angle determination. For the experimental satellite a high turnaround time is not required, thus a carrier wave ranging technique was chosen to minimize the power requirements of SCANNAR. For the operation satellite, a pulse ranging technique could be used to permit a larger number of fixes per unit time.

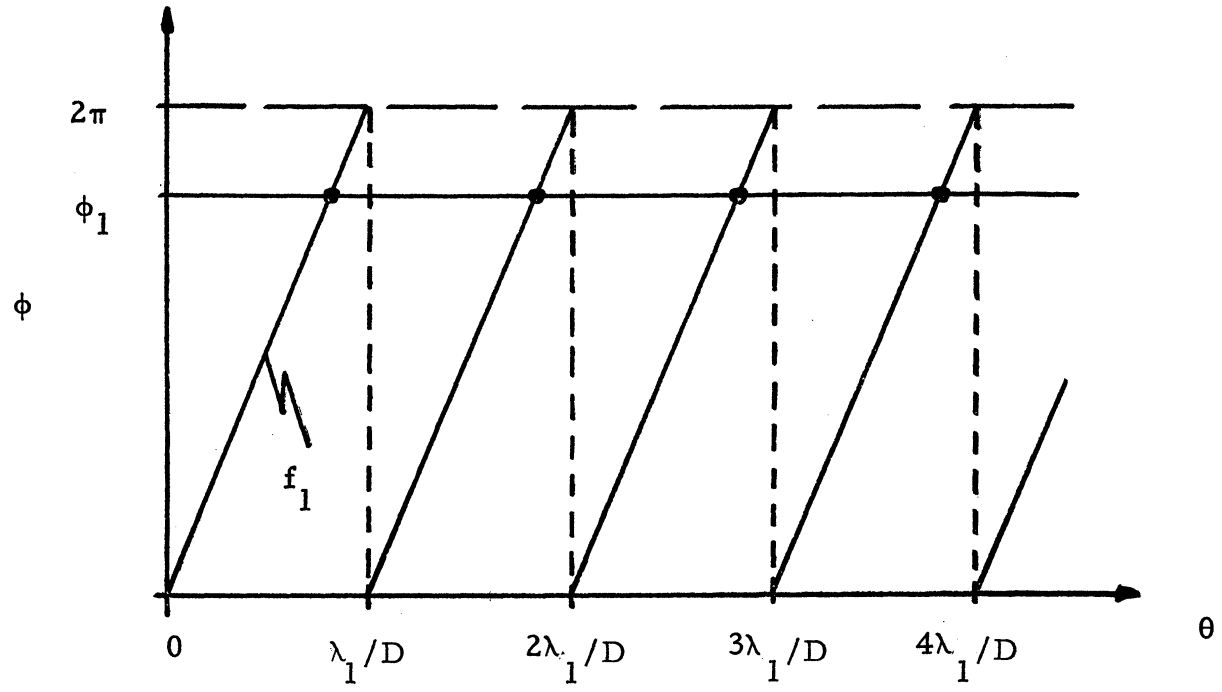

Figure 2.3 Single Frequency Measurement Ambiguities (Reference 2.3)

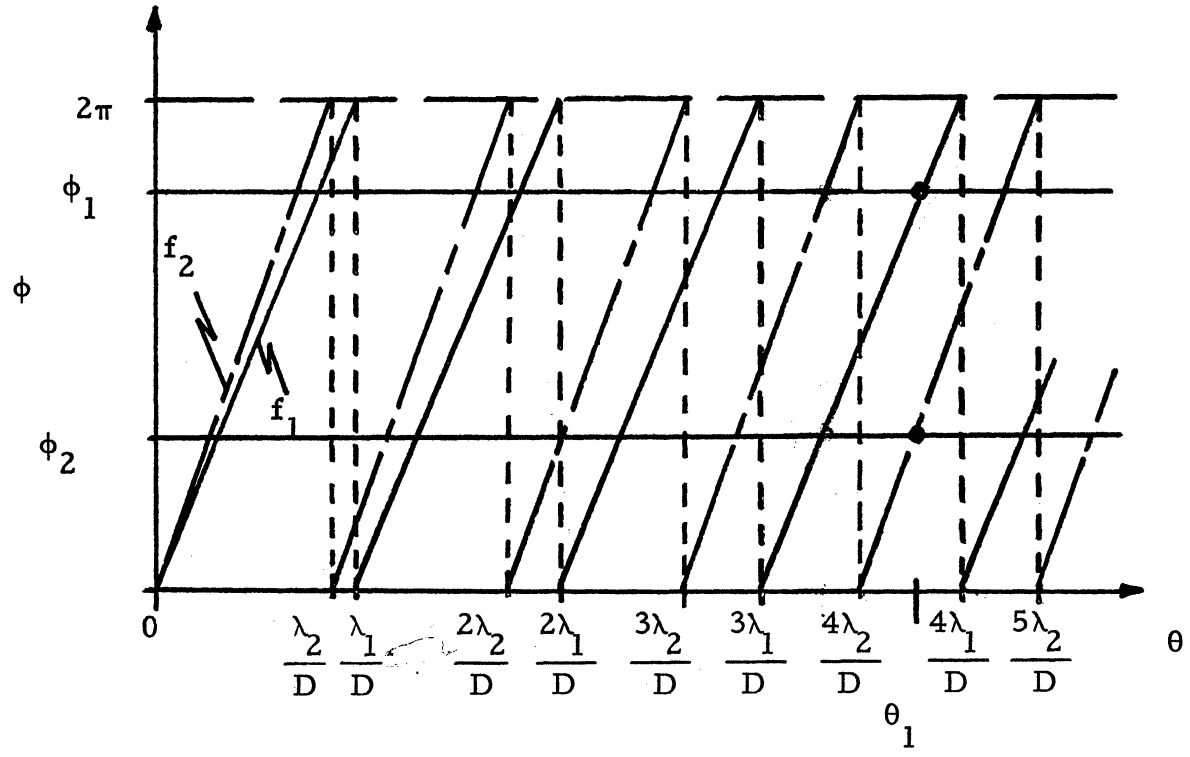

Figure 2.4 Two Frequency Ambiguity Resolution (Reference 2.3)

2.4 SYSTEM ERRORS

Because of SCANNAR's anticipated dynamic environment, a calibration procedure using ground reference stations to determine unknown constants will be employed (Sections 2.1.1 and 2.7). Some of the errors, however, cannot be corrected through calibration. These are discussed in Appendix A.2.

SCANNAR's total navigation system accuracy is 2.08 nautical miles ($3\sigma_{rms}$).

2.5 SATELLITE EQUIPMENT

The four interferometric antennas are positioned on the ends of four forty-five foot booms. The boom length was determined by the Attitude & Control and Structures groups with consideration for their respective requirements. The booms are oriented so that the interferometer antennas are parallel to the earth's surface and are rotated 45° from a North-South and East-West orientation. Due to possible errors caused by multipath, from the satellite body, being received by the sidelobes of the interferometer antennas, the booms are positioned down from the local horizontal 15°. The antennas may have a typical sin x/x amplitude distribution for which the first sidelobe gain is about 25 db below the primary lobe. Even so, the boom position angle should be based on antenna characteristics found from tests. With the three foot diameter of the satellite body between boom mechanisms, and forty-five foot booms located at 15°, the effective interferometric baseline, D, is 89.5 feet.

The four interferometric antennas will be aimed by construction at 30° north latitude and 37.5° west longitude for optimum North Atlantic coverage (Figure 3.1). All four antennas are 2.92 feet in diameter with a beamwidth of 15° and a gain of 21 db.

Interferometric and range data will be frequency multiplexed (Appendix B.7 and Section 3.3) before being sent to the ground station where the position will be calculated. The phase comparison will be an open-loop measurement in which the combined angle signals from one interferometer and a reference signal will be directly compared in phase. In a phase-comparison system with two separate IF channels, the amplifiers cause a phase shift in the signals. To avoid this problem, identical linear RF amps and a dual local oscillator system will be employed.

The local oscillator actually consists of two oscillators, with one mixer frequency being 3000 Hz higher than the other (Figure 2.5). The outputs of the two mixers are summed and amplified by a single IF amp, thus reducing the magnitudes of the phase shift. The signals out of the IF amplifier will be mixed and the 3000 Hz output will be phase compared with the 3000 Hz reference signal.

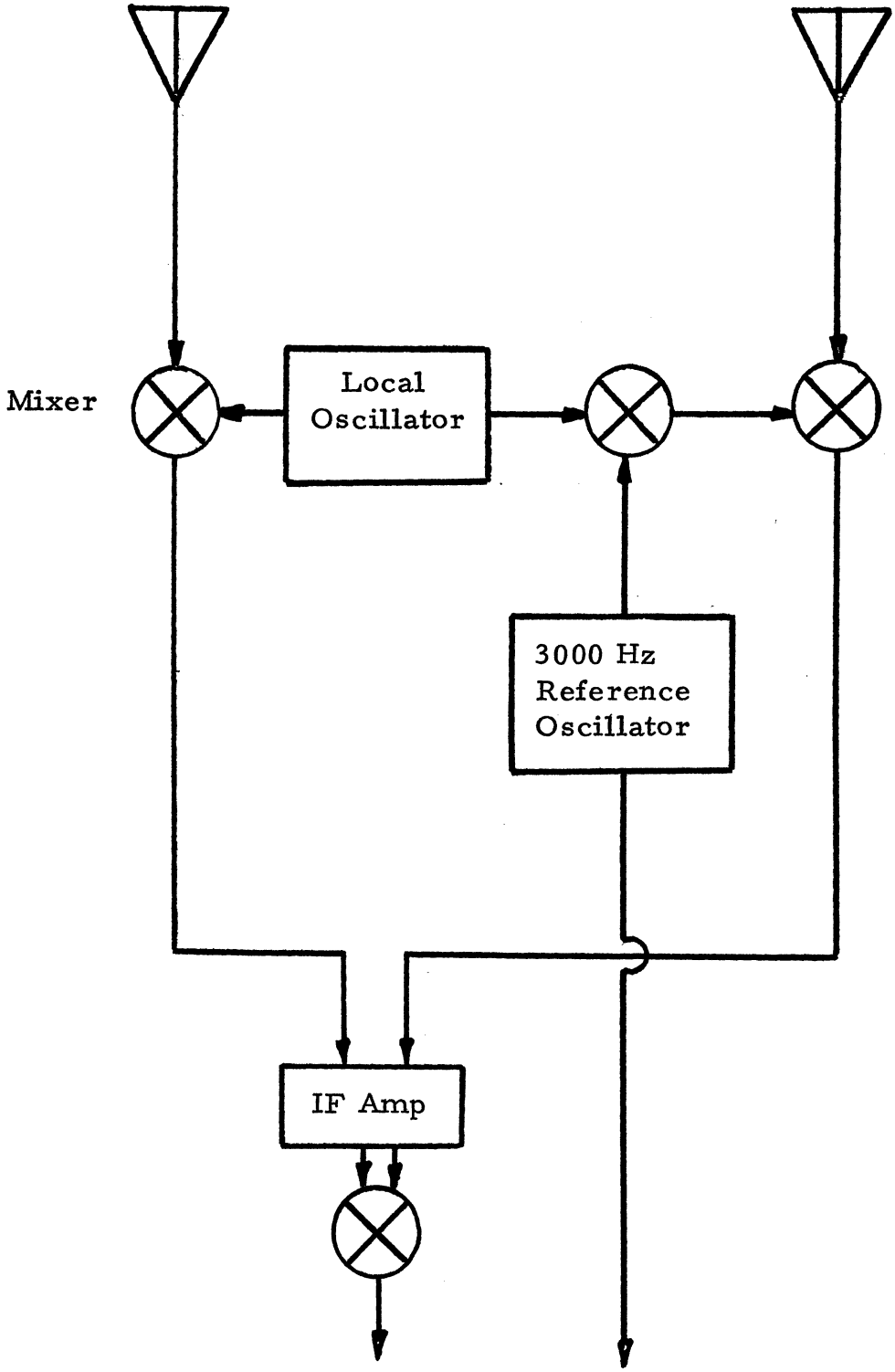

Figure 2.5 Dual Local Oscillator System

The satellite equipment (Figure 2.6) receives, amplifies, and frequency multiplexes the signals from the antennas and transmits them, together with the reference oscillator signal, to the ground. The linear RF amplifiers are located on the ends of the booms to reduce RF losses associated with long cable runs. To further reduce phase errors caused by amplification, RF filters have been placed before the RF preamps to reduce the amplifier bandwidth. These RF amps will be identically constructed (as close as possible) to insure equal amplification to each signal received by a set of interferometer antennas. To further reduce errors, the amplifiers at the ends of the booms will be insulated to prevent unequal amplification due to temperature differences, should one of the booms be shadowed by the satellite body.

To increase the reliability of the angle processing subsystem, two local, two reference, and two subcarrier oscillators will be provided should one of them fail.

The transponded range signals will be downconverted using a double conversion process before they are multiplexed with the reference range signals.

2.6 AIRCRAFT EQUIPMENT

Nominal L-Band aircraft equipment includes flush-mounted, port and starboard, linear array antenna with 15 db gain. The beam will be 72^{o} (azimuth angle) by 10^{o} (elevation angle), and can be manually or automatically selected among ten beams (two sets of five). (Figure 2.7). Each set is mounted at 60^{o} from the centerline of the fuselage.

The aircraft ranging transponder can be similar to that used for tracking satellites (Figure B.5) with the following changes:

1) phase modulator ⟶ frequency modulator
2) delete the modulator summer
3) there will be only one channel filter since tracking is done with only one satellite.

The aircraft navigation equipment is shown in Figure 2.8.

2.7 GROUND EQUIPMENT

The central ground station is the primary collection center, since it receives and analyzes the phase difference measurements received from the user aircraft and the four ground reference stations. The signals from the satellite are separated by frequency selective channels, and the zero crossing phase measurements are made (Figure 2.9). There will be a time delay

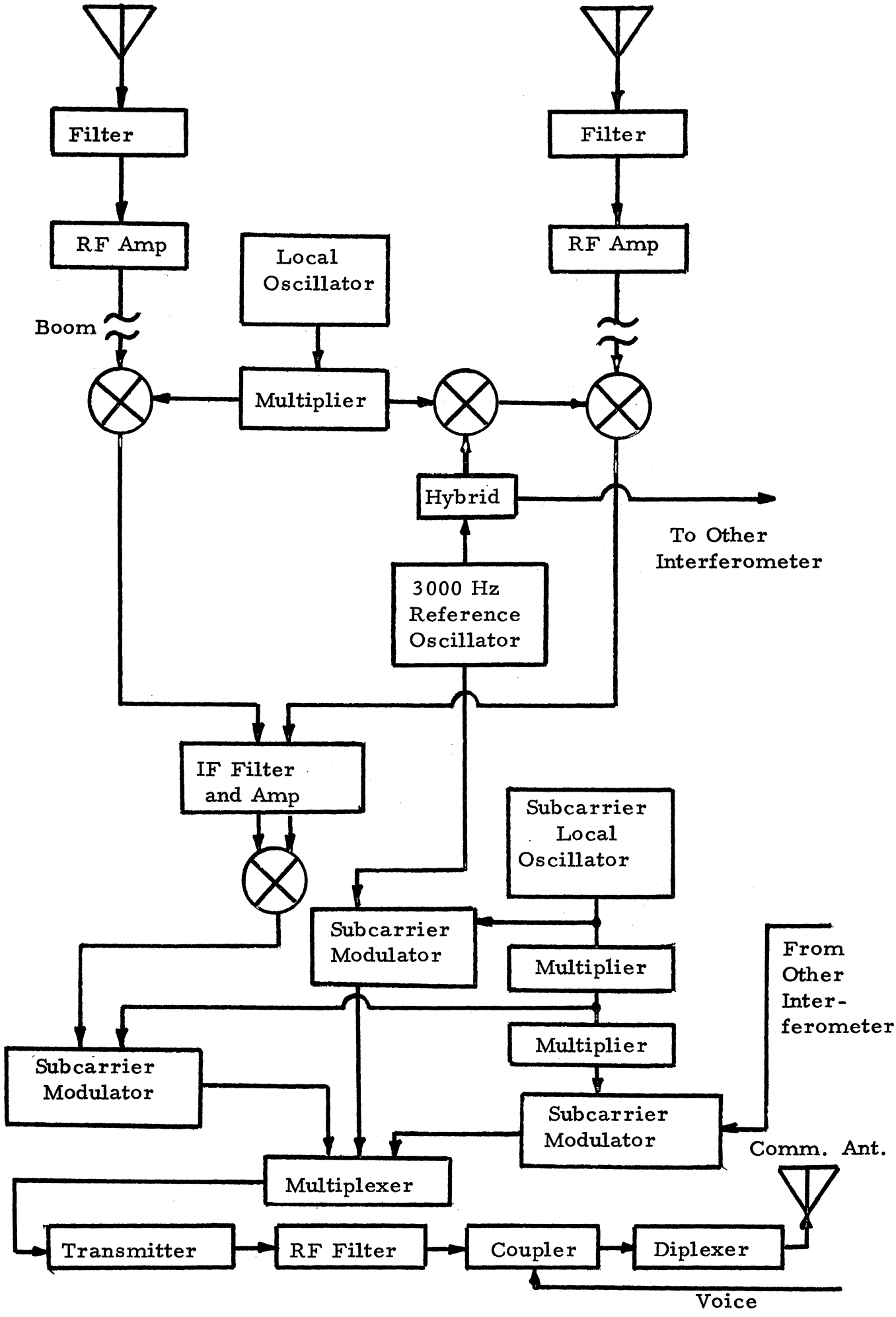

Figure 2.6 Satellite Interferometer Equipment

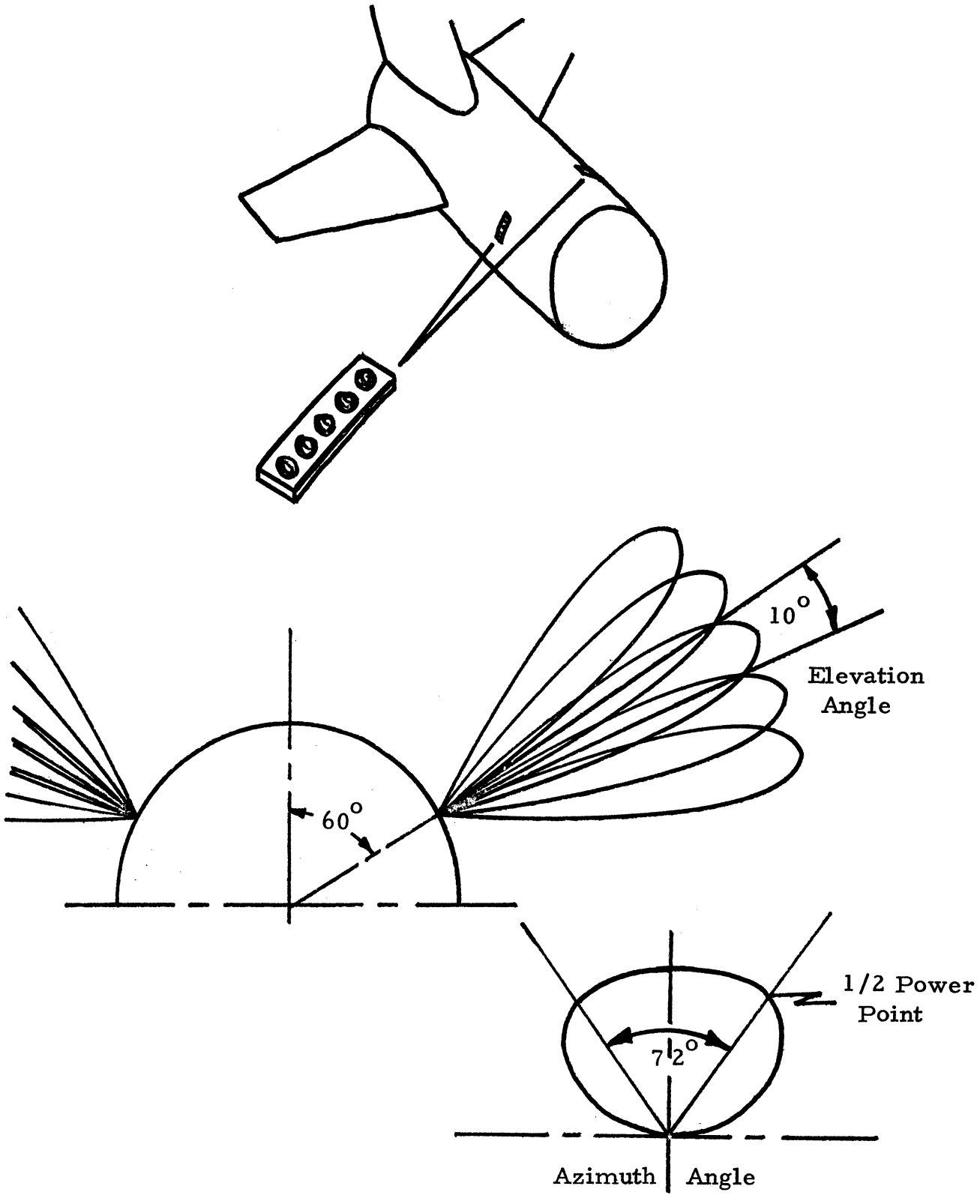

Figure 2.7 Aircraft L-Band Antenna (Reference 2.6, p. 51)

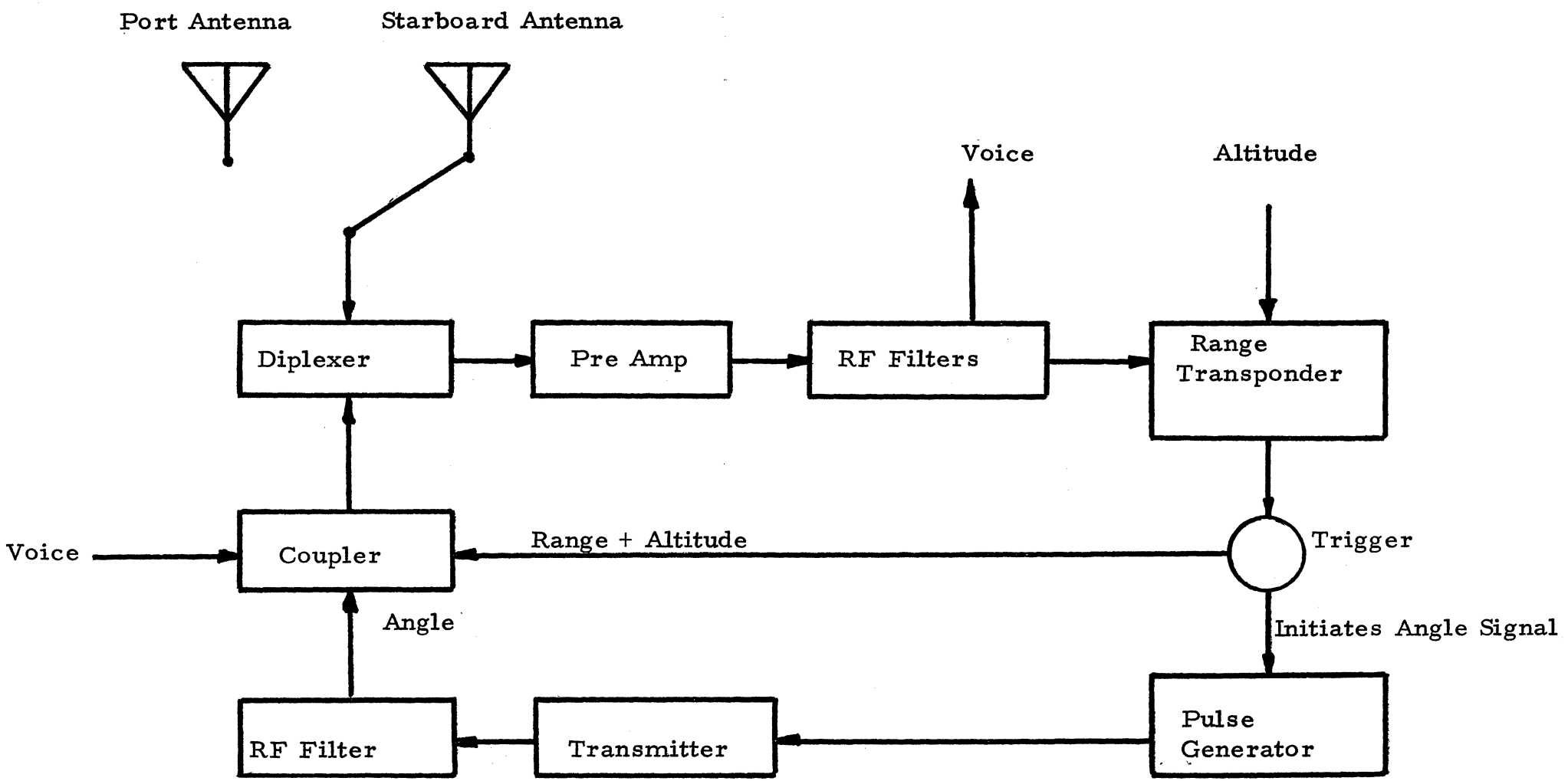

Figure 2.8 Aircraft Navigation Equipment

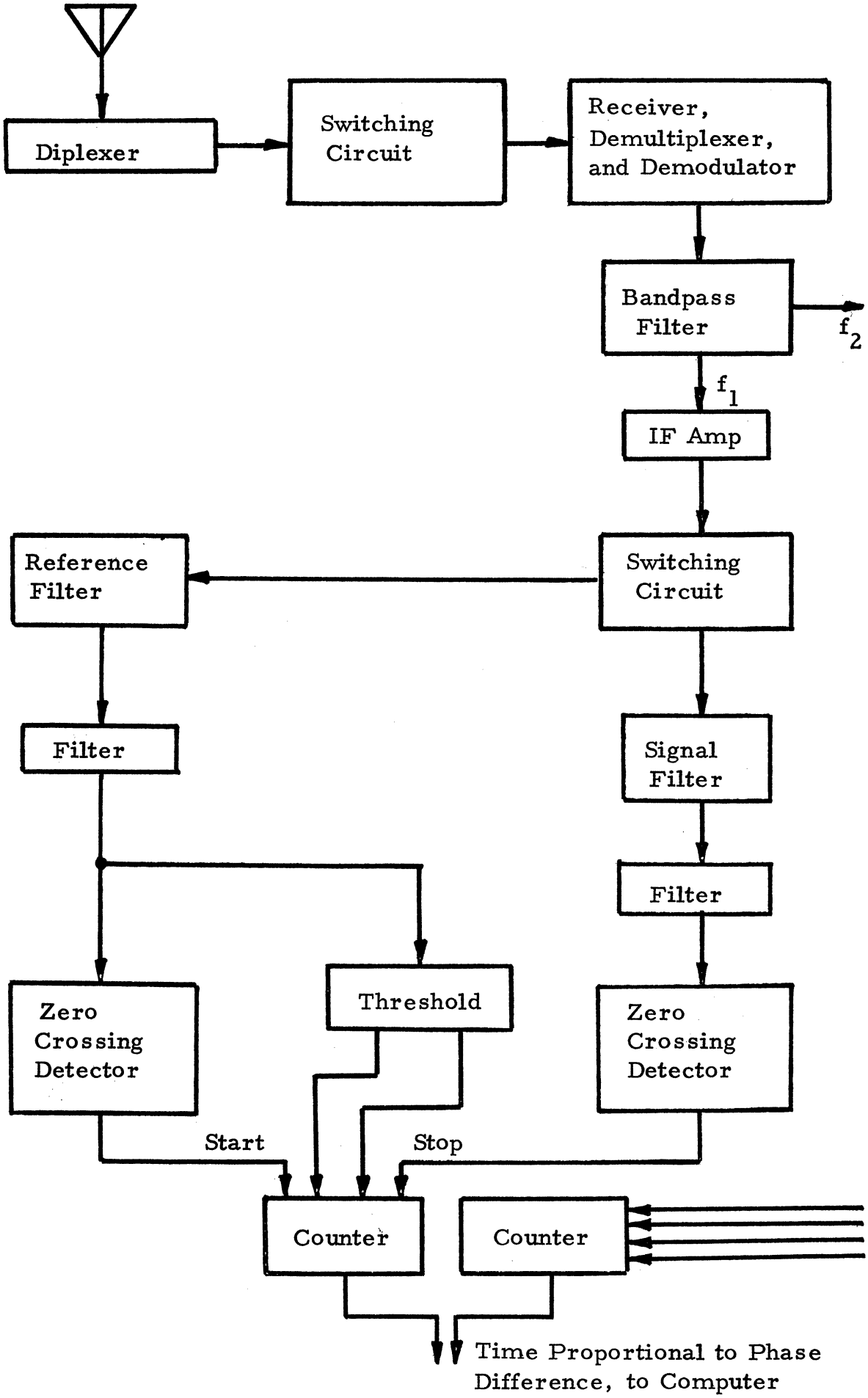

Figure 2.9 Ground Station Angle Measuring Equipment

between the received signals at the ground, and the signals will be received (and satellite-transmitted) in the following order:

1) Aircraft
2) Reference Station #1
3) Reference Station #2
4) Reference Station #3
5) Reference Station #4

The frequencies for the four reference stations are given in Figure B.2. For experimental purposes, each of the three reference stations (the central ground station in the U.S. is the fourth reference station) could be trailer-mounted and contain a lightweight antenna that is similar to the aircrafts'. The portability of the stations allows for investigation of terrain, altitude, and elevation angle on navigation measurement accuracy (Reference 2.4).

REFERENCES

2.1 Keats, E.S., "Navigational Satellites; Beacons for Ships and Planes," Electronics, February 9, 1965, pp 79-86.

2.2 Navigation Satellite System, Phase I, Westinghouse Electric Corp., Baltimore, Maryland, January 30, 1964.

2.3 Navigation Satellite System, Phase II, Westinghouse Electric Corp., Baltimore, Maryland, October 15, 1964.

2.4 Klein, P.I., Analysis of a Short-Baseline Radiating Interferometer Navigation Satellite Concept Incorporating Methods to Eliminate Systematic Navigation Error, Philadelphia, Penn., May 1968.

* * *

Jorasch, R.E., Communication System Implementation, Philco-Ford Corp., Palo Alto, Calif., October 22, 1969.

Jorasch, R.E. and Murphy, Synthesis of an Aeronautical Service Satellite System, Philco-Ford Corp., Palo Alto, California.

Klein, P.I., Analysis of a Synthetic Aperture Radiating Interferometer Navigation Satellite Concept, Philadelphia, Penn., May 1969.

Kronmiller, G.C. and Baghdady, E.J., "The Goddard Range and Range Rate Tracking System: Concept, Design, and Performance," Publications of Goddard Space Flight Center, Vol. II, Space Technology, 1965, pp 782-818.

3
COMMUNICATIONS

3.1 INTRODUCTION

An integral part of SCANNAR is the establishment of navigational data and voice communication links. Since the VHF band of the frequency spectrum is fairly crowded, recent allocations for aeronautical navigation have been in the L-band spectrum (1540 MHz - 1660 MHz) (see Figure B.1, Appendix B.1). The allocations for SCANNAR are shown in Figure B.2. The choice of frequencies that would be used for the actual satellite can be made at the time of the final design. For the purpose of calculations a frequency of 1600 MHz was chosen.

The communications subsystem is capable of providing five voice channels along with the requirements for aeronautical navigation. A narrow band FM scheme was chosen for the voice links to conserve bandwidth and thus satellite power. The on-station power requirements for the various links appear in Table 3.1.

Table 3.1 Power Requirements

Voice	
Power amplifiers	100 watts
Equipment	15 watts
Navigation	
Transmitter	28 watts
Equipment	15 watts
Interferometer antenna preamps	4 watts
Telemetry, Tracking and Command	18 watts
Total	180 watts

A 10^{o} beam was selected as providing sufficient overlap onto land areas around the North Atlantic for installation of control and calibration stations as needed. The coverage area is shown in Figure 3.1 as determined by use of Reference 3.1. For the experimental stage, the ground system could include the installation at Rosman, North Carolina. The calibration stations could be located in the Azores, Newfoundland, and Iceland (or Great Britain).

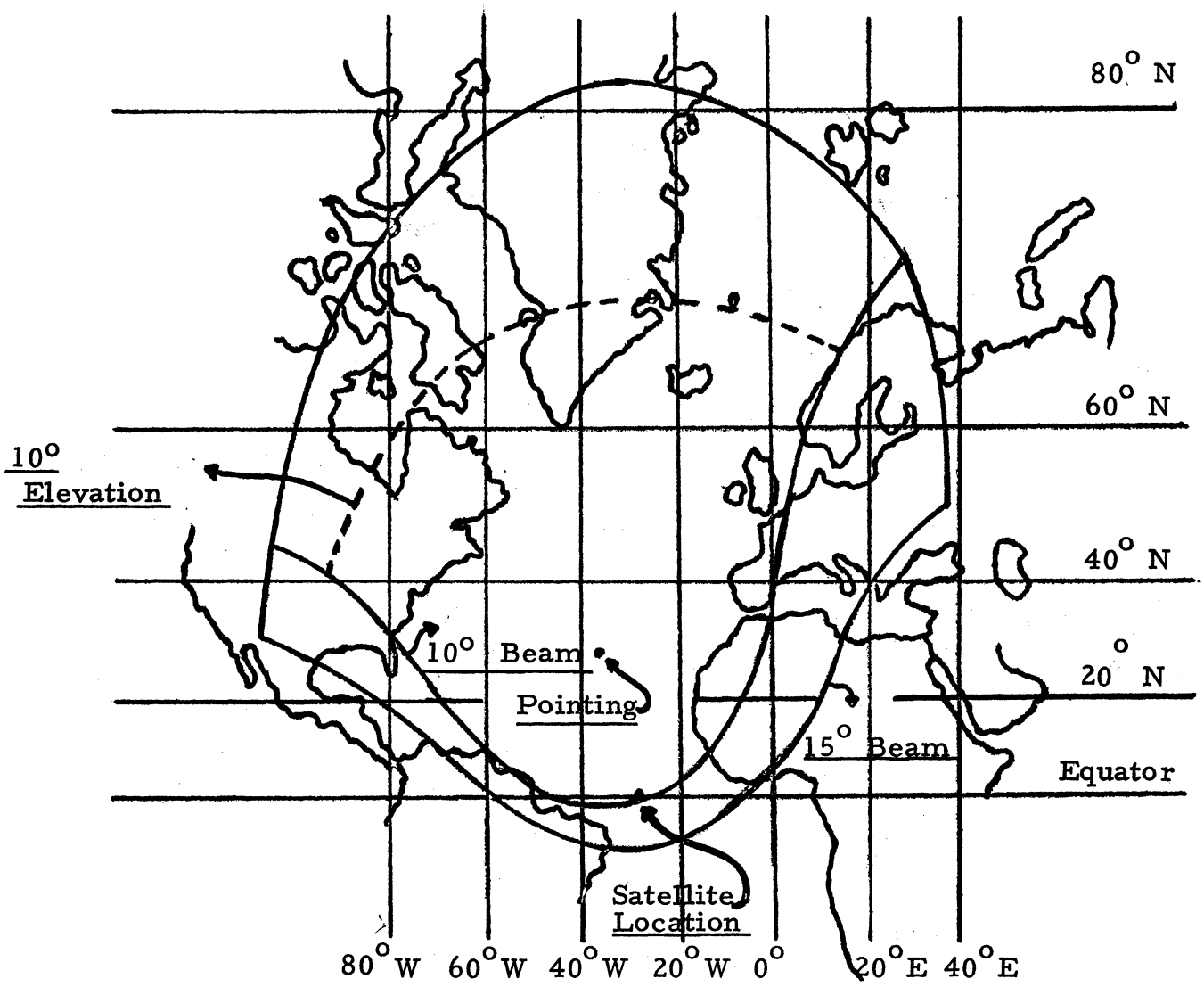

Figure 3.1 Antenna Coverage

Figure 3.2 presents the general block diagram of the electronic components for the satellite, and Appendix B.2 contains a breakdown of the equipment.

3.2 VOICE COMMUNICATIONS

3.2.1 System Operation

When the aircraft pilot desires to talk to the ground control station, he will transmit a signal containing his code number and priority (determined by set standards) on a common control channel. The satellite will frequency translate this signal and relay it to the ground station by way of the body mounted parabolic antenna. The ground station will then transmit a coded signal back to the aircraft stating that it has received the request. At the same time, or when a channel is free, the control station will transmit a coded signal informing the pilot on which of the five narrowband FM channels he may talk.

The system, operating in a simplex mode, will provide six channels, the first five being voice channels and the sixth for request and confirmation. In the event of an emergency, one of the channels may be freed to allow the pilot to communicate immediately. A multiplexing scheme was not chosen because there will be only six channels. In the operational satellite provisions could, and should, be made to allow for a larger aircraft capacity by providing more channels.

3.2.2 System Description

3.2.2.1 Link Budgets. The narrow band FM voice link will incorporate a message bandwidth of 3 KHz and will disregard all sidebands whose amplitude is less than one tenth of the unmodulated carrier amplitude. A deviation ratio of unity was chosen resulting in an IF bandwidth of 12.6 KHz and a threshold $(S/N)_{in}$ of 6.6 db. The $(S/N)_{out}$ at the demodulator output will be 33 db below the S/N_o ratio for the link. The calculations for the above characteristics appear in Appendix B.3. Tables 3.2 through 3.5 present the link budgets for the voice portion of SCANNAR. The important contributions are described in Appendix B.4.

The channels are spaced 50 KHz apart to allow for bandwidth, aircraft oscillator instability and Doppler shifts. This is ample spacing as the initial consideration was to eliminate the need for a very stable aircraft oscillator and thus reduce user costs.

The effective radiated power from the satellite to the ground and to the aircraft is approximately 64 dbm. The $(S/N)_{out}$ at the aircraft demodulator output is 18.5 db. In the operational mode, more power could be supplied to

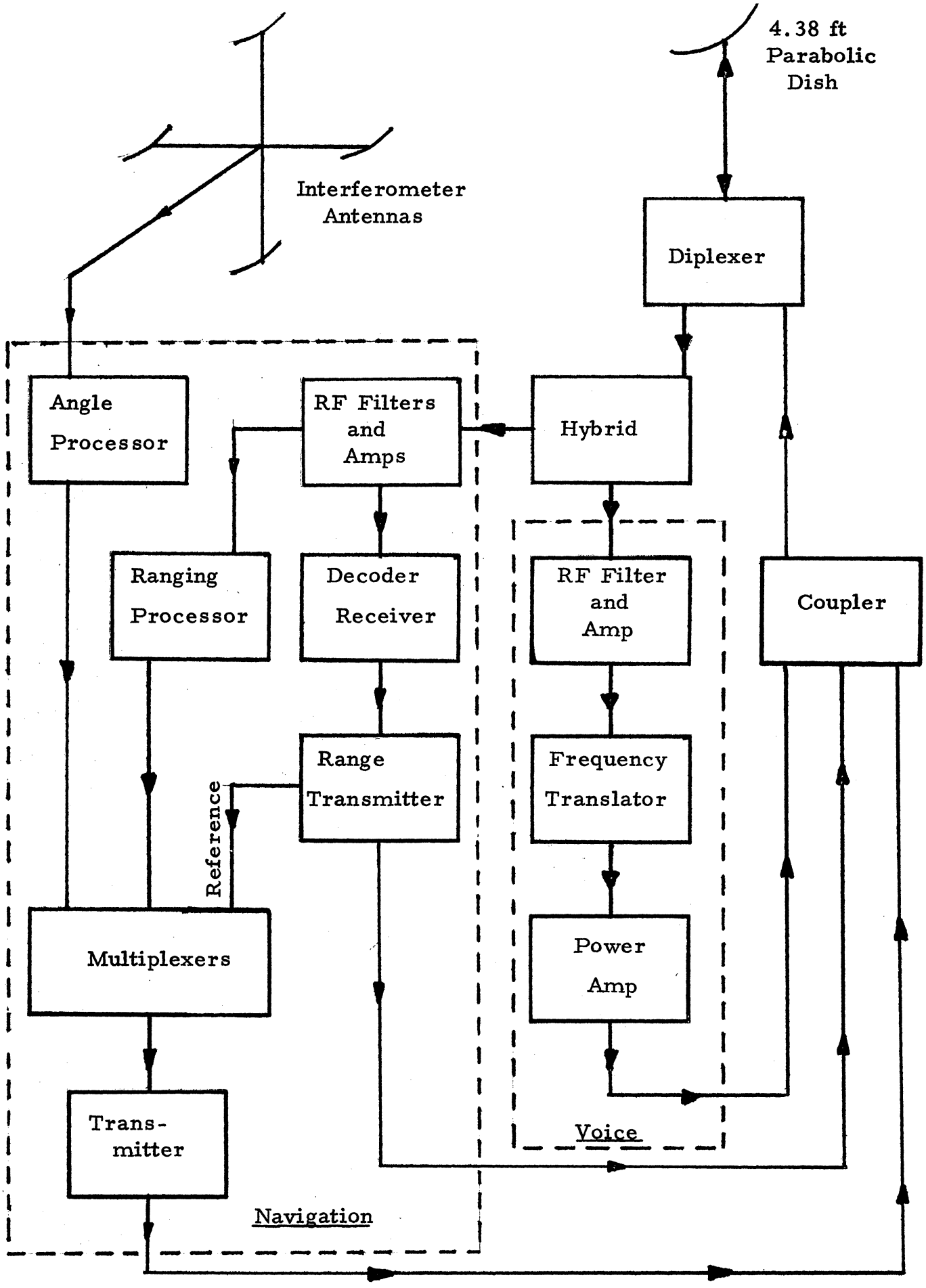

Figure 3.2 Satellite Functional Block Diagram

Table 3.2 Satellite to Aircraft Voice Link

	db
sat. transmitter power per channel	+10 (10 watts)
sat. antenna coupling loss	- 1
sat. antenna gain	+24.4
sat. off-beam losses	- 2.8
free space attenuation	-188.8
atmospheric attenuation	- 1
polarization losses	- 0.5
aircraft antenna gain	+15
aircraft off-beam losses	- 1
aircraft antenna coupling loss	- 1
aircraft effective system temperature	-28.4
Boltzman constant	+228.6 db/^{o}K-Hz
safety factor	- 2

$S/N_o = 51.5$ db-Hz

$(S/N)_{in} = 10.5$ db

$(S/N)_{out, FM} = 18.5$ db

Table 3.3 Satellite to Ground Voice Link

	db
sat. transmitter power per channel	+10 (10 watts)
sat. antenna coupling loss	- 1
sat. antenna gain	+24.4
sat. off-beam losses	- 3
free space attenuation	-188.8
atmospheric attenuation	- 3
polarization loss	- 0.5
gnd. antenna gain (40' parabolic dish)	+43
gnd. off-beam loss	- 0.5
gnd. coupling loss	- 0.5
gnd. effective system temperature	-20
Boltzman constant	+228.6 db/^{o}K-Hz
other system losses	- 2

$S/N_o = 86.7$ db-Hz

$(S/N)_{in} = 45.7$ db

$(S/N)_{out, FM} = 53.7$ db

Table 3.4 Aircraft to Satellite Voice Link

	db
aircraft transmitter power	+20 db (100 watts)
aircraft antenna coupling loss	- 1
aircraft antenna gain	+15
aircraft off-beam losses	- 1
free space attenuation	-188.8
atmospheric attenuation	- 1
polarization losses	- 0.5
sat. antenna gain	+24.4
sat. off-beam losses	-2.8
sat. antenna coupling loss	- 1
sat. effective system temperature	-28.8
Boltzman constant	+228.6 db/^{o}K-Hz
safety factor	- 2

$$S/N_o = 61.1 \text{ db-Hz}$$

Table 3.5 Ground to Satellite Voice Link

	db
gnd. transmitter power per channel	+20 db (100 watts)
gnd. antenna coupling loss	- 0.5
gnd. antenna gain	+43
gnd. off-beam losses	- 0.5
free space attenuation	-188.8
atmospheric attenuation	- 3
polarization loss	- 0.5
sat. antenna gain	+24.4
sat. off-beam loss	- 3
sat. coupling loss	- 1
sat. effective system temperature	-28.8
Boltzman constant	+228.6 db/^{o}K-Hz
safety factor	- 2

$$S/N_o = 87.9 \text{ db-Hz}$$

each channel to improve the quality somewhat; although, if a multiplexing scheme were to be used, this would in itself increase the FM improvement of the link while requiring more power for the larger IF bandwidth. The multiplexing scheme would become advantageous if the number of channels increased significantly over the present system.

Philco (Reference 3.2, pp 36-37) chose a nominal L-band design point for 95% reliability at (S/N_o) = 45 db-Hz which results in a 92% word intelligibility when operating at a 20^o elevation angle. Assuming a similar design point is practical for the present design, then a slight improvement would be realizable for the satellite to aircraft voice link where (S/N_o) = 51.5 db-Hz.

3.2.2.2 Voice Equipment. The voice links will be frequency translated at the satellite by a simple, redundant repeater which takes the signals down to an IF to strip off some of the noise added in the up links.

The receiver front end is completely redundant in that it incorporates two bandpass filters, RF amplifiers, and mixers which can be switched in event of a system failure. Two master oscillators are also provided to increase the redundancy.

The six channels are all down converted by the same amount and each channel has its own IF filter, IF amplifier and up converter. The translated signals are fed through six solid state power amplifiers after which the RF signals are sent through a coupler, a filter and then to the diplexer for transmission.

The IF and power amplification stages are all redundant since each channel has its own chain. If one of these were to fail, the satellite could still provide four voice channels, so that a loss of five of these stages is needed before the system is incapacitated.

Each of the power amplifiers has an output of 10 watts and is 60% efficient, thus requiring a total of 100 watts for the voice transmission. The equipment will absorb another 15 watts bringing the total voice power requirement to 115 watts.

Both of the receiving links (from ground and from aircraft) will go through the same translator. A block diagram of the system appears in Figure 3.3.

Solid state power amplifiers were chosen because the desired output per channel is only 10 watts. Since solid state components are more compact and operate sufficiently well for low power requirements, they were chosen

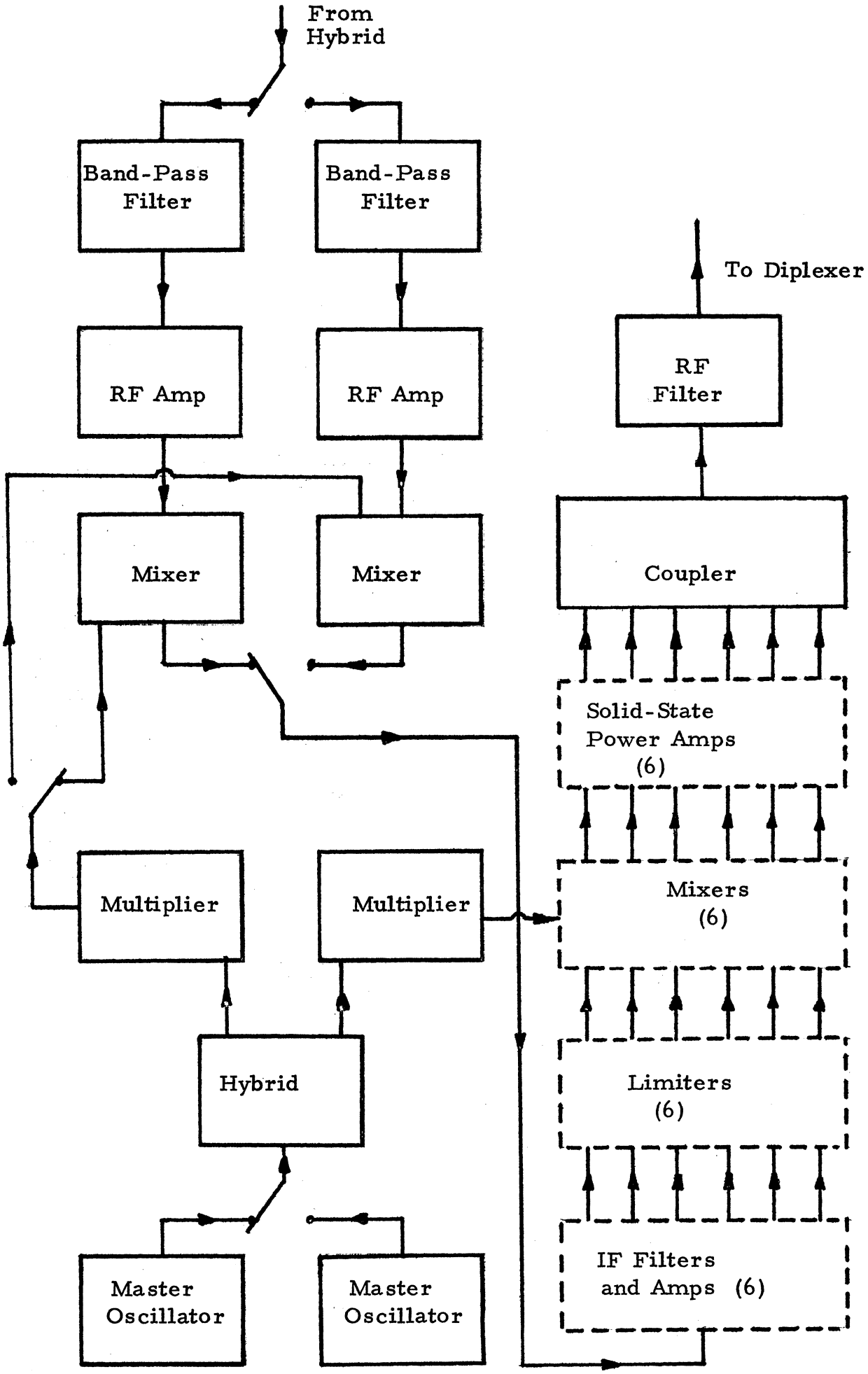

Figure 3.3 Satellite Voice Subsystem

over a traveling wave tube (TWT) which would not supply the needed redundancy. If a larger capacity is desired for the operational satellite, a TWT would probably serve better because of its broadband characteristics.

3.2.2.3 Antenna. The antenna used for the reception and transmission of signals will be a parabolic reflector with a steerable feed. The steerable feed is provided as a redundancy in case the antenna is deployed improperly or if the attitude of the satellite cannot be maintained as tightly as needed. In the transit mode, the antenna will be folded in an umbrella shape and unfolded on command once the satellite is on-station. The mesh antenna provides an average gain of 24.4 db for the frequency range used, and is nominally pointed at 30° N latitude, 37.5° W longitude. This pointing is accomplished structurally. A diplexer is incorporated into the system to allow for simultaneous reception and transmission via the same antenna.

The actual design and deployment of the antenna should be considered in more detail than time has warranted. Some other possible types of erectable antennas are: inflatable, Nitinol wire, hinged pedals, and the "Swirlabola" by Goodyear. (For further details see Reference 3.2, pp. 67-68.)

3.2.2.4 Aircraft Equipment. The user aircraft will require an L-band superheterodyne receiver which is tuneable to the six voice channels. The voice transmit-receive operation will be simplex with a diplexer being used to allow navigation functions to be performed simultaneously.

A channel spacing of 50 KHz was selected to provide sufficient room for frequency and tuning errors at the aircraft.

A switch is provided at the output of the down mixer. It will automatically switch the incoming signal to the desired detection circuit. One circuit is the relayed status and channel assignment which will be decoded and displayed so that the pilot knows which channel to talk on. The other circuit is the normal voice receiving demodulator. The switch will be operated when the pilot tunes to either the request channel or one of the five voice channels. This could also be accomplished by dividing the mixer output into separate filters for the voice channels and request channel.

The system block diagram appears in Figure 3.4.

The aircraft antenna will be an electronically steerable phased array antenna having 15 db gain and a 72° azimuth 3 db beamwidth and a 10° elevation 3 db beamwidth as described in Section 2.6.

3.2.2.5 Ground Equipment. Due to the many possible systems, the ground equipment has not been specified for the voice link. A practical limit should be placed on the equipment used to make the experiment feasible. For the experimental satellite, a simple ground receiving-transmitting voice system could be used.

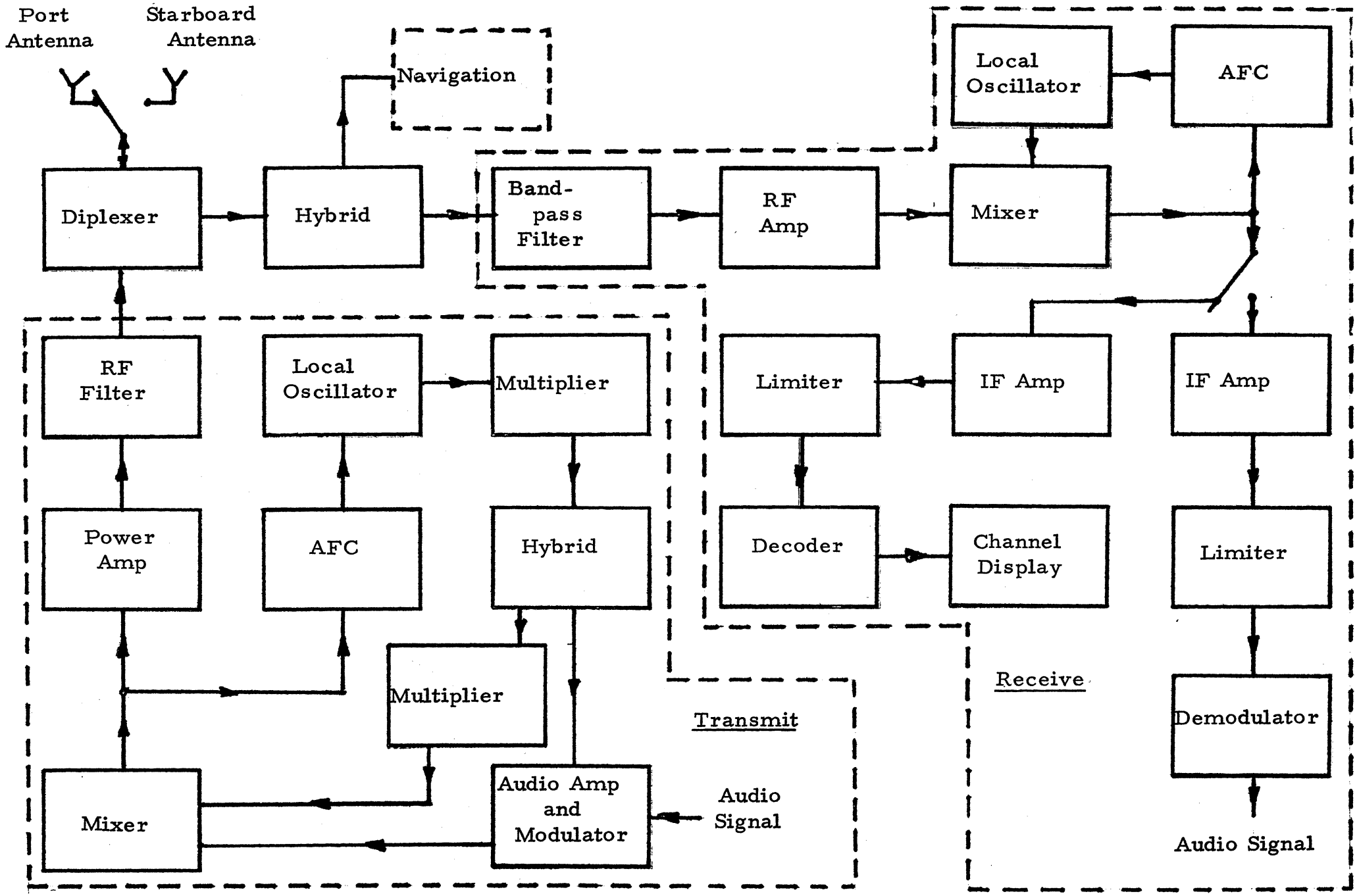

Figure 3.4 Aircraft Voice System

3.3 NAVIGATION DATA

3.3.1 System Operation

The signals processed according to Section 2.5 will be multiplexed by separate equipment because of the difference in data type. The range signal, along with aircraft altitude data will be received and multiplexed first. After a short delay, the angle signals will be received and multiplexed. The calibration stations will have a set delay between them so that the order of multiplexing and transmission will be aircraft, station one, etc.

If the aircraft pilot desires to know his position, the voice links will be used for this purpose. In the operational satellite it would be feasible and strongly recommended to supply a return link for the position location to be displayed at the aircraft.

3.3.2 System Description

3.3.2.1 Power Budgets. The two ranging sidetones will be modulated onto the carrier wave using a deviation ratio of two and disregarding all sidebands whose amplitudes are less than one tenth of the unmodulated carrier amplitude. The IF bandwidth will be 67 KHz and the threshold condition will be 7.6 db (Appendix B.6). The link budget appears in Table 3.6.

The multiplexing of the navigational data is described in Appendix B.7. The link budget appears in Table 3.7.

The $(S/N)_{in}$ at the ground will be improved after the detection stage, since the postdetection bandwidth will decrease to that of the relatively narrowband raw data, thus providing a good (S/N) for the comparison of signals.

3.3.2.2 Aircraft Link Budgets. The link budgets for the user aircraft appear in Tables 3.8 and 3.9. The aircraft range transponder can be similar to the ones used for tracking satellites. (Figure B.5). The total aircraft power required appears in Table 3.10.

3.4 TELEMETRY, TRACKING, AND COMMAND

During the transit mode the satellite will be tracked by NASA's STADAN system. Both the Minitrack and the Range and Range Rate (RARR) systems will be used to enable a high degree of accuracy in determining the location of the satellite during its long transfer orbit. Minitrack provides a nominal 20 arcsecond accuracy while the RARR system provides an accuracy of $\pm$ 15 meters and $\pm$ 0.1 meters/sec.

Table 3.6 Satellite to Aircraft Range Link

	db
sat. transmitter power	+17.5
sat. antenna coupling loss	- 1
sat. antenna gain	+24.4
sat. off-beam losses	- 2.8
free space attenuation	-188.8
atmospheric attenuation	- 1
polarization losses	- 0.5
aircraft antenna gain	+15
aircraft off-beam losses	- 1
aircraft antenna coupling loss	- 1
aircraft effective system temperature	-28.4
Boltzman constant	+228.6 db/^{o}K-Hz
safety factor	- 2

(S/N_o) = 59 db-Hz

B_{IF} = 48.3 db

$(S/N)_{in}$ = 10.7 db

P_t = 56 watts peak

0.5 sec CW signal

2 sec/fix

duty cycle = 25%

P_t = 14 watts average

Table 3.7 Satellite to Ground Data Link

	db
sat. transmitter power	+11.5 db (14 watts)
sat. antenna coupling loss	- 1
sat. antenna gain	+24.4
sat. off-beam losses	- 3
free space attenuation	-188.8
atmospheric attenuation	- 3
polarization losses	- 0.5
gnd. antenna gain	+43
gnd. off-beam loss	- 0.5
gnd. coupling loss	- 0.5
gnd. effective system temperature	-20
Boltzman constant	+228.6 db/^{o}K-Hz
other system losses	- 2

(S/N_o) = 88.2 db-Hz

Range $(S/N)_{in}$ = 25.9 db

Angle $(S/N)_{in}$ = 29.3 db

Range $(S/N)_{postdetection}$ = 39.9 db

Angle $(S/N)_{postdetection}$ = 53.5 db

Table 3.8 Aircraft to Satellite Range Link

	db
aircraft transmitter power	+20 db(100 watts)
aircraft antenna coupling loss	- 1
aircraft antenna gain	+15
aircraft off-beam losses	- 1
free space attenuation	-188.8
atmospheric attenuation	- 1
polarization losses	- 0.5
sat. antenna gain	+24.4
sat. off-beam losses	- 2.8
sat. antenna coupling loss	- 1
sat. effective system temperature	-28.8
Boltzman constant	+228.6 db/^{o}K-Hz
safety factor	- 2

(S/N_o) = 61.1 db-Hz

B_{IF} = 48.3 db

$(S/N)_{in}$ = 12.8 db

peak power = 100 watts

duty cycle = 0.25%

average power = 0.25 watts

Table 3.9 Aircraft to Satellite Angle Link

	db
aircraft transmitter power	+30 db
aircraft antenna coupling loss	- 1
aircraft antenna gain	+15
aircraft off-beam losses	- 1
free space attenuation	-188.8
atmospheric attenuation	- 1
polarization losses	- 0.5
sat. antenna gain	+24.4
sat. off-beam losses	- 2.8
sat. antenna coupling loss	- 1
sat. effective system temperature	-28.8
Boltzman constant	+228.6 db/^{o}K-Hz
safety factor	- 2

(S/N_o) = 71.1 db-Hz

B_{IF} = 300 Hz (24.7 db)

$(S/N)_{in}$ = 46.4 db

peak power = 1000 watts

duty cycle = negligible

average power: less than 1 watt

Table 3.10 Aircraft Power Requirements

	Average (watts)	Peak (watts)
Voice	100	---
Navigation		
Range	0.25	100
Angle	1	1000

This mode of tracking requires a simple S-band transponder for the RARR system and a VHF beacon for the Minitrack system. These systems have wide global coverage and are also compatible with other systems in order to provide excellent tracking of the satellite prior to its on-station operation.

Once on station the RARR system will be used by itself since Minitrack is not suitable for synchronous orbit satellites.

The telemetry subsystem will be used to report housekeeping operations and functions as well as receive the various command signals from the ground control station. Prior to the on station operation the tracking transponder antennas will be used to telemeter and to receive commands. The on station telemetry antenna is described in Appendix B.5.

A small lightweight clock is provided to fulfill NASA's requirement of telemetering a time signal as a reliability check with ground signals. These time signals are telemetered via the prime commutator

The command subsystem will provide local and override commands as well as ground originated commands. To insure success of the mission, a second command receiver is supplied as a redundancy. If both of these receivers were to fail the L-band receiver could function as a command receiver.

The equipment breakdown and power required is shown in Appendix B.2. The total telemetry, tracking and command power requirement is 18 watts.

A more complete discussion of the telemetry, tracking and command subsystem appears in Appendix B.8.

REFERENCES

3.1 Sollfrey, E., Earth Coverage Patterns with High-Gain Antennas on Stationary Satellites, The Rand Corporation, Memorandum RM-4894-NASA, February, 1966.

3.2 Communications System Implementation, Jorasch, R.F., Sr. Engineering Specialist, Philco-Ford, SRS Division, October 22, 1969.

3.3 Rauch, L.L., Aerospace Engineering 485 (Communications Systems), The University of Michigan, Class notes and handouts, Winter term 1970.

3.4 "Space Attenuation at Telemetry Frequencies", Cnudde, G.M., Lockheed Missiles and Space Co., Sunnyvale, California, Telemetry Journal, August/September 1969, pp. 73-75.

3.5 Hogg, D.C. and Mumford, W.W., "The Effective Noise Temperature of the Sky", Microwave Journal, vol. 3, March 1960, p. 80.

3.6 American Electronic Laboratories, Inc., Bulletin, 20-50.

3.7 Stiltz, H.L. ed., Aerospace Telemetry, vol. I, 1961, Prentice Hall, Inc., Englewood Cliffs, N.J.

3.8 Cuccia, C.L., "Sensitivity of Microwave Earth Stations for Analog and Digital Communications", Part II, Microwave Journal, February 1969.

* * *

Corliss, W., Scientific Satellites, NASA SP-133, 1967.

Filipowsky, R.F., and Muehldorf, E.I., Space Communications Systems, Prentice-Hall, Englewood Cliffs, N.J., 1965.

Harvey, A.F., Microwave Engineering, 1963.

Koelle, H.H., ed., Handbook of Astronautical Engineering, 1961, Chapter 16.

Mueller and Sprangler, Communication Satellites, 1964.

Navigation Satellite System, Westinghouse Electric Corporation Defense and Space Center, contract NASw-785, Phase I Report, January 30, 1964 and Phase II Report, October 15, 1964.

Project MISSAC, Department of Aerospace Engineering, The University of Michigan, Winter term, 1968.

Useful Applications of Earth-Oriented Satellites: Navigation and Traffic Control, Panel 11 of Summer Study on Space Applications, NAS, Washington, D.C., 1969.

4
ATTITUDE AND CONTROL

4.1 INTRODUCTION

The proposed attitude determination and control system for Project SCANNAR consists of five sun sensors, a planar scanner, and three position gyros for attitude sensing while control is maintained by using three reaction wheels in conjunction with thrusters for unloading of the wheels, rotational maneuvers, and translational corrections. The conceptual description of the system and its major components is presented in this chapter. Component specifications are found in Appendix C. 2.

4.2 SYSTEM REQUIREMENTS

The requirements dictated by Project SCANNAR for the attitude and control system are the following:

1. Attitude determination to within $\pm 1^{o}$ on all three axes must be provided from the circular parking orbit through the two-year operational period at synchronous altitude.

2. Control over all three axes must be maintained at all times during this period to an accuracy of 1^{o}. While on-station at synchronous altitude, the satellite communications apparatus must be kept pointed toward a fixed latitude and longitude on the Earth to maintain coverage of the North Atlantic.

3. The system must provide translational capability to correct satellite drift within the equatorial plane from its prescribed longitudinal position.

4.3 COORDINATE SYSTEM

An orbit-plane axes system was chosen to describe the idealized configuration of the satellite. The origin is centered at the center of mass of the satellite with three orthogonal axes: X, Y, and Z. The Y, pitch, axis is parallel with the Earth's axis of rotation and is positive South. The Z, yaw, axis is positive toward the Earth and is pointed toward the Earth geocenter. The X, roll, axis completes the right-hand coordinate system and is positive in the approximate direction of the velocity vector (see Figure 4.1). The coordinate system rotates one revolution per day about the Y-axis (see Figure 4.2).

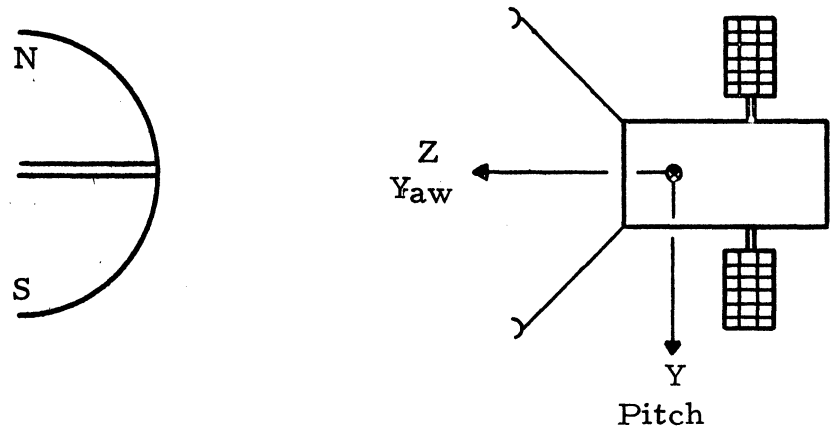

Figure 4.1 Coordinate System

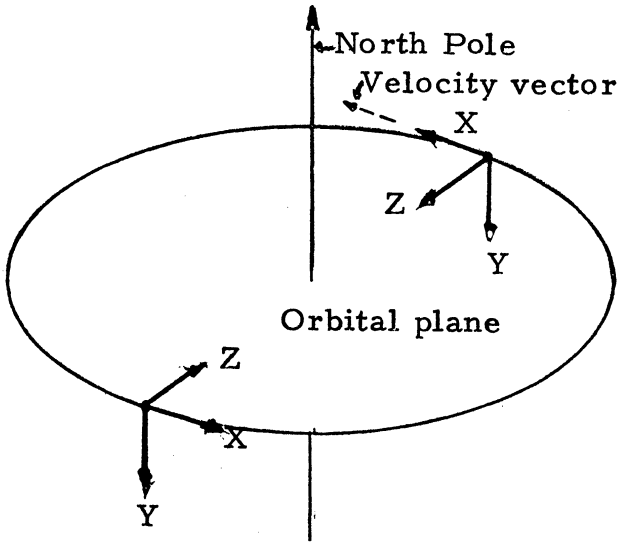

Figure 4.2 Axes of Revolution

On station, the booms will be deployed along two perpendicular lines: one positioned in a Northeast-Southwest direction, the other in a Northwest-Southeast direction. The communication antenna is offset on the satellite body to the East (along the positive roll axis), and is pointed toward 30° N latitude and 37.5° W longitude. The initial eastward direction before deployment of the booms will be determined by the sun sensors described in Section 4.5.

4.4 OVERALL SYSTEM DESCRIPTION

The satellite body attitude information will be provided by a system of solar aspect sensors, planar scanner, and position gyroscopes. The data from the sensors will be reduced by a small onboard digital computer. Any errors will result in the computer sending actuating commands to the torquing apparatus consisting of reaction wheels and monopropellant hydrazine rocket motors. Each of the system components and their respective function is described below, and is shown in block diagram form in Figure 4.3. A consolidated description of system modes is found in Appendix C.1.

It should be noted that all attitude referencing is concerned exclusively with the rigid body of the satellite, excluding the booms.

4.5 ATTITUDE SENSING

The sensing equipment consists of three body-mounted position gyros, five solar aspect sensors, and one infrared planar scanner earth sensor. The proposed system will provide at least 1° attitude determinations along all three axes through the launch phase. During synchronous altitude operation, the system will provide better than 0.1° sensing accuracy about the pitch and roll axis and better than 1° along the yaw axis. A description of each sensor and its mode of operation is presented below.

4.5.1 Solar Aspect Sensors

A system of five solar aspect sensors will provide full spherical coverage as shown in Figure 4.4. Each sensor has a field of view of 128° x 128° and has a two axis accuracy of 0.25°. The solar aspect sensors will be the primary attitude sensing system employed during the launch phase along the orthogonal axes perpendicular to the sun's rays as shown in Figure 4.5. The solar aspect sensors will provide primary yaw axis information and resetting information for the gyros while on station.

4.5.2 Position Gyros

Because the axis parallel to the sun's rays cannot be resolved using the solar aspect sensors, a three axis gyro system was adopted. The approrpiate position gyro will be used for information along the unresolved

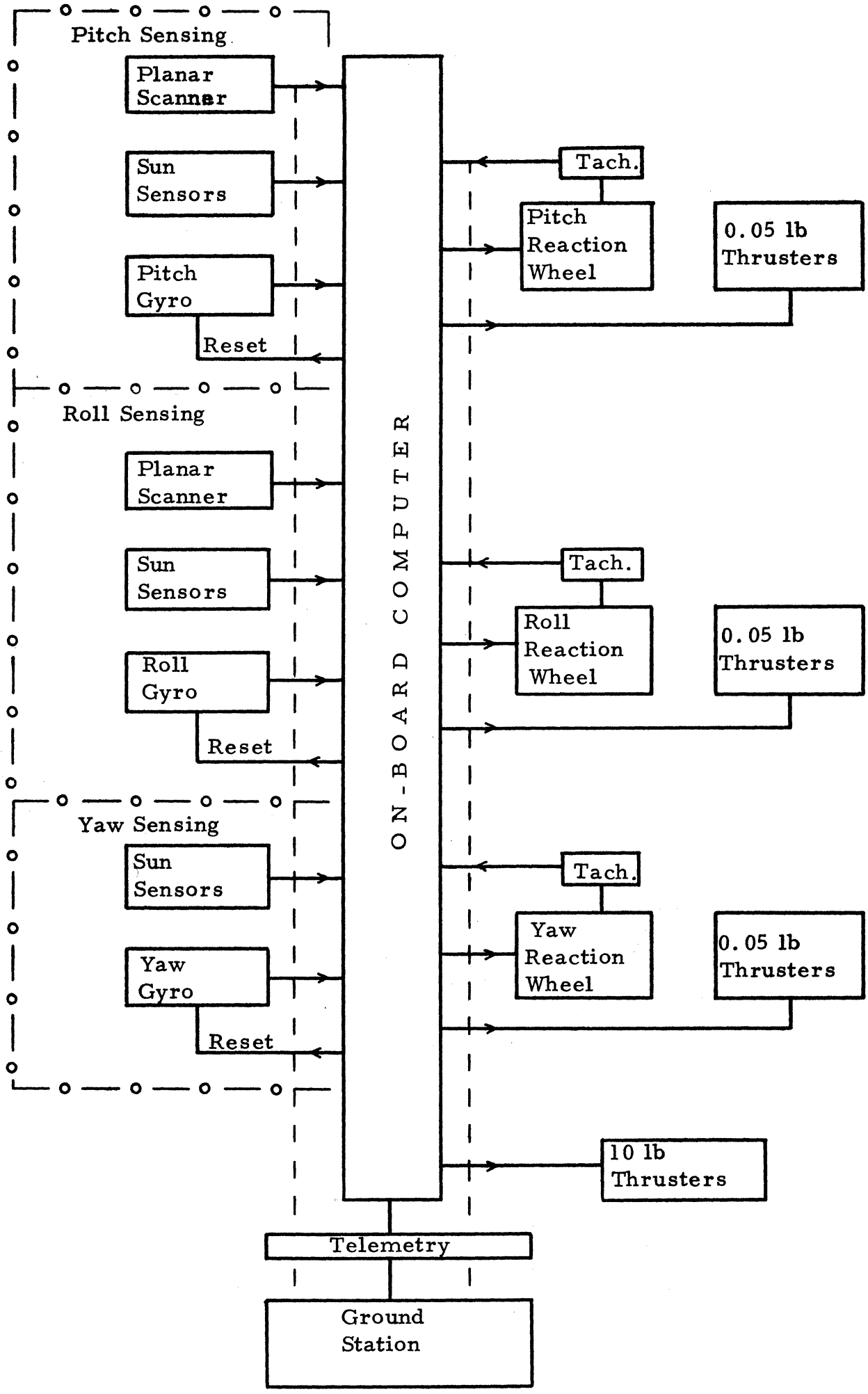

Figure 4.3 Attitude and Control Block Diagram

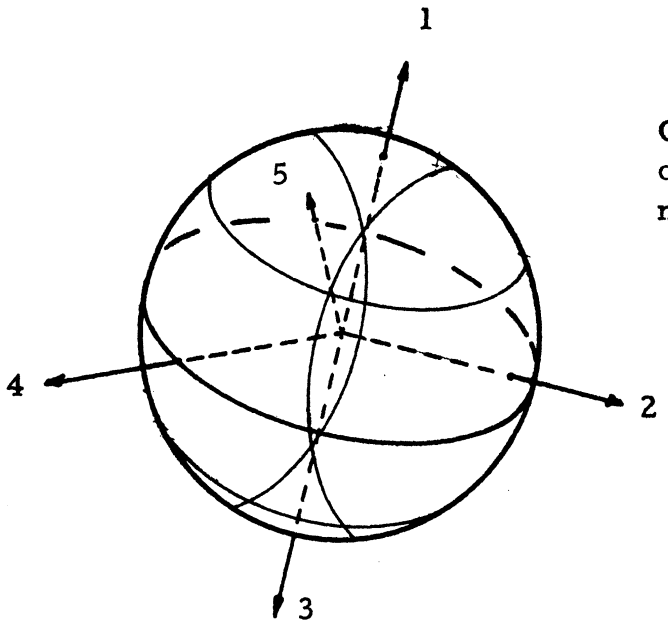

Figure 4.4 Solar Aspect Sensor Coverage

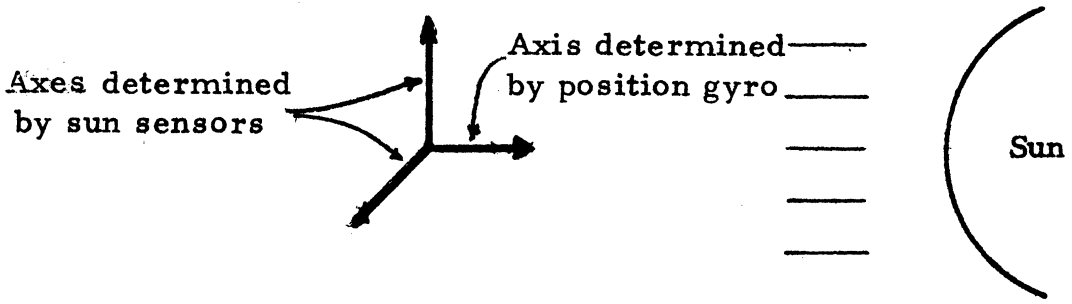

Figure 4.5

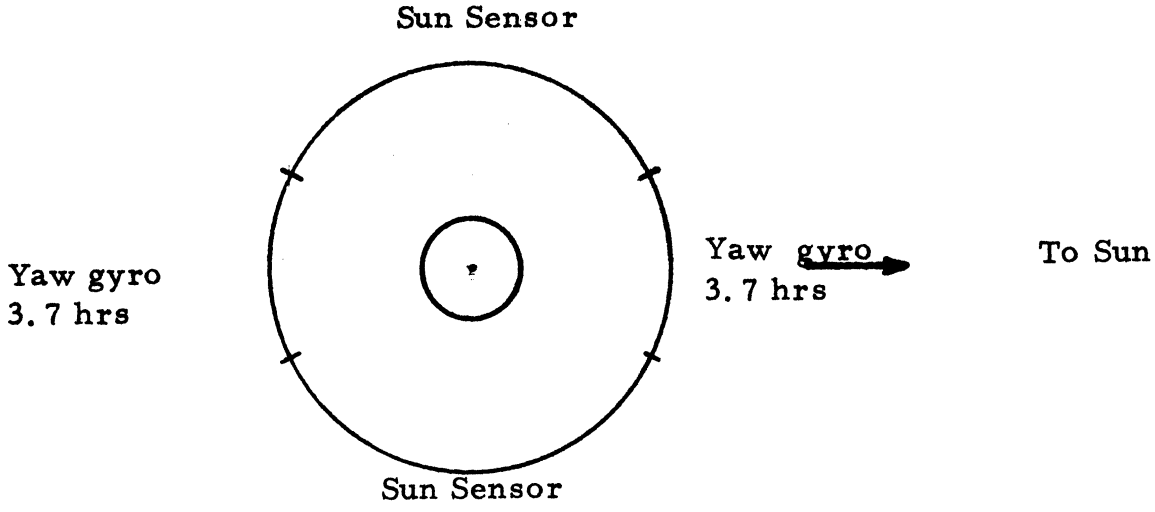

Figure 4.6 Sensing Modes

axis. The gyros will be spun-up prior to launch and will be reset periodically from solar aspect sensors and planar scanner to correct for gyro drift. With current gyro technology, the drift error can be held to within 1^{o} over a period of a few hours. Therefore, the gyros cannot be relied upon as a primary attitude sensor for long periods of time. During the launch phase, the gyros must be reset prior to critical maneuvers. While on station, the gyros will be used normally only for yaw information during two 3.7 hour periods each day and during solar eclipse. The gyros will be reset prior to these periods for the desired accuracy. The on-station sensing modes are shown in Figure 4.6.

4.5.3 Planar Scanner

An infrared planar scanner will provide pitch and roll attitude information to within 0.1^{o} at all times while on station. The instrument is pointed toward the Earth along the yaw axis and will remain in that orientation during synchronous orbit.

Infrared sensors, in general, detect thermal radiation discontinuities at opposite horizons of a planetary body. The term "planar scanner" denotes a specific method of applying this concept.

The unit contains four infrared radiation detectors whose fields of view are rotated in two perpendicular planes from space across the horizon, or edges, of the planetary body as shown in Figure 4.7. The two fields of view in each plane are rotated synchronously; that is, at any instant during their scan cycle the two fields of view make equal angles with the primary axis of the scanner. If a pointing error exists, the field of view of one detector will cross the horizon before the field of view of the second detector in the same scanning plane crosses the opposite horizon. Since the scanning rate is constant, the time difference between crossing opposite horizons in one scanning plane is directly proportional to pointing error in this plane. The direction of pointing error is determined by noting which of the detectors first detects the radiation discontinuity (Reference 4.1).

4.5.4 Digital Computer

A digital computer will provide the necessary interface between the attitude sensing equipment and the control torquing devices. The total computational requirements for the modular attitude and control system, as implemented by the onboard digital computer, can be accomplished by present state-of-the-art aerospace computers (Reference 4.2).

The proposed unit will provide capability for constant attitude information reduction, control logic, and command initiation as well as a capability for storing and sequencing commands for future initiation.

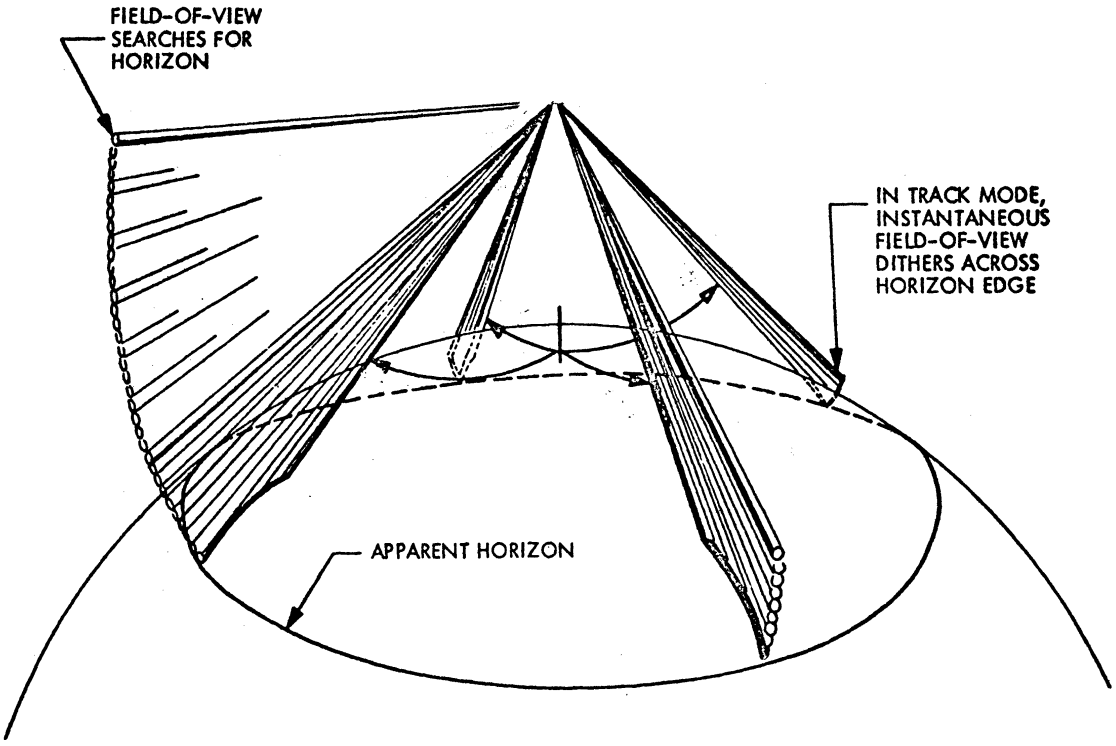

Figure 4.7 Planar Scanner

Storage and sequencing capability will be used for maneuvers during the launch and rendezvous phase, for reaction wheel unloading operations, and for station-keeping maneuvers.

4.5.5 Redundancy and System Accuracy

All of the sensing apparatus chosen has been used on spacecraft and is of high reliability. The system does, however, provide back-up capability for a considerable amount of system failure.

The planar scanner will normally provide attitude resolution along the roll and pitch axes to an accuracy of less than 0.1^{o}. In case of its failure, two axis attitude information can be drawn from the solar aspect sensors and the third axis from the appropriate position gyro. Each gyro can be reset from solar data to within 0.25^{o}.

The yaw axis attitude is derived from the sun sensors or the reset yaw position gyro. In case of a sensor failure, the gyro dependency time would be expanded. In the case of a gyro failure, the satellite would be without any yaw information for about two 3.7 hours periods each day.

4.6 REACTION WHEELS

Three reaction wheels control the vehicle's attitude about the three axes. Their operation is based on the principle of conservation of momentum. A disturbing torque acting on the satellite results in a change in satellite angular momentum, its magnitude dependent on the duration of action and magnitude of the disturbing torque. By accelerating the reaction wheels at this point, their momentum will increase and the momentum of the satellite will decrease so that the total momentum of the satellite-wheel system remains unchanged. To determine which reaction wheels to activate and what their respective magnitudes and directions of acceleration should be, the resulting total wheel momentum vector should have the same magnitude and direction as the satellite momentum vector before the reaction wheels are activated.

The reaction wheel method is limited because the wheels cannot store infinite momentum. Therefore, when wheel momentum saturation is reached, the reaction wheels must be unloaded by using thrusters. When unloading, the thruster momentum vector must be equal but opposite in direction to the wheel momentum vector, bringing the net momentum of the satellite-wheel system to zero. Now, the reaction wheels can again store momentum and the process continues.

When sizing reaction wheels, the value of momentum saturation must not be so small that for their particular application they must be unloaded at unreasonably frequent intervals. Also, the drive torque of the wheels must not be greater than the maximum torque which the satellite can structurally withstand and not smaller than the disturbing torques which they are supposed to counteract in the worst case.

The reaction wheels used in Project SCANNAR have a momentum storage capability of 1.456 ft-lb-sec at 1000 rpm with a stall torque of 0.01 lb-ft. They are driven by three brushless DC motors. These values of stall momentum and restoring torque are sufficient to satisfactorily counterbalance all the disturbing torques which will be encountered by the satellite (see Appendices C. 3 and C.4).

One reaction wheel is placed along each axis. The speed of the wheels is controlled by the onboard computer, which processes sensor signals into attitude errors. The angular velocity of each wheel is measured by a tachometer which sends a signal to the computer which in turn sends a command to fire appropriate thrusters when the wheel motor reaches maximum speed and the wheel momentum has to be unloaded.

4.7 PROPULSION SYSTEM

Monopropellant hydrazine thrusters will be used to perform orbit trim, rendezvou and rotational maneuvers, and to unload the reaction wheels. Two ten-pound thrust rocket motors, located on either side of

the apogee motor, will be used to provide translational thrust for the second perigee burn and rendezvous. Since these thrusters are used when the satellite is in a non-spinning mode, misalignment of the thrust vectors creates a disturbing torque on the satellite. However, this torque is easily corrected using the 0.05 pound thrusters (see Appendix C.5).

Sixteen 0.05 lb thrust rocket motors will accomplish all rotational corrections before arrival on station. The satellite must be despun prior to satellite maneuvering because of instabilities that occur in maneuvering a spinning body. The yo-yo despin technique (see Section 4.8) is used after third-stage burnout. Later, rotational maneuvers are made to orient the satellite for second perigee and apogee burns. Just before apogee burn, the satellite is spun-up around the Z-axis using the 0.05 lb thrusters to avoid the large torque created by apogee motor thrust misalignment. After apogee burn, prior to rendezvous maneuvering, the satellite is again despun using the 0.05 lb thrusters. When on station, the 0.05 lb thrusters will function to unload the reaction wheels and will provide translational thrust for small drift corrections. Thruster location and operational modes are shown in Figure 4.8.

Table 4.1 Fuel Budget

Operational Function	Fuel Weight
360^{o} maneuvers before apogee	.095 lbs
360^{o} maneuvers after apogee	.088 lbs
Orbit trim (ΔV = 60 fps)	9.048 lbs
Rendezvous (ΔV = 163 fps)	12.881 lbs
Thruster misalignment corrections	.077 lbs
Spin-Up (1)	.939 lbs
Despin (1)	.806 lbs
Drift corrections (2 years)	.698 lbs
	24.632 lbs
Contingency	5.368 lbs
Total fuel weight	30.000 lbs

Figure 4.8 Thruster Location and Operational Modes

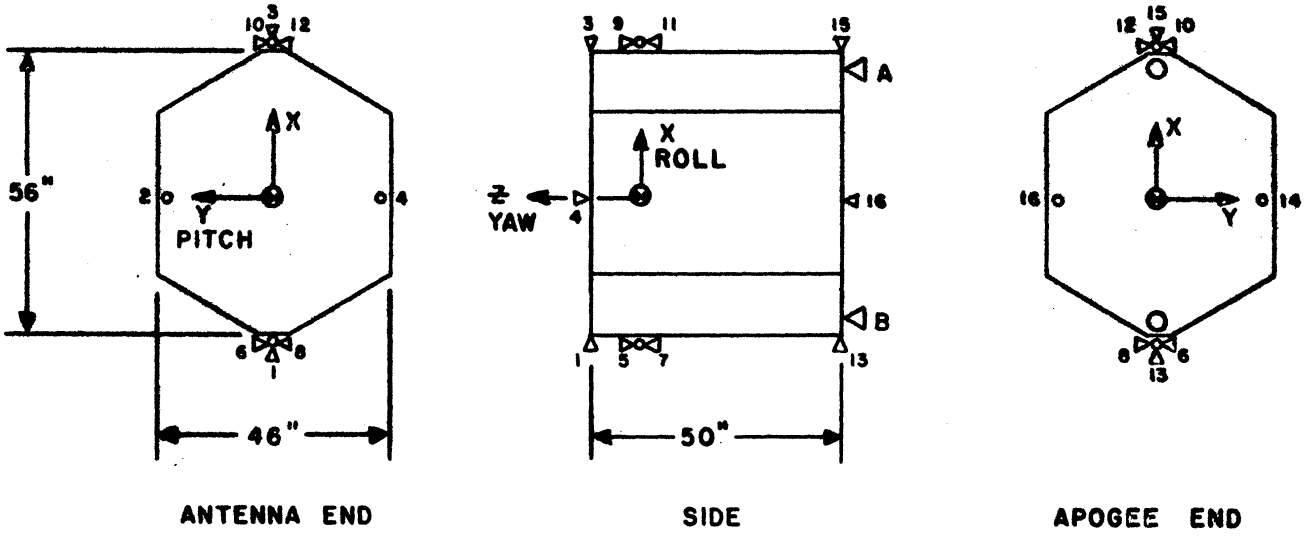

Motion	Thrusters	Thrust	Torque
Positive X	1 & 13	.1 lbs	
Negative X	3 & 15	.1 lbs	
Positive Y	12 & 8	.1 lbs	
Negative Y	6 & 10	.1 lbs	
Positive Z	A & B	20 lbs	
	7 & 11	.1 lbs	
	14 & 16	.1 lbs	
Negative Z	5 & 9	.1 lbs	
	2 & 4	.1 lbs	
Positive Roll	4 & 14		.1917 ft-lbs
Negative Roll	2 & 16		.1917 ft-lbs
Positive Pitch	7 & 9		.2333 ft-lbs
	1 & 15		.2083 ft-lbs
Negative Pitch	5 &11		.2333 ft-lbs
	3 & 13		.2083 ft-lbs
Positive Yaw	6 & 12		.2333 ft-lbs
Negative Yaw	8 & 10		.2333 ft-lbs

The torque generated by the thrusters in rotational maneuvering is the product of the thrust applied and the effective moment arm through which the thrust acts. This torque has to be at least equal to the stall torque of the reaction wheels and smaller than the maximum torque which the satellite can structurally withstand. The maximum torque generated by two 0.05 lb thrusters working in conjunction to overcome a rotational error is 0.2333 ft-lb and the minimum is 0.1917 ft-lb (from Figure 4.8). These values of torques are within the design limits of the satellite structure, including the booms, and are larger than the stall torque of the reaction wheels.

The total thrust impulse required is a function of the velocity increments necessary for different mission operations. A capability of one 360° maneuver about each of the three axes is provided before apogee burn. This requires .095 lbs of fuel (see Appendix C.6). For translational maneuvering prior to apogee burn, a possible velocity increment of 60 fps is required by using the two ten-pound thrust rocket motors. Using a satellite weight of 1020 pounds before apogee burn, these maneuvers require an impulse of

$$I_1 = 60\left(\frac{1020}{32.174}\right) = 1900 \text{ lb-sec.}$$

Assuming a specific impulse of $I_{sp} = 210$ sec for the ten-pound thrusters, the above impulse corresponds to a fuel weight of 9.048 pounds. Corrections for a possible 0.25° misalignment of the 10 pound thrusters require 0.0265 pounds of fuel using the 0.05 pound thrusters (see Appendix C.5).

Just before apogee burn, the satellite is spun-up to 100 rpm around the Z-axis using the 0.05 pound thrusters. This requires 0.939 pounds of fuel. After apogee burn, the satellite is despun using the 0.05 pound thrusters, requiring 0.806 pounds of fuel (see Appendix C.7).

Another capability of one 360° maneuver about each axis is provided after the apogee burn, now requiring .088 lbs of fuel (see Appendix C.6). Translational maneuvering after apogee burn, including rendezvous, will require a possible velocity increment of 163 fps, again using the two ten-pound thrust rocket motors. After apogee burn, the satellite weight is approximately 534 pounds, which, with the ΔV of 163 fps, results in an impulse of

$$I_2 = 163\left(\frac{534}{32.174}\right) = 2705 \text{ lb-sec.}$$

Using the specific impulse of 210 sec, this means an additional fuel weight of 12.881 lbs. In this case, corrections for a possible 0.25° misalignment of the 10 lb thrusters require 0.0501 lbs of fuel (see Appendix C.5). Therefore, the total fuel consumption prior to arrival on station is 23.934 lbs. The on station satellite weight is approximately 534 - 13 or 521 pounds.

On station maneuvering will consist of drift corrections and reaction wheel unloading using only the 0.05 lb thrust rocket motors. For a two-year period, a possible velocity increment of 6.46 fps is required for drift corrections. This means an impulse of

$$I_3 = 6.46 \left(\frac{521}{32.174} \right) = 104.7 \text{ lb-sec.}$$

A specific impulse of $I_{sp} = 150$ sec is assumed for the 0.05 lb thrusters, which will be operated in a pulse mode. This results in a fuel weight required for drift correction over a two-year period of .698 pounds.

Thus far, 24,632 lbs of fuel are required for various mission operations. Reaction wheel unloadings require only 0.005 lbs of fuel per unloading (see Appendix C.4). Calculations of the disturbing torques (see Appendix C.3) show that the reaction wheels will not have to be unloaded very often during the two-year operational life of the satellite. Using a total fuel weight of 30 lbs, a contingency factor of 5.368 lbs will be more than sufficient to accomplish all necessary reaction wheel unloadings as well as provide for unpredictable, potential fuel needs.

Hydrazine thrusters utilize Shell 405 as the spontaneous catalyst which decomposes the hydrazine into 1800°F gases consisting of ammonia, nitrogen, and hydrogen. Hydrazine (N_2H_4) has a propellant density of 62.7 lb/ft^3, a freezing temperature of 34.7°F and a boiling temperature of 236.3°F.

For Project SCANNAR, the monopropellant hydrazine will be supplied to the thrusters using a "blow-down" pressurization system. The "blow-down" system will consist of two collapsible bladders containing hydrazine, each bladder contained within a sphere filled with pressurized nitrogen gas. Thirty pounds of hydrazine will be supplied for the mission, with a volume of 827 in^3. The volume ratio of hydrazine to nitrogen will be 6 to 4. Hence, since 827 in^3 of fuel will comprise 60% of the total volume necessary, the resulting total volume is 1378 in^3. Dividing this into twospheres, each sphere will have a volume of 689 in^3 and therefore a diameter of 11 inches.

The ten-pound thrust rocket motors operate at a propellant pressure of 250 psi and the 0.05 lb thrusters require 80 psi. The initial pressure of the nitrogen gas will be 250 psi. As hydrazine is expelled, the pressure will decrease to a final pressure of 100 psi. A fluidic pressure dropping device will be placed in line with the 0.05 lb thrusters to keep the propellant pressure at 80 psi.

As the pressure of the propellant fed to the ten-pound thrusters decreases from the optimum pressure of 250 psi, the actual thrust output will decrease proportionately. This change will be accounted for by increasing the firing time to make up for the decrease in thrust. To correct for changing thrust levels, a pressure gage will monitor the propellant pressure

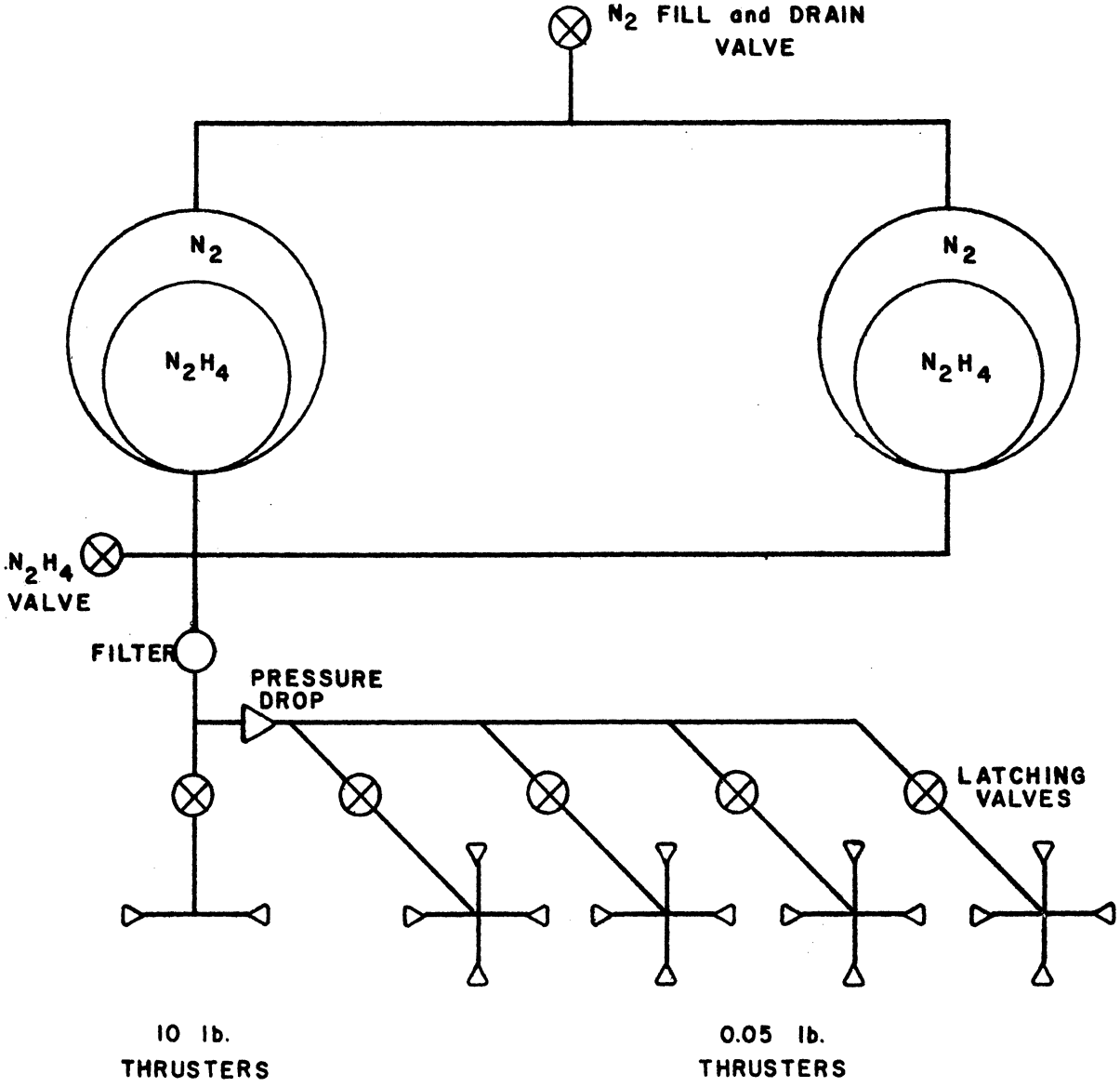

Figure 4.9 Propellant Pressurization System

and feed this information into the onboard computer. A calibration of propellant pressure versus thrust will be programmed into the computer so that the correct firing time can be calculated for any desired ΔV.

Latching valves will be used to provide redundancy in stopping fuel flow to the thrusters. These valves will receive commands at the same time the individual thruster solenoid valves are actuated. This redundancy prevents fuel leakage through a thruster due to a faulty solenoid valve. By regarding the sixteen 0.05 lb thrusters as four quads, only four latching valves are needed since there would never be more than one thruster from any quad being fired at any time.

A filter is used to guard against impurities in the propellant. A diagram of the "blow-down" pressurization system is shown in Figure 4.9.

4.8 YO-YO DESPIN SYSTEM

During the launch phase of the mission, the third stage uses spin stabilization for injection accuracy. After third stage burnout, and before separation from the third stage and the attach fitting, the satellite is despun using the yo-yo despin technique. This is done by unwinding two diametrically opposed weights that are wrapped around the periphery of the attach fitting. The two weights are connected to the attach fitting by steel cables. These cables unwind tangentially until the final spin rate is reached. At this time the cables are perpendicular to the spacecraft and detach from the body.

An initial spin rate of 100 rpm is reduced to nearly zero rpm by releasing two 3.94 pound weights that spin out 18.50 feet from the attach fitting (see Appendix C.8).

System Parameters

I - spin moment of inertia (45.246 slugs-feet^2)
L - length of one cable (18.50 feet)
M - end weight (3.94 pounds)
M_c - weight of one cable (0.687 pounds)
R_i - initial spin rate (100 rpm)
R_f - final spin rate (0 rpm)
cable is 1/8 inch steel, 0.0031 pounds/inch
a - radius of attach fitting (0.75 feet)

REFERENCES

4.1 Hatcher, N.M., et al, "Development of a Proposed Infra-Red Horizon Scanner for Use in Spacecraft Attitude Determination", NASA TND-2995, September 1965.

4.2 "Radio/Optical/Strapdown Inertial Guidance Study for Advanced Application", TRW, Inc., NASA CR-1496, Volume I - Summary, December 1969.

4.3 Greensite, Arthur L., "Attitude Control in Space", Analysis and Design of Space Vehicle Flight Control Systems - Volume XII, General Dynamics Convair Report No. GDC-DD#67-001, NASA CR-831, August 1967.

4.4 Eide, D.G., and Vaughn, C.A., "Equations of Motion and Design Criteria for the Despin of a Vehicle by the Radial Release of Weight and Cables of Finite Mass", Langley Research Center, NASA TN D-1012, January 1962.

* * *

Cassady, W.M., "Reaction Wheel with Brushless DC Motor Drive," Sperry Farragut Company Contract No. NAS5-9016, NASA CR-388, April 1966.

Cliff, R.A., "SDP-3--A Computer for Use On Board Small Scientific Spacecraft", EASCON 68 Conference.

Final Report for Lunar Libration Point Flight Dynamics Study, General Electric Company Contract No. NAS5-11551, May 1968, November 1968.

Fulcher, R., "A Brushless DC Torquer-Driven Reaction Wheel for Spacecraft Attitude Control", NASA TN D-5265, July 1969.

Hatcher, Norman M., "A Survey of Attitude Sensors for Spacecraft", NASA SP-145, 1967.

Leondes, C.T., Guidance and Control of Aerospace, New York, McGraw-Hill, 1963.

MISSAC- Michigan Instructional Satellite for South American Countries, Feasibility Design Report, The University of Michigan Department of Aerospace Engineering, April 1968.

Modern Navigational Systems - Fundamentals and Applications - Volume II, U. of M. Engineering Summer Conferences, 1969.

Singer, S.F., Torques and Attitude Sensing in Earth Satellites, New York Academic Press, 1964.

Staffan, K.F., "Positioning and Stationkeeping and Orbital Navigation", Course Notes, University of California at Los Angeles,

"U.S. Rocket Motors", Aviation Week and Space Technology - Inventory Report, March 10, 1969.

5
POWER

5.1 INTRODUCTION

Electrical power for SCANNAR is provided by a system of solar panels, body mounted solar cells and silver cadmium batteries weighing a total of 115 pounds. The system is designed to provide the required power level of 238 watts over the two year lifetime of the satellite.

Before selecting this design, several factors were considered. The power requirement and the two year lifetime of the satellite eliminated all but solar power and radioisotope thermoelectric generators (RTG's) as possible power sources. Solar power systems have the disadvantage of requiring batteries for use when the satellite is in shadow. RTG's operate independent of sunlight, but they are heavier and more expensive when used in earth orbit than comparable solar power systems. The radioactive materials they use for fuel must be shielded from other spacecraft equipment, adding to the weight of the satellite. Solar cell-battery combinations have been used on satellite for many years and have proven to be very reliable. For these reasons, a solar power system was chosen for use on SCANNAR.

5.2 POWER REQUIREMENTS

The SCANNAR mission can be divided into four separate phases: launch, the period from liftoff until shroud separation; transfer, the period from launch until the satellite is on station; orbit, extending over the two year operating life of the satellite; and eclipse, the periods when the satellite is in shadow. The power requirements of each of the satellite subsystems are summaried in Table 5.1.

Table 5.1 Power Requirements

System	Launch	Transfer	Orbit	Eclipse
Communications, Navigation and Telemetry	11 watts	11 watts	180 watts	180 watts
Attitude Control and Station Keeping	30	30	40	40
Battery Charging	-	12	12	-
Solar Panel Orientation	-	-	6*	-
TOTALS	41	53	238	220

*When the orientation motors are not operating, this power can be used for battery charging.

A graph of power required and power available is shown in Figures 5.1 and 5.2. The decrease in power available from the solar panels over two years reflects a 15 percent allowance made for solar cell degradation. This degradation is caused by cell aging, radiation damage, micrometeorite impact and other factors. However, the actual power loss cannot be predicted exactly. The 15 percent allowance includes a safety margin, making it possible for the actual operating life of the satellite to extend beyond the two year design lifetime.

5.3 SYSTEM COMPONENTS

A block diagram of the power system, showing each of the individual components is shown in Figure 5.3. The function of each piece of equipment is described in the following sections.

5.3.1 Solar Panels

The primary power source for SCANNAR is a pair of solar panels which extend from the sides of the satellite. Each panel consists of two sections of honeycomb aluminum, measuring 2.5 ft by 4 ft by 1 in, on which the solar cells are mounted. The panels are supported by a two foot shaft connected to a brushless DC motor which rotates the panel and keeps it oriented toward the sun.

During the transfer phase, the panels are folded and held against the sides of the satellite. This configuration is shown in Figure 5.4. When they are folded, the cell side of the outboard sections, sections one and four, face outward. This allows them to supplement the power output of the body cells during transfer. When the satellite reaches its final position over the Atlantic, a command is sent to deploy the panels. They are released from the sides of the satellite and spring loaded hinges force them outward until locking pins engage and hold them in place. Sun sensors mounted on each shaft then allow the panels to orient themselves toward the sun, bringing the power available up to 280 watts. During the lifetime of the satellite, the panels will rotate once each day about an axis perpendicular to the plane of the satellite's orbit and remain pointed toward the sun. The final configuration is shown in Figure 5.5.

The solar cells used are 2 cm by 2 cm, N/P silicon cells with a base resistivity of 2 ohm-centimeters. Each cell is 0.014 in thick and has a 0.006 in red-blue coverglass with an antireflective coating. The coverglass extends the life of the cell and limits its operating temperature to a maximum of 115^{o}F by filtering out ultraviolet and infrared radiation.

Each cell produces 0.130 amperes at 0.41 volts in direct sunlight. Since all satellite equipment operates at 28 volts DC, 72 cells are connected in series strings to produce a nominal bus voltage of 28 volts. To produce

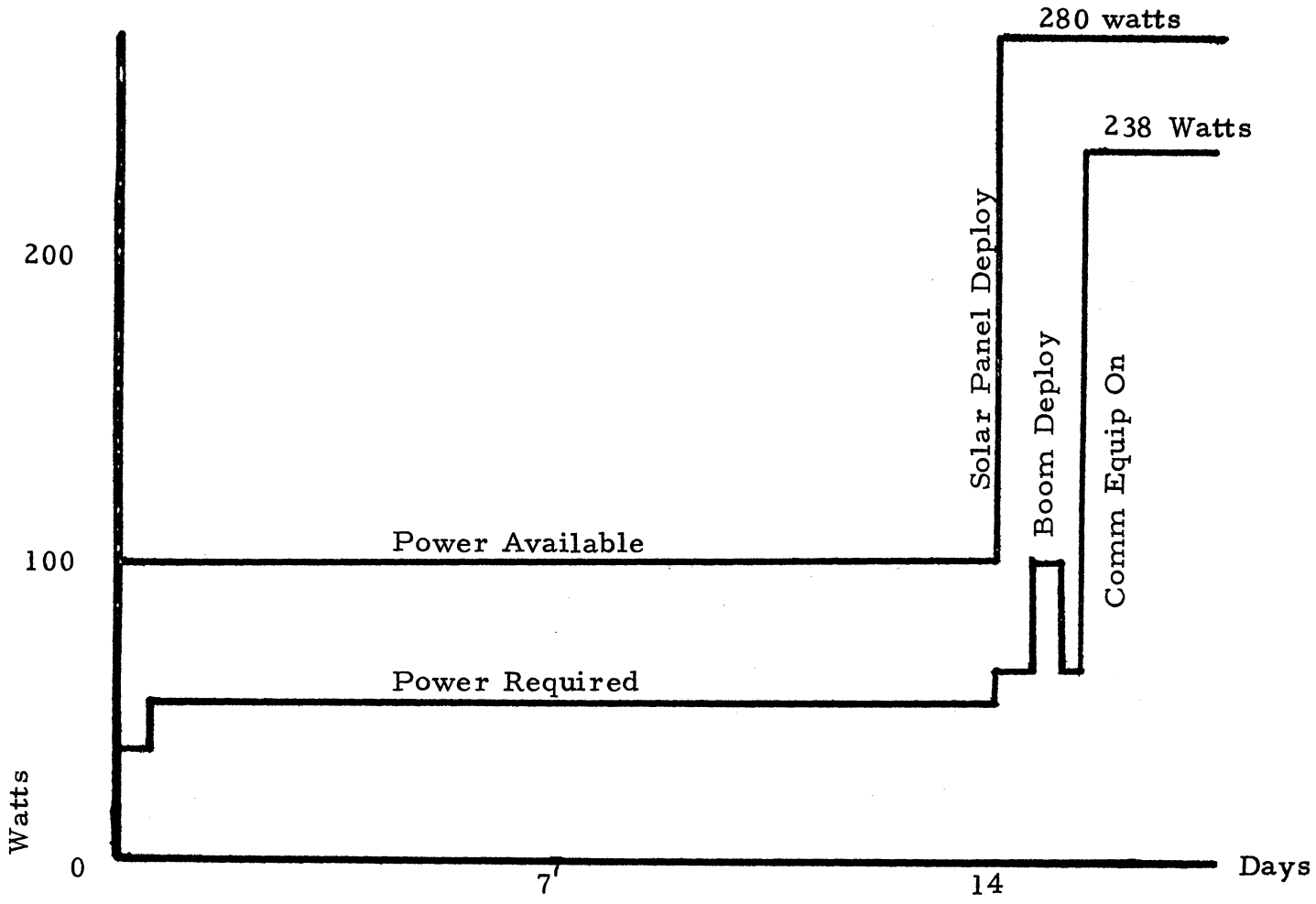

Figure 5.1 Power Profile: Launch and Transfer

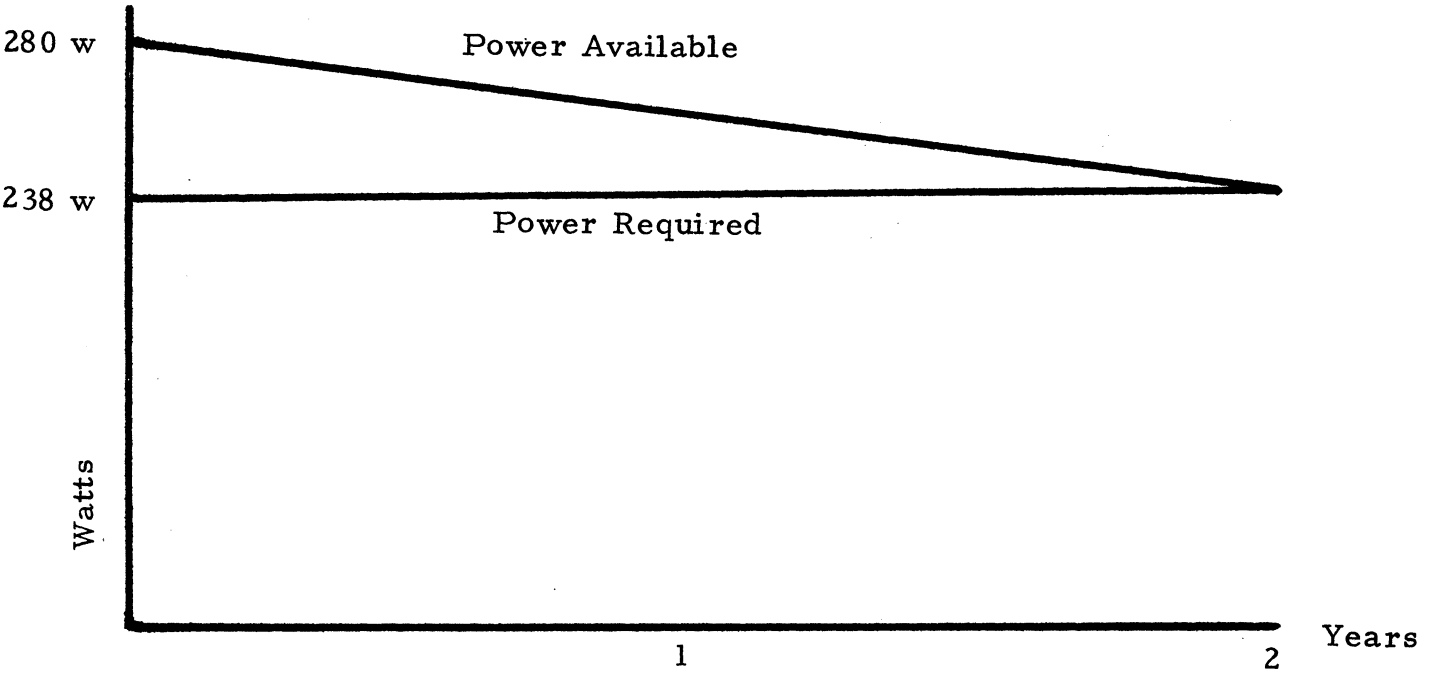

Figure 5.2 Power Profile: Orbit Phase

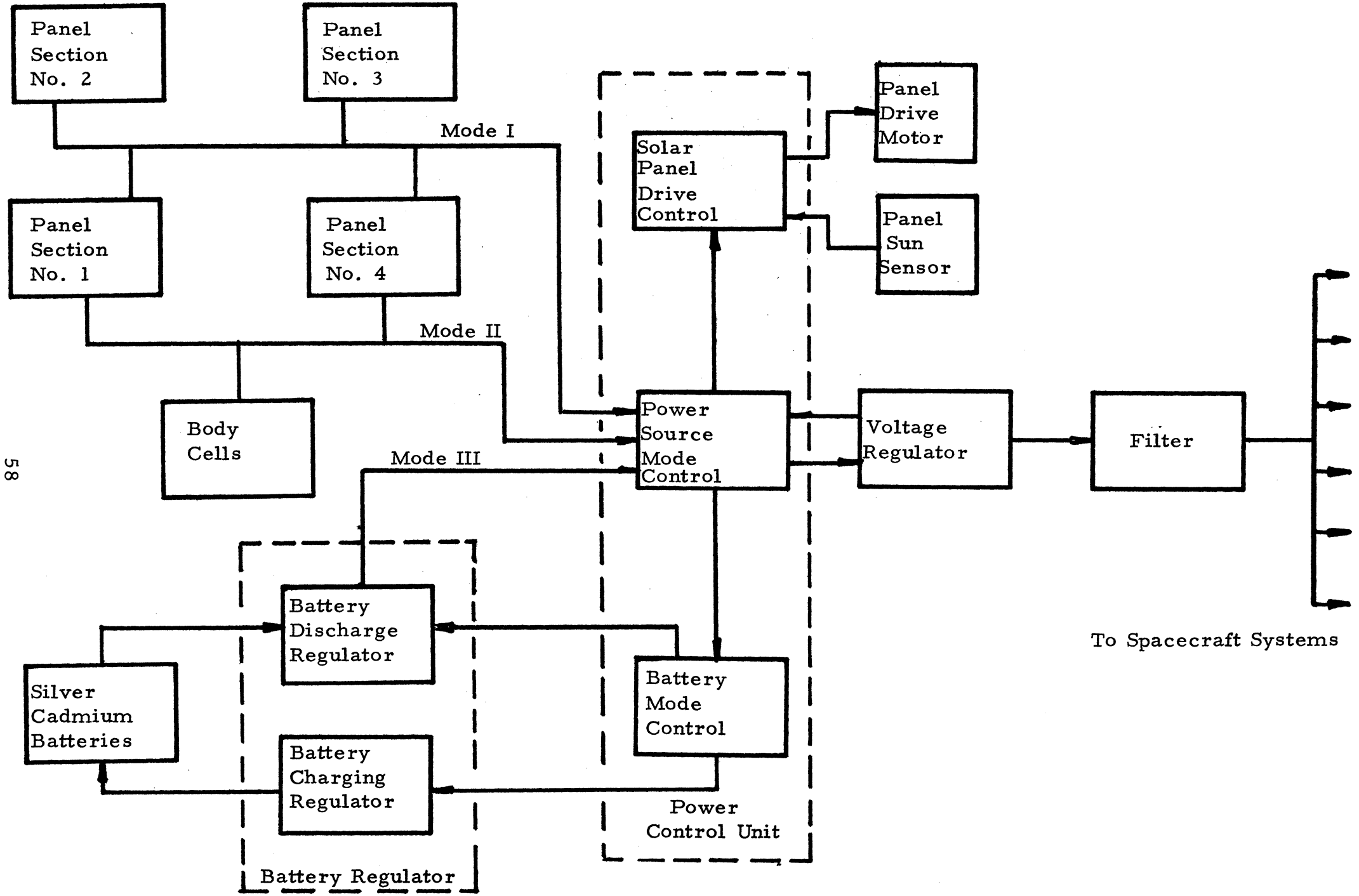

Figure 5.3 Power System Block Diagram

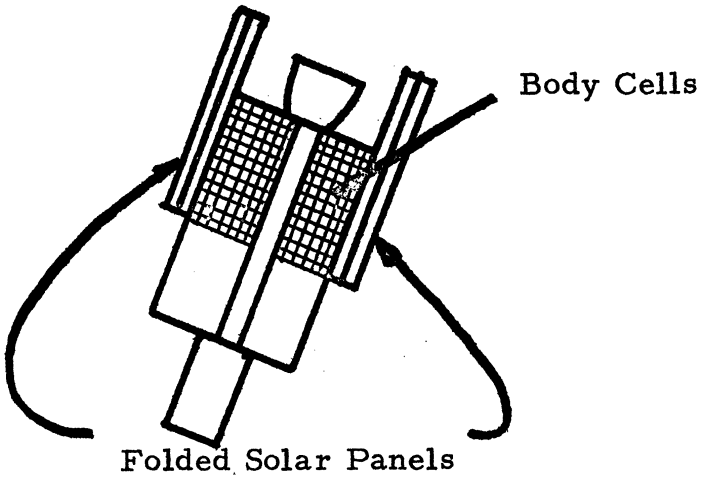

Figure 5.4 Solar Panels Folded

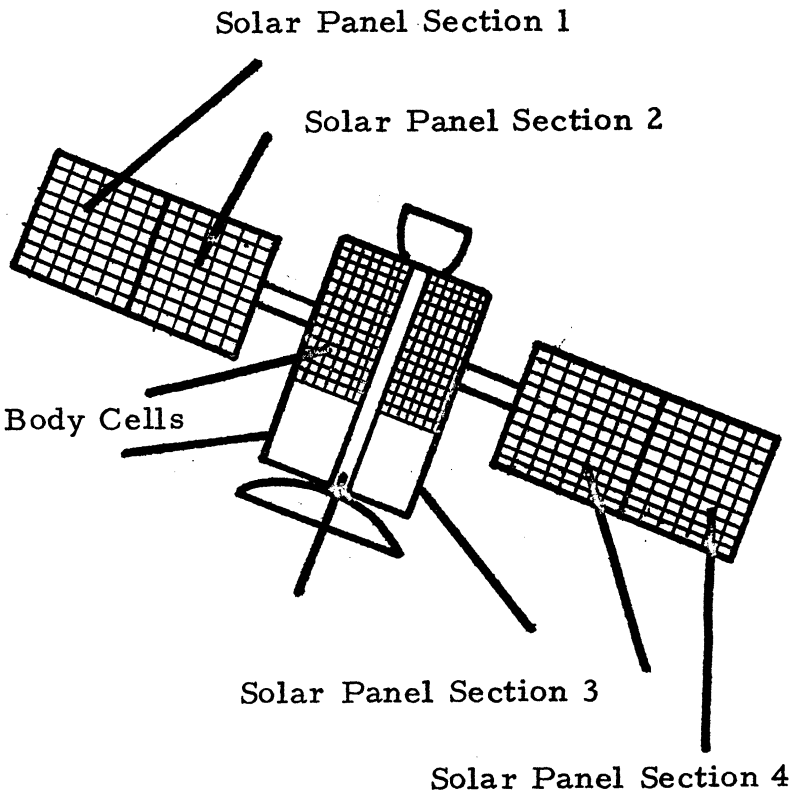

Figure 5.5 Solar Panels Deployed

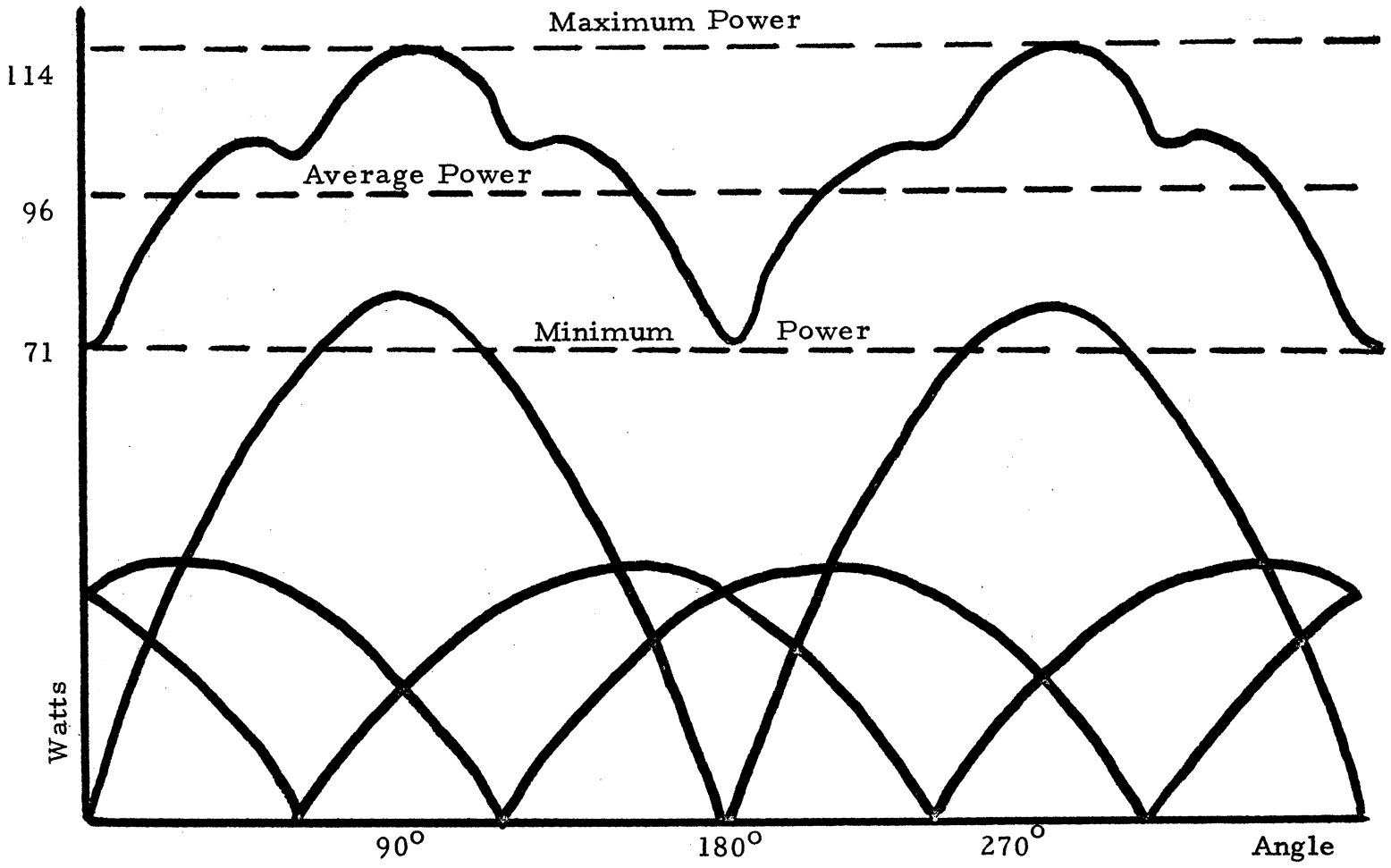

Figure 5.6 Power Available During Transfer

the required power, 112 of these strings are connected in parallel. A diode is wired in series with each string to prevent active cells from discharging into any cells which might be in shadow.

The solar cells are mounted on the panels in blocks of 7 cells by 36 cells. Each panel section contains eight of these blocks, or a total of 28 series strings.

The total number of solar cells on the two panels is 8064.

5.3.2 Body Cells

During the transfer phase, power is supplied by solar cells mounted on the body of the satellite and by the two exposed sections of the folded solar panels. The area of cells is distributed evenly around the surface of the satellite to minimize the effect of spacecraft attitude on the power output.

The body cells are arranged in four areas, each measuring 2 ft by 2.5 ft. These are located on the faces of the satellite not covered by the folded solar panels. A graph of the power available from the solar panel sections and the body cells as the satellite revolves around its z axis is shown in Figure 5.6. The angle of revolution is measured from the x axis. The power levels shown assume that the sun's rays are parallel to the satellite's x-y plane and that no cell degradation has yet occurred. The actual angle of incidence can be as high 30 degrees before the minimum power available equals the power requirement of 53 watts. This reduces the need for attitude control during the transfer phase. Once the satellite is at synchronous altitude, keeping it within this 30 degree limit will be sufficient to ensure full operation. The apogee motor and the communications antenna prevent placement of cells on the upper and lower surface of the satellite, but if angles of incidence of more than 30 degrees are required during orbital maneuvers, the batteries can supplement the solar cell power temporarily.

The body cells are identical to the cells used on the solar panels. Each of the four areas contains 14 strings of 72 cells, connected in the same series-parallel arrangment. The total number of body cells is 4032.

5.3.3 Batteries

A satellite operating at synchronous altitude goes into the earth's shadow 92 times per year with a maximum time in darkness of 1.2 hours. During these periods, the solar cells cannot operate and power must be supplied by batteries.

Three different types of batteries were considered for use on SCANNAR: nickel-cadmium, silver-cadmium and silver-zinc. Silver-zinc cells were

eliminated because of their low cycle life. Either nickel-cadmium or silver-cadmium cells could have been used, but silver-cadmium cells were chosen because of their lower weight.

The sizing of the battery system depends on several factors. The nominal operating voltage of silver-cadmium cells is 1.1 volts. Therefore, 26 cells are connected in series to produce the required 28 volts DC. A diode is wired in series with the negative lead of the battery system to prevent discharge into the solar cells during battery charging. During eclipse, the power requirement is 220 watts for 1.2 hours, or 264 watt-hours. Allowing for losses in power conditioning equipment, the maximum drain on the batteries will be 311 watt-hours. Cells with a capacity of 18 amp-hours, or 515 watt-hours at 28 volts, were chosen. This limits the maximum depth of discharge to about 60 percent, occurring only twice per year. With this depth of discharge, the cycle life of the batteries will be over 1500 cycles.

When the satellite is in sunlight, from 12 to 18 watts from the solar cells are used for battery charging. This is below the maximum charging current allowable but is high enough to allow the batteries to be completely recharged in the 23 hours between one eclipse period and the next.

5.3.4 Power Control Unit

During the four phases of the mission, the power system operates in three different modes. Mode I is used during the orbit phase. At this time, power comes from the solar panels. Mode II is used during transfer, drawing power from the body cells and two exposed panel sections. Mode III is used during launch and eclipse periods when power comes from batteries. The power control unit (PCU) is primarily a switching mechanism which monitors the power required and power available for all of the satellite systems and selects the power mode which is to be used.

The PCU performs several secondary functions. During Mode I and Mode II, the PCU supplies current to the battery charging regulator. During Mode III operation, the PCU selects the discharge function of the battery regulator and the batteries become the primary power source.

The power control unit also monitors the output of the sun sensors on the solar panel shafts. When these sensors indicate that the panel is no longer pointed toward the sun, the PCU delivers 6 watts to the drive motors which reposition the panels.

During any periods when the communications equipment is turned off, the power control unit supplies power to a shunt resistor to be dissipated as heat. This prevents the satellite temperature from dropping below its lower limit.

The final function of the PCU is fault sensing. The PCU monitors the operation of the battery regulator, the voltage regulator and the PCU itself. In the event of a malfunction in any of these units, it can switch to a back-up.

5.3.5 Battery Regulator

The battery regulator controls the charge-discharge operation of the battery system. The voltage of the batteries can vary from 1.05 to 1.5 volts per cell, depending on the level of discharge. The regulator acts as a transformer to adjust the voltage of the charging current to the proper level, from 28 to 40 volts for 26 cells. During discharge, it lowers the output voltage of the system to a nominal 28 volts.

5.3.6 Voltage Regulator

The voltage regulator is a transistor step-down circuit which accepts power from the solar cells and batteries and provides an output of 28 volts DC with a maximum variation of 0.05 volts. The efficiency of this unit is a function of the actual input voltage and should be above 85 percent for normal operating conditions.

5.3.7 Filter

To compensate for any variation in input voltage, the voltage regulator will generate a spike in its output voltage. Since this spike can affect the accuracy of the phase measuring equipment in the navigation system a filter has been included to minimize these effects. The filter attenuates any spike by a factor of ten to one, and improves the electromagnetic radiation characteristics of the power system, thereby decreasing interference with communication equipment.

5.4 SYSTEM RELIABILITY

All of the components of the power system have been used on satellites for many years and have proven to be very reliable. The use of back-up equipment and separate modes of operation also acts to improve the total system reliability.

The most critical failure in the power system would be failure of the solar panels to deploy properly. The squibs which release the panels are redundant so that proper operation of any one is sufficient to deploy the panels. The spring loaded hinges are simple mechanisms and present little chance for failure. If they did fail to unfold completely, there is sufficient fuel in the thruster system to allow the satellite to be spun about the z axis and centrifugal force used to pull them outward until they lock.

The use of series-parallel arrays in the solar cells provides a current path around any defective cell without significant loss of power. An independent orientation system for each panel minimizes the chance that both panels would be inoperable.

Back-up equipment for the power control unit, the battery regulator and the voltage regulator decreases the chance for failure in these areas.

The separate modes of operation would allow partial functioning of the satellite if any one of the power sources failed to operate. Only complete failure of both primary and back-up equipment, or a combination of failures would result in a total loss of power. The probability of this occurring does not justify the weight of additional back-up equipment.

In all design analysis, conservative estimates of cell degradiation, converter efficiencies, etc., were used. The actual operating life of the power system could continue beyond the two year design lifetime with full operation, and much longer with partial satellite operation.

REFERENCES

Gibson, R., "Design Data for Space Power Systems," The Bendix Corporation, Aerospace Systems Division, February 16, 1970.

Szego, G.C. and Taylor, J.E., Space Power Systems Engineering, Progress in Astronautics and Aeronautics, Volume 16, 1966.

Abbott Power Supply Catalog, 1970, Abbott Transistor Laboratories Inc.

"Space Power Systems Advanced Technology Conference" NASA Report SP-131, 1966.

Corliss, William R., Scientific Satellites, NASA Report SP-133, 1967.

Yardney Silcad Cell Data, Yardney Electric Corporation, 1966.

6
THERMAL CONTROL

6.1 INTRODUCTION

The purpose of thermal control is to provide an environment for the efficient operation of all temperature dependent components in the satellite. This can be accomplished by either an active or a passive system. A passive system was chosen for its reliability and simplicity.

SCANNAR's equipment provides constant internal heat and therefore the internal temperature of the satellite will not change radically during the mission. However, in synchronous orbit, there are variations in the amount of solar input to the satellite for the duration of the mission. SCANNAR will have eclipse periods of 44 days centered about each equinox. The internal temperature of the satellite must be controlled during these eclipses, the longest being a period of 1.2 hours.

Generally, several components have a restrictive temperature operating range or a high heat output. These factors are critical in determining the control system and the placement of components. In SCANNAR, the voice package and the voltage regulator both have high heat outputs, while the batteries have a restrictive temperature range ($14^{\circ}F$-$104^{\circ}F$). These components therefore, will determine, to a large extent, the thermal control system used.

6.2 SYSTEM DESCRIPTION

As are most thermal control systems SCANNAR's is based on a basic heat balance equation:

$$q_{in} = q_{out}$$

The internal heat of the spacecraft is composed of power dissipations from the components and input of solar radiation in areas which are not insulated. This total heat must then be conducted to an area which can radiate it back to space. This area will consist of two surfaces, on opposite sides of the spacecraft, which are free from insulation, but controlled to a certain degree by a specified thermal coating.

SCANNAR's internal power dissipation is relatively high and constant. Therefore, the radiating areas will be an efficient heat sink. They are designed to minimize the variation of solar input and in this way q_{in} will be kept in a range allowing their temperatures and the temperatures of the components to vary only slightly.

Scale: 1 1/2" = 1'

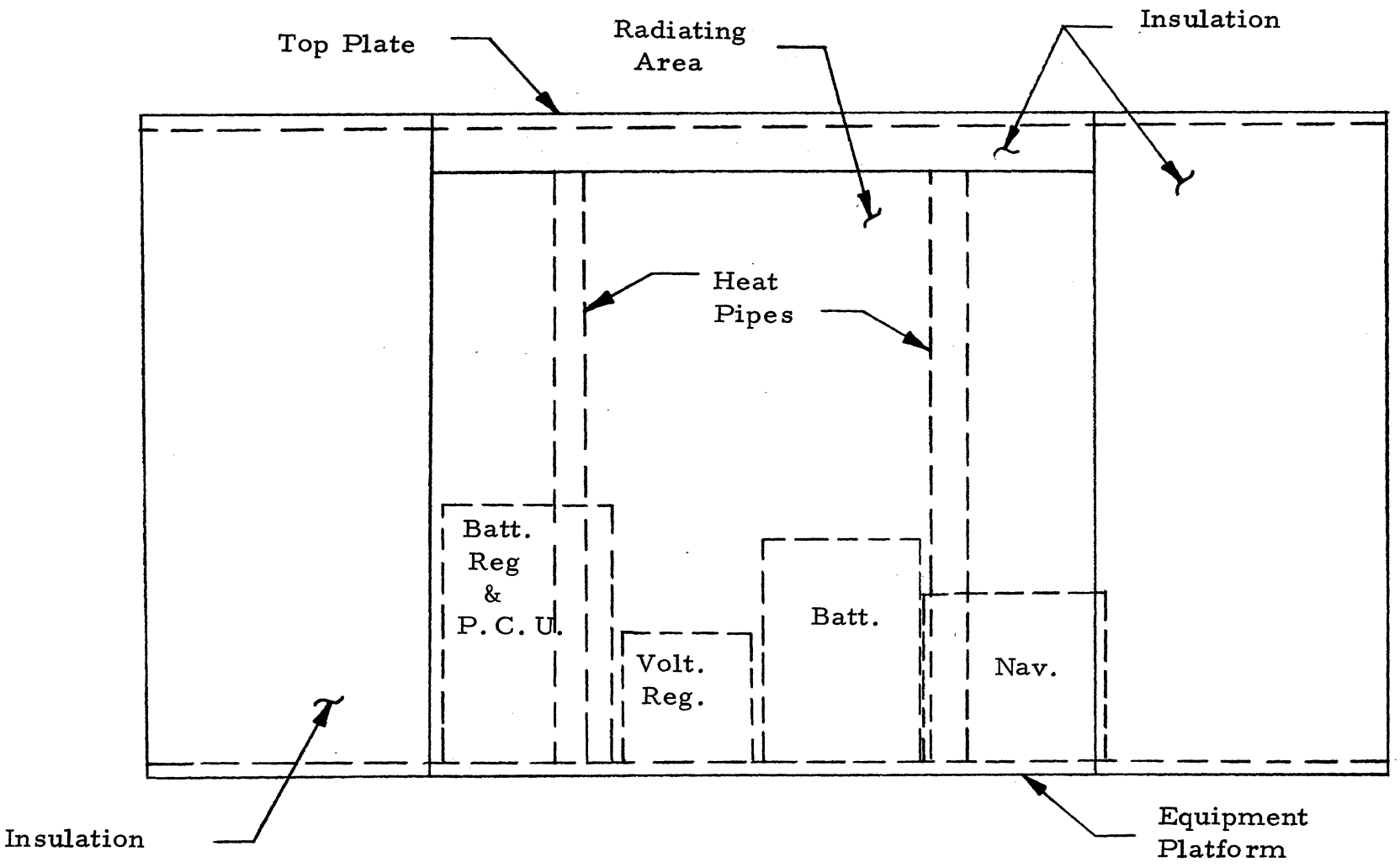

Figure 6.1 Radiating Area I (see Figure 7.5)

Since the most important requirement of thermal control is to keep the components at a temperature within their operating range, and since the system we have designed is passive, the placement of the component packages, relative to the radiating areas, is quite important. The role that these locations play in the temperature range of the components can be seen in Appendix E.3. The individual placements can be seen in Figure 7.5.

Table 6.1 shows the thermal specifications for the components of SCANNAR and the design range they will experience.

Table 6.1 Thermal Specifications

Component	Operating Range (^{o}F)	Design Range (^{o}F)
Voice Comm.	32^{o} to 160^{o}	85^{o} to 113^{o}
Tracking Command, Telemetry	32^{o} to 160^{o}	70^{o} to 98^{o}
Navigation	32^{o} to 160^{o}	67^{o} to 95^{o}
Voltage Reg.	-65^{o} to 212^{o}	30^{o} to 127^{o}
Batteries	14^{o} to 104^{o}	21^{o} to 88^{o}
Battery Reg. & Power Cont.	-65^{o} to 212^{o}	76^{o} to 104^{o}
Computer	-30^{o} to 230^{o}	123^{o} to 151^{o}
Sensor Elect.	-30^{o} to 230^{o}	45^{o} to 138^{o}
Fuel Tanks	35^{o} to 237^{o}	40^{o} to 160^{o}

Since SCANNAR is an experimental satellite, there may be instances when all the packages on the equipment platform are not operating. At this time, the voltage regulator will transfer power through shunts near the components, to be dissipated as heat in the satellite. This will maintain suitable component temperatures.

6.3 THERMAL COMPONENTS

6.3.1 Radiators

The radiating surfaces will be the heat sink mechanism by which q_{int} will be radiated to space. There are two radiating surfaces, located

on faces which never see direct sunlight after the satellite is on station. This surface is conductively connected at one edge to the equipment platform (see Figure 6.1).

Each radiating surface is 2.5 ft x 2.34 ft and will always have a temperature between $4^{o}F$ and $32^{o}F$, depending upon its position with respect to the sun. The surface is made of 0.25 in thick aluminum honeycomb between 2 aluminum sheets, each 0.048 in thick.

6.3.2 Thermal Coatings

Thermal coatings are used to control the solar energy abosrbed and the infrared energy emitted.

The radiating surface will be coated with S-13G, a white organic stable paint, (α = 0.20, ϵ = 0.90), to minimize solar input to the satellite and to maximize radiation from the satellite to space.

The solar panels and body cells have a blue-red cover glass with α/ϵ = 0.70/0.84. The back side of the solar panels will be painted with S-13G paint.

The booms will be coated with a metalized film. This film is made of silver and 0.008 in quartz with the quartz on the outside. It has an α/ϵ = 0.1/0.8. This will minimize thermal boom deflections to less than 1 ft (see Appendix E.4).

6.3.3 Insulation

Insulation is used to minimize thermal conduction. All internal surfaces of SCANNAR which are not radiating surfaces will be insulated to minimize solar input and heat radiation from those surfaces. Forty layers of Al/$\frac{1}{4}$ mil Mylar at sixty layers per inch will be used.

In addition, the booms must be isolated from the body of the satellite to minimize thermal deflection. This is done by insulating the boom package.

Special consideration must be given to insulating the apogee motor and the support tube from the equipment platform and body of the satellite.

6.3.4 Heat Pipes

Heat pipes are needed on the radiating surface to dissipate heat from the equipment platform over the whole radiating area. The heat pipe is a closed, evacuated chamber, whose inner surfaces are lined with a capillary wicking structure that is saturated with a volatile liquid. Heat, upon entering one area of the heat pipe, causes the fluid in that area to evaporate.

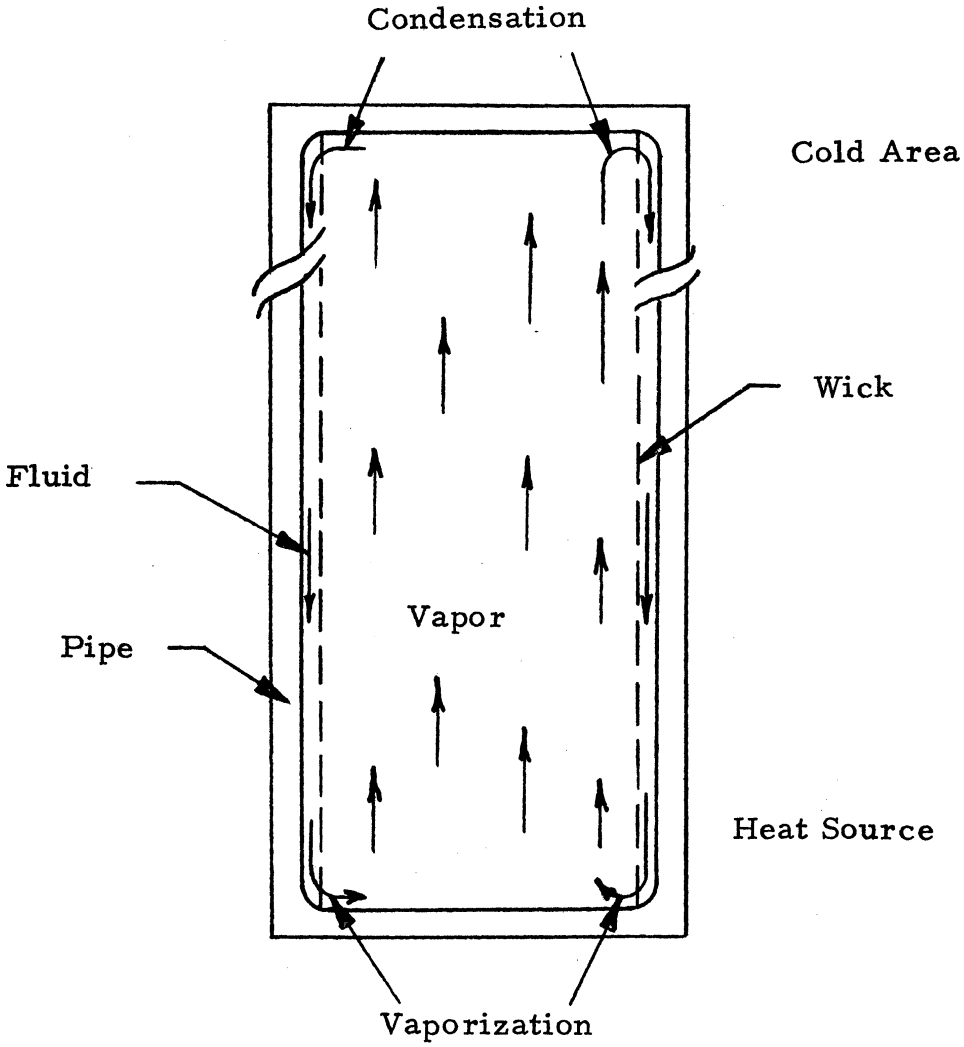

Figure 6.2 Heat Pipe

The vapor traverses the chamber and condenses at cool areas, giving up its large heat of vaporization. The fluid is then drawn back to the evaporator sections by capillary forces in the wick structure (see Figure 6.2).

The source and sink temperatures, as well as the amount of heat to be transferred, determine the choice of heat pipe working fluid, wick geometry, pipe diameter, wick pore size, etc.

Heat pipes in SCANNAR will be mounted perpendicular to the equipment platform on the radiating surfaces. There are two 2.34 ft long heat pipes per radiating surface (see Figure 6.1).

6.4 THERMAL COMPONENT WEIGHTS

Component	Weight
Insulation	2.9 lbs
Heat Pipes	3.3 lbs
Total	6.2 lbs

REFERENCES

Krieth, Frank, Radiation Heat Transfer for Spacecraft and Solar Power Plant Design, Scranton, Pa: International Textbook Company, 1962.

Project LINUS, University of Michigan design project, December 1969.

Westinghouse Heat Pipes, No. WANL-MP-051, Westinghouse Electric Corporation Astronuclear Lab, Pittsburgh, Pa.

API Thermal Control Systems Standardization Study, No. ETM-038, Bendix Aerospace Systems Division, Ann Arbor, Michigan, Dec. 11, 1967.

Bannister, Tommy C., and Eby, Robert J., Pegasus Thermal Design, NASA Report No. TN D-3625, November 1966.

7
STRUCTURES

7.1 INTRODUCTION

The SCANNAR structure was designed to adequately support and protect satellite components in prelaunch, launch, and orbital environments.

Equipment was placed to satisfy weight and inertia requirements, with special consideration given to the placement of sensors and antennas to provide them with unobstructed "windows". Critical for accurate angle measurements were the torsional and flexural stiffness of the interferometric antenna booms. Electronic equipment required thermal control which necessitated outer walls for insulating the satellite from solar heat as well as providing radiating areas to dissipate the satellite's internal heat. The need for reliability dictated that a minimum of moving parts be used, and that all mechanical systems be as simple as possible. Overall constraints of light weight and ease of fabrication also had to be considered.

Aluminum alloys were chosen for structural members because of their low weight and high strength. Aluminum honeycomb was used for panels and platforms for similar reasons. Mechanical fittings and connections were used throughout to allow easy access to the satellite interior prior to launch, and to avoid the difficulties of welding heat treated aluminum alloys.

The launch subjects the satellite to its severest loadings and thus sizes the structural members. It further specifies that all members of the satellite have fundamental frequencies higher than 40 cps axially and 25 cps laterally. The center of mass must be within 0.015 inches of the axis passing through the attach fitting center and one of the satellite's principal axes of inertia must allign with this centerline to within 0.002 radians. The SCANNAR structure is designed to meet these restrictions.

The structural components are described separately in sections 7.2 to 7.12; their location is shown in Figure 7.1.

7.2 SUPPORT TUBE

The support tube is the main structural member of the satellite. It is the primary means by which loads are transferred from the satellite components to the booster interface. The equipment platform, antenna platform, and cover plate are all connected to the tube which is in turn connected to the apogee motor mounting ring with six thermal insulating fixtures. The tube is made of 7075-T6 aluminum and is 50 in long, 22 in in diameter, and 0.030 in thick.

7.3 STRUTS AND PINS

Tubular struts are used to support the equipment and antenna platforms. The top of each strut is connected to the support tube with a bolt on fitting. Connections are made at the platform with bolts and an annular ring 0.05 in thick to distribute the loadings. Six struts are used with each platform. The struts are pinned at their midpoints to the support tube to increase their fundamental frequencies to acceptable levels. They are made of 7075-T6 aluminum. Their dimensions are given in Section 7.13.

7.4 EQUIPMENT PLATFORM

The equipment platform is the mounting surface for all electronic equipment as well as the two hydrazine tanks. The platform is attached to the support tube with struts and a mounting bracket. Individual components are fastened to the platform using plastic filler inserts installed with any of several patented tools. The platform is made of 0.5 in honeycomb with 0.040 in facings. The facings are heavier than necessary for structural support to give the necessary heat conduction properties. The facings are bonded to the honeycomb with thermally conductive adhesive. At the ends of the platform the facings are closed using a strip of perforated fiberglass. The shape of the platform was chosen to accommodate the solar panels in the launch configuration.

7.5 ANTENNA PLATFORM

The antenna platform is essentially the same as the equipment platform, except that the facings are 0.020 in thick and thermally insulating adhesive is used to bond the facings to the honeycomb core. The four boom mechanisms are mounted to the platform on insulating pads to reduce heat transfer. Six struts and a mounting bracket attach it to the support tube.

7.6 COVER PLATE

The cover plate is 0.020 in aluminum and is used for adding support to the side panels and as a mounting surface for the communication antenna and planar scanner. It is connected to the support tube with a mounting bracket and bolted to the stringers at its outer edges. Provision is made in its mounting bracket for fastening ground handling tools.

7.7 MOUNTING BRACKETS

Mounting brackets are used to fasten the platforms and cover plate to the support tube. They are 1.5 in by 1.5 in right angle sections 0.10 in thick, and are fastened to the support tube with rivets.

7.8 SIDE PANELS

The side panels serve as mounting surfaces for solar cells, thermal insulation, and thrusters. Two panels are used as radiating surfaces for thermal control. All are constructed of 0.25 in perforated aluminum honeycomb. The non-radiating surfaces have 0.016 in facings bonded with thermally insulating adhesive to the honeycomb core, while the radiating panels have 0.048 in facings bonded with thermally conductive adhesive. The panels are bolted to the stringers.

7.9 STRINGERS

Stringers are conventional aluminum extruded channels running from the equipment platform to the cover plate. They provide mounting surfaces for the side panels and transfer the axial loads on the panels to the antenna and equipment platforms. The stringers are connected to the platforms with blind rivets and to the cover plate with bolts.

7.10 LAUNCH RING

The launch ring provides the interface between the satellite and the booster third stage. It is connected to the apogee motor mounting ring and the attach fitting is clamped on at its opposite end. It is machined from 7075-T6 aluminum and tapers in diameter from 21 in to 18 in with a thickness of 0.035 in and a length of 15 in.

7.11 SOLAR PANEL MECHANISMS

The solar panels are supported by spring loaded hinged rods. During launch the panels are fastened to the satellite side panels with squibs. The ends of the supporting rods are attached to brushless DC motor driving mechanisms which are bolted directly to the support tube.

7.12 BOOM MECHANISMS

Forty-five ft deployable booms were used to place the interferometric antennas at the large separation needed for accurate angle measurements. Such booms have proven quite reliable. They consist of flat tapes stored on motor driven drums that form a cylindrical shape when unrolled. Our design constraints limited torsional and flexural deflections to $\pm 2^{o}$. These constraints were met using a stainless steel interlocking boom with a 1.5 in diameter. Thermal deflections were reduced by using thermal coatings on the booms and small, 0.05 lb, thrusters were employed to minimize deflections arising from satellite dynamics. The boom mechanisms were bolted to the antenna platform to give the necessary 15^{o} down angle. The cabling from the antennas to the satellite body is an integral part of the boom and is supplied by the manufacturer. The boom deflection calculations are found in Appendix F.3.

7.13 PARTS SPECIFICATION

Item	Number	Total Weight	Material
Support tube	1	7.04	7075-T6 aluminum
Struts			
Ant. platform	6	2.56	7075-T6 alum. 1.5" dia. 0.050" thick, 16" long
Equipment platform	6	6.54	7075-T6 alum. 1.5" dia. 0.10" thick, 16 " long
Pins	12	1.4	2014 alum. 6" long
Cover plate	1	4.42	7075-T6 alum. 0.020"thick
Antenna platform	1	9.82	Honeycomb sandwich Core: 0.5" 5052-H39 alum 0.1875" hex cells 0.001" wall thickness. Facings: 0.020" 7075-T6 aluminum
Equipment platform	1	18.81	Same as ant. platform except facings 0.040" 7075-T6 aluminum
Mounting brackets	3	2.3	2014-T6 alum. 0.10"thick
Side panels			
Radiating sides	2	11.7	Honeycomb sandwich Core: 0.25" 5052-H39 alum. 0.1875" hex cells 0.001" thick wall Facings: 0.048" 7075-T6 aluminum
Non-radiating sides	6	6.8	Same as radiating sides except facings are 0.016" 7075-T6 aluminum
Stringers	14	3.9	2014-T6 aluminum
Booms and boom mechanisms	4	28.8	301 stainless steel
Annular rings	2	1.2	2014-T6 aluminum
Launch ring	1	8.6	7075-T6 aluminum
Hardware		6	
Total Weight		119.89 lbs	

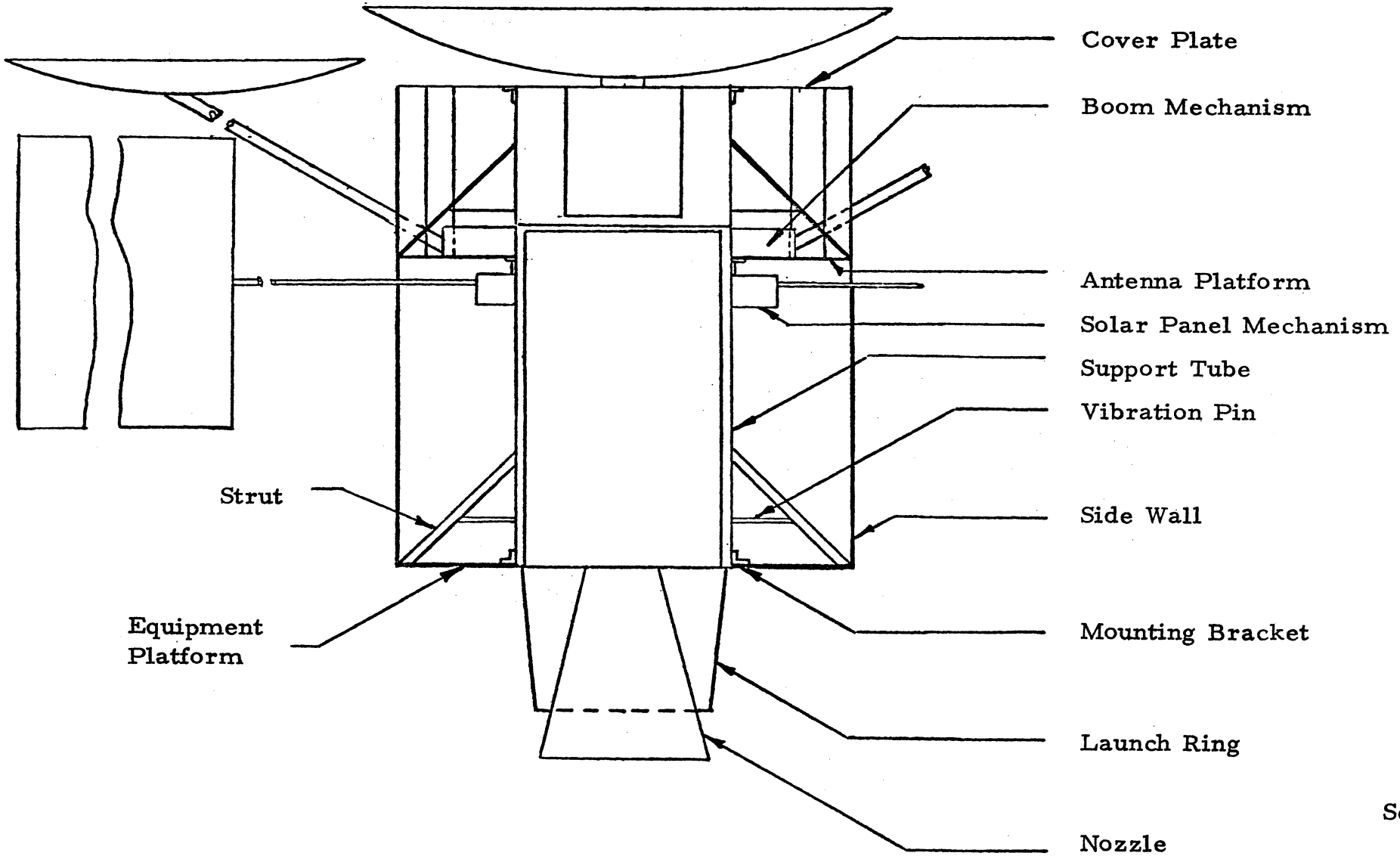

Figure 7.1 Structural Cross Section

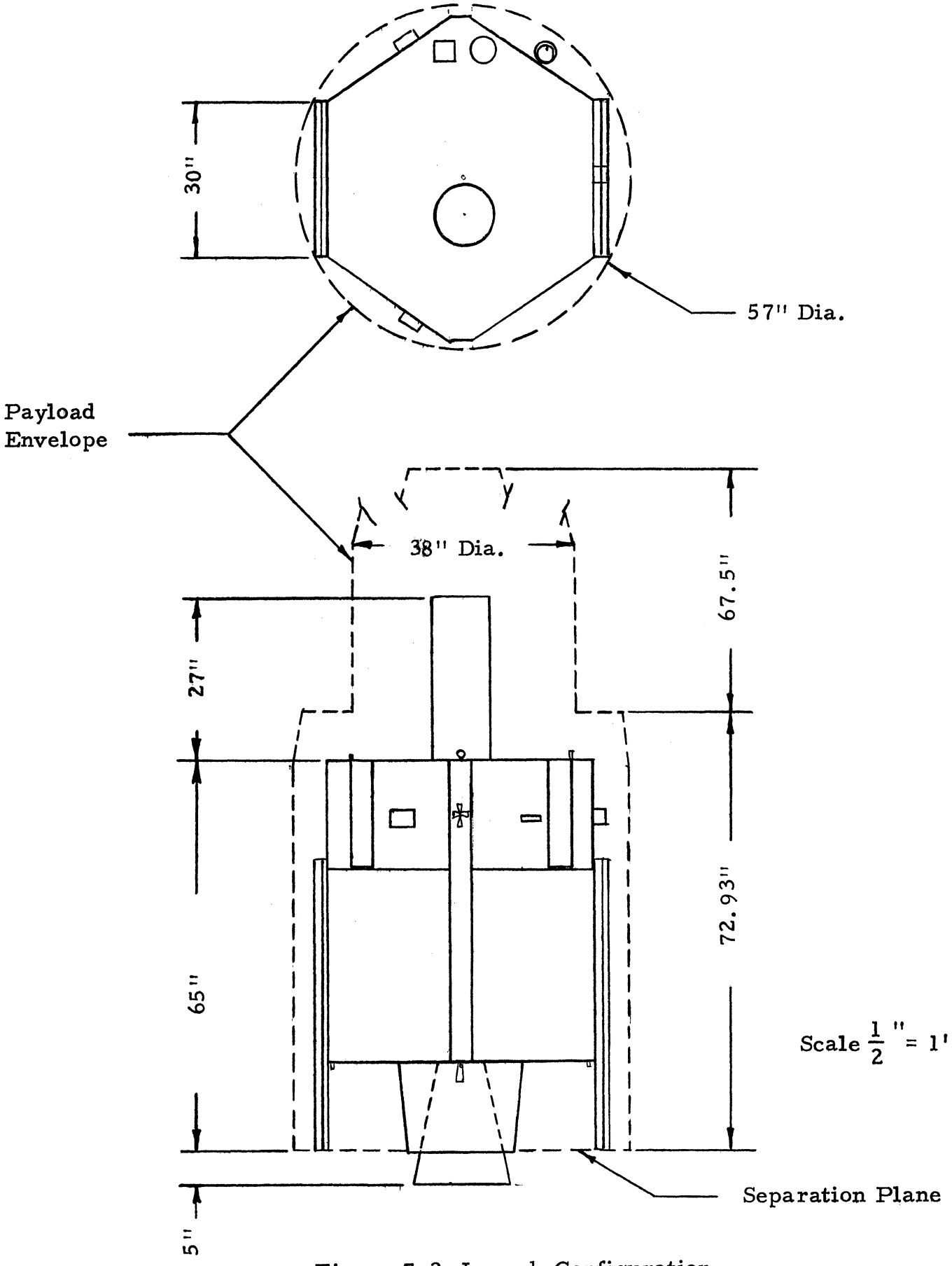

Figure 7.2 Launch Configuration

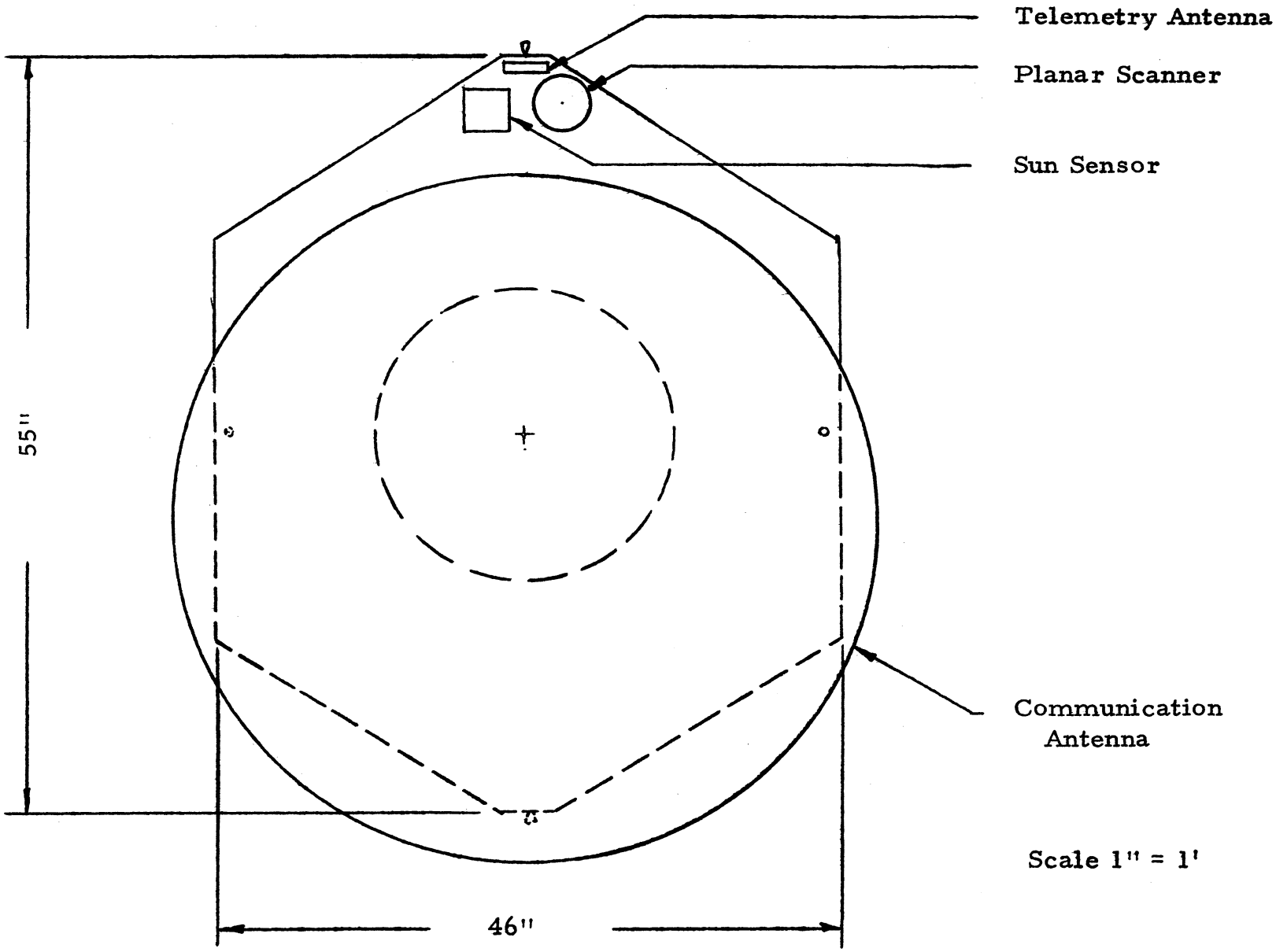

Figure 7.3 Cover Plate Detail

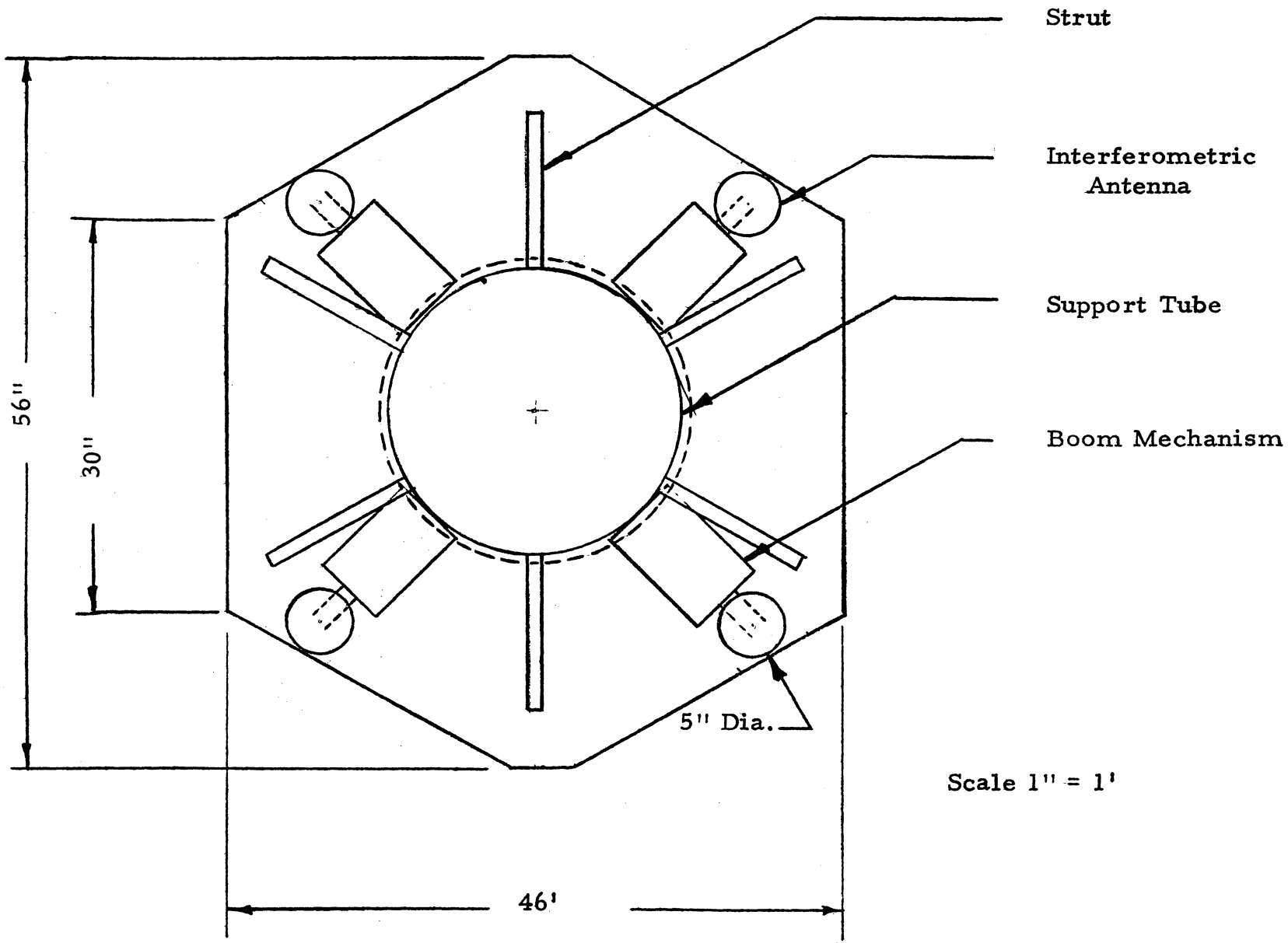

Figure 7.4 Antenna Platform Detail

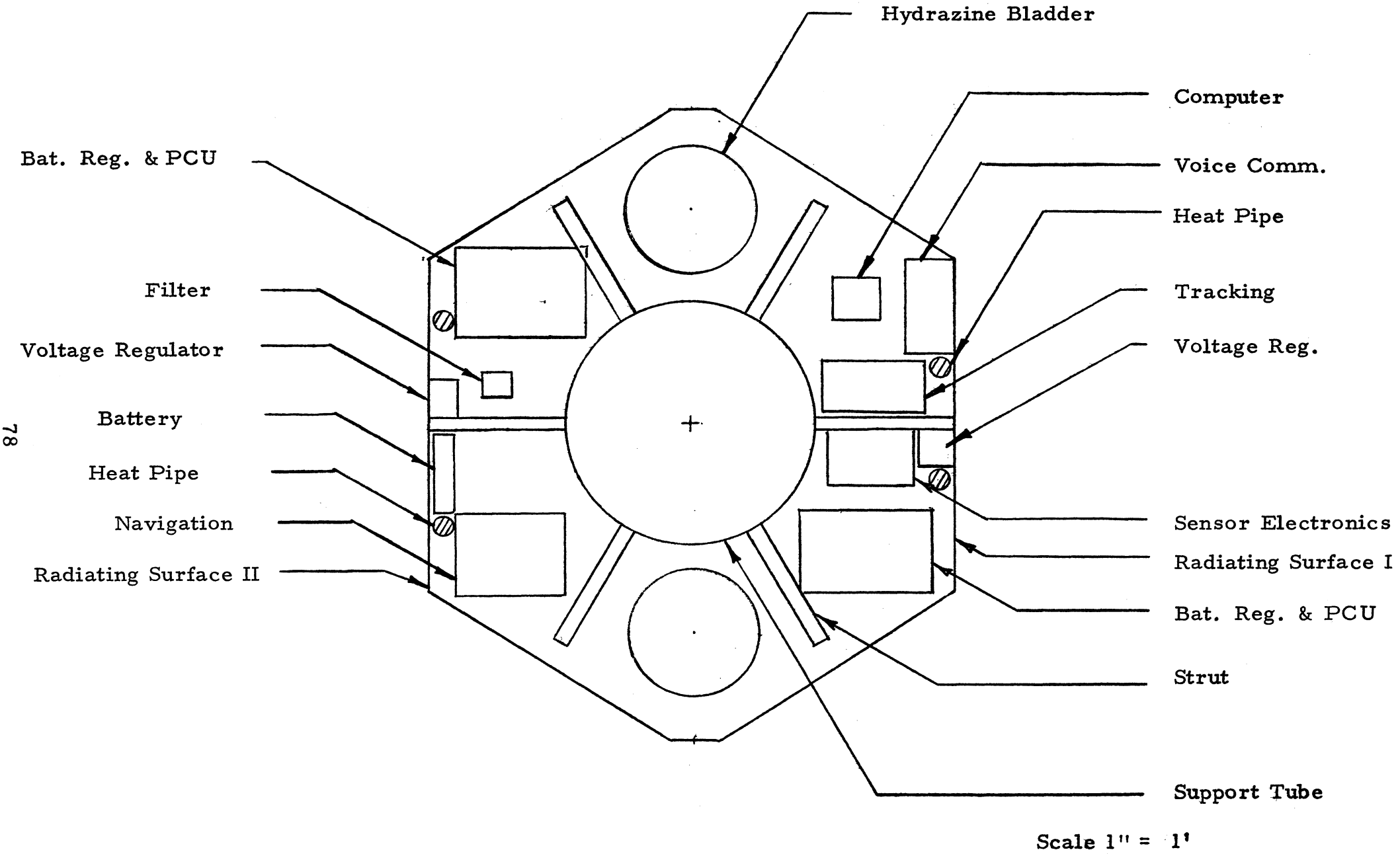

Figure 7.5 Equipment Platform Detail

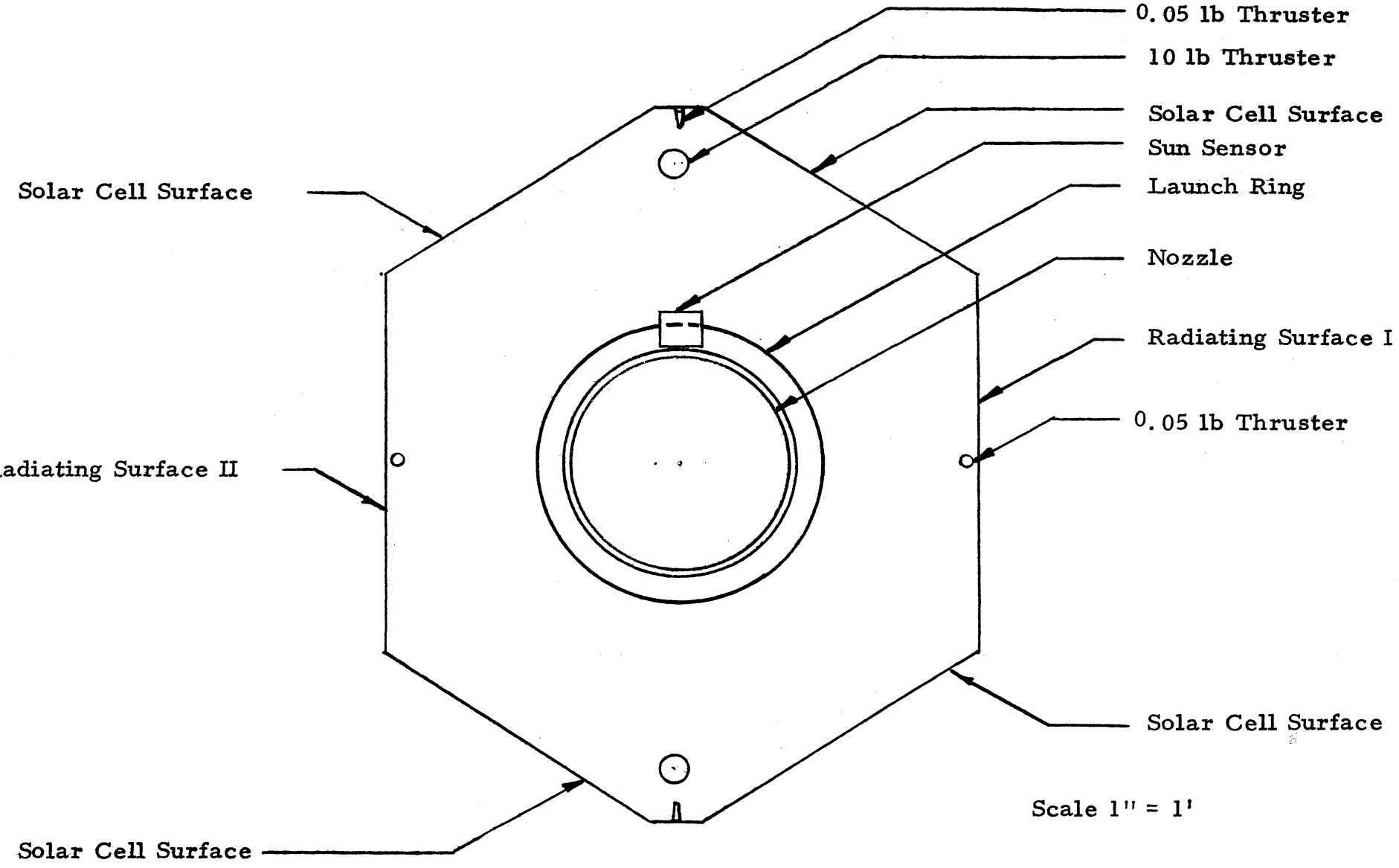

Figure 7.6 Bottom Detail

Table 7.1

	Launch	After Apogee Burn	On Station
D_{cm} in	11	15	41
I_{xx} slug-ft^2	44.0	39.8	923
I_{yy} slug-ft^2	41.5	34.6	840
I_{zz} slug-ft^2	31.4	27.0	1250
Wt lbs	1054	534	521

D_{cm} is the distance from the bottom of the equipment platform to the center of mass. The center of mass always lies along the satellite centerline.

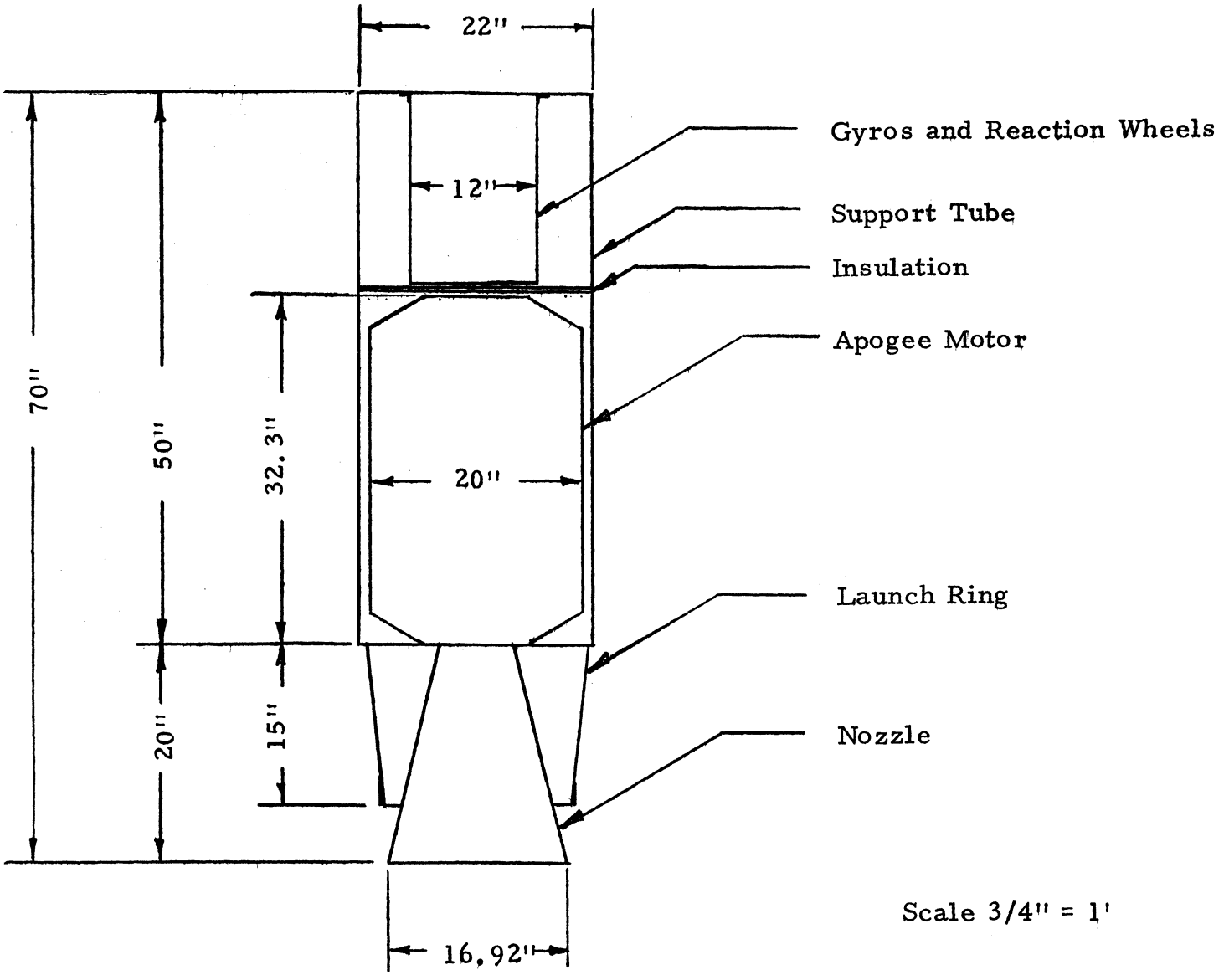

Figure 7.7 Support Tube Detail

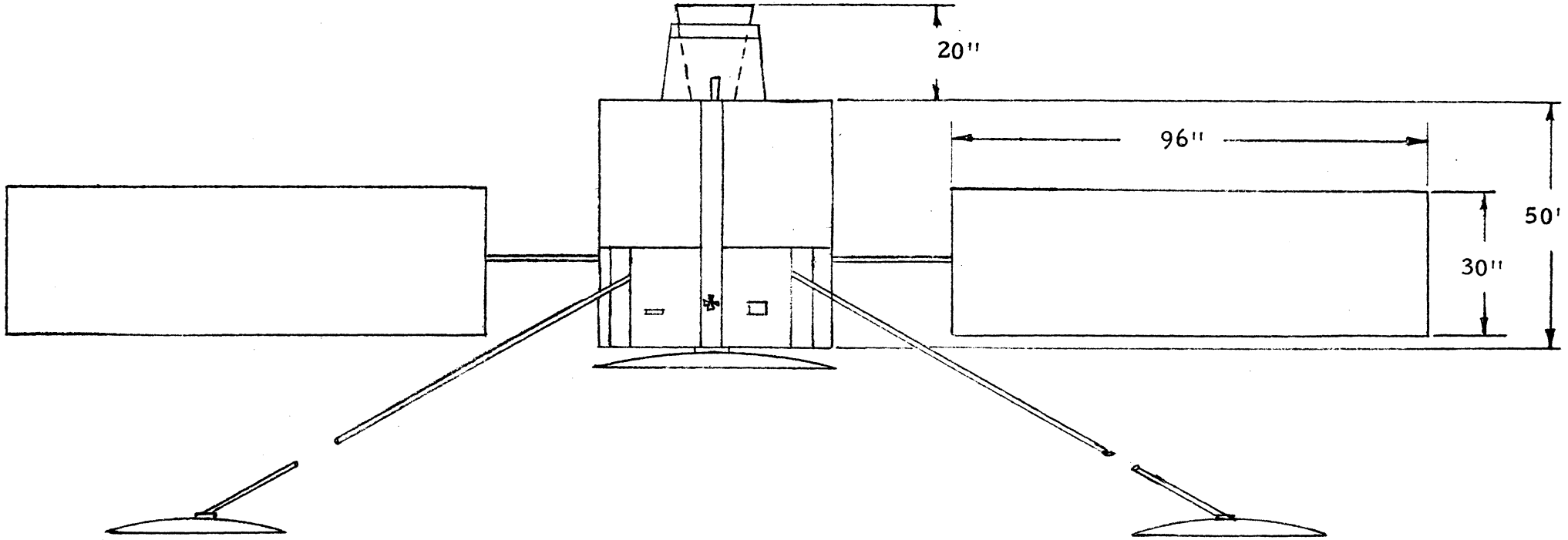

Scale 3/8" = 1'

Figure 7.8 Front View On-Station Configuration

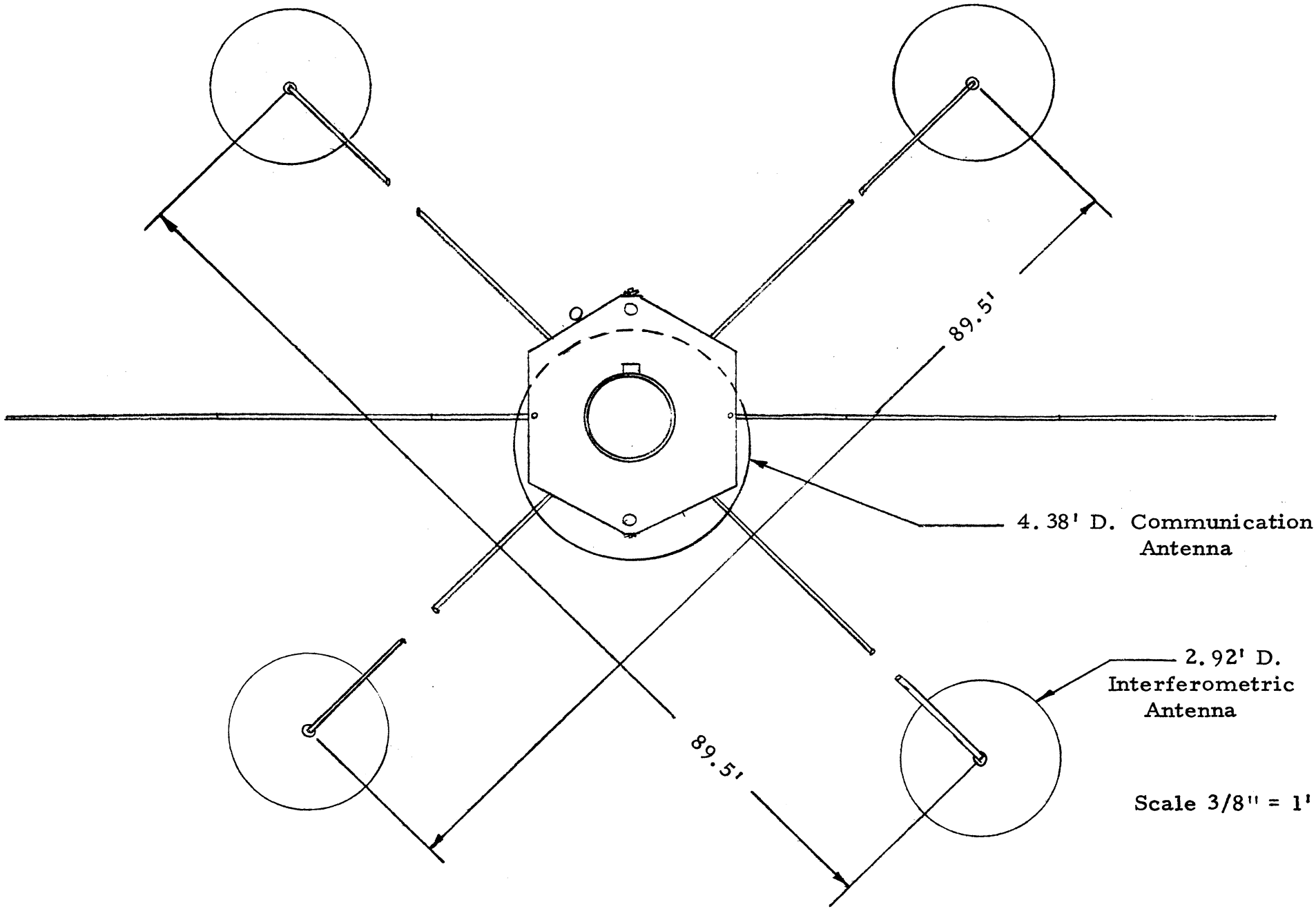

Figure 7.9 Top View On-Station Configuration

7.14 EQUIPMENT PLACEMENT

Once all satellite components were identified they had to be assembled and placed to satisfy launch vehicle restrictions on center of mass and moment of inertia locations. Compatability and packing limitations in the shroud further restricted the design. The apogee motor set the minimum length of the satellite, and the position gyroscopes and reaction wheels had to be placed along its centerline to lie along the principal moments of inertia. The down angle of the antenna booms necessary to reduce interference of the antenna lobes and satellite body made it difficult to keep the center of mass within the satellite body and resulted in an offset between the center of mass and the center of pressure. Thermal considerations played the most significant role in positioning components on the equipment platform. Tradeoffs between various demands resulted in the final SCANNAR configuration.

Table 7.1 shows moments of inertia, center of mass location, and system weight for various configurations. Figure 7.2 shows the satellite within the shroud for launch, while Figures 7.8 and 7.9 show the on station configuration. Figures 7.3, 7.4, 7.5, and 7.6 give details of the cover plate, antenna platform, equipment platform, and equipment platform bottom, respectively. Figure 7.7 shows component placement within the support tube.

REFERENCES

7.1 Timoshenko and Gere, Theory of Elastic Stability, New York, McGraw-Hill, 1966.

7.2 STEM, a profile, Spar Aerospace Products Limited, Toronto, Ontario.

7.3 Crandall and Dahl, Introduction to the Mechanics of Solids, New York, McGraw-Hill, 1959.

7.4 Navigation Satellite System, Westinghouse Electric Corp., Baltimore, Maryland, 1964.

8
LAUNCH VEHICLE

8.1 INTRODUCTION

In choosing a launch vehicle, three basic considerations were taken into account: 1) capability, 2) reliability, and 3) cost effectiveness. A vehicle is needed capable of putting a 1054 lb useful payload into earth synchronous orbit. This requirement rules out the Scout family of vehicles as too weak and makes the Atlas family of vehicles too powerful for our payload. The new Douglas Spacecraft Vehicle DSV-603, with 6 solid strap-on engines (Castor II's), incorporating the TE 364-3 solid fuel third stage, and having a maximum useful payload of 1200 lbs for the transfer orbit inclination of 27.84^{o}, meets the SCANNAR capability requirement (see Figure 8.1 and Reference 8.1).

The Delta family of vehicles is very reliable, as their history indicates. They have successfully orbited 59 of 63 mission payloads from 1960 through December 1968. Cost effectiveness for the Delta vehicles is good as a direct result of the vehicles' low launch costs and their inherent reliability. With all the above taken into consideration, the choice for the launch vehicle is the DSV-603 as described.

8.2 LAUNCH SITE

SCANNAR will be launched due east from the Eastern Test Range (ETR).

8.3 LAUNCH VEHICLE WEIGHTS

First Stage	
Lift-off	214,938 lbs
Main Engine Cut-off (MECO)	10,082.4 lbs
Vernier Engine Cut-off (VECO)	9,980.4 lbs
Second Stage	
Ignition	12,519.1 lbs
Cutoff	1,661.1 lbs
Third Stage	
Ignition	1,749.5 lbs
Burnout	122.4 lbs

8.4 LAUNCH SEQUENCE

Because the launch sequence for the vehicle configuration with 6 Castor II's was not available, the sequence for the 9 Castor II's configuration is presented for this mission.

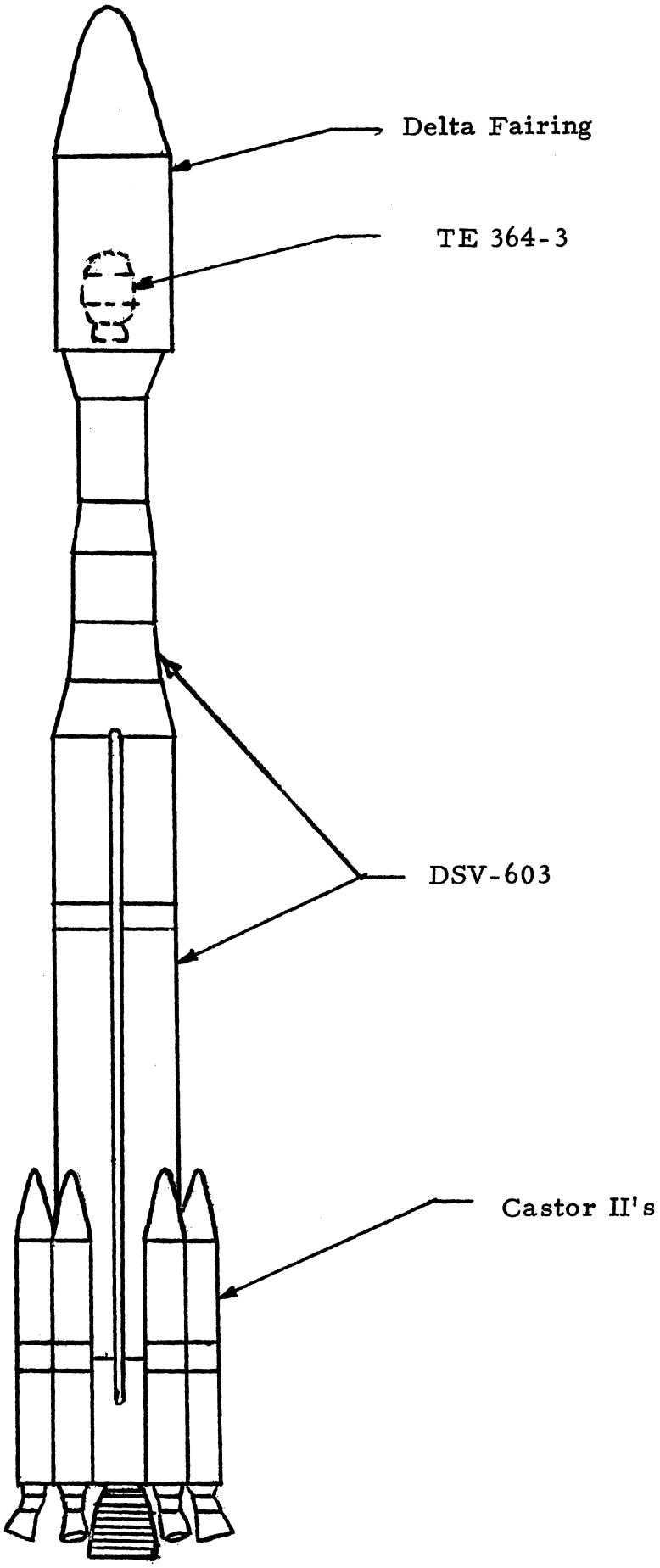

Figure 8.1 Delta Launch Vehicle

Time (sec)	Event
T + 0	Vehicle Liftoff
T + 40	Castor II Separation
T + 220.5	Main Engine Cutoff (MECO)
M + 0	Start Stage II Programmer
M + 4	Start Stage II Engine
	Fire Separation Bolts
M + 41	Fairing Separation
M + 302	Stage II Engine Cutoff (SECO)
M + 30,304	Initiate Ullage Jets
M + 30,344	Restart Stage II*
M + 30,372	Stage II Engine Cutoff
M + 30,374	Fire Spin Rockets**
M + 30,376	Stage II/Stage III Separation
M + 30,389	Stage III Ignition
M + 30,433	Stage III Burnout
M + 30,443	Despin Stage III/Spacecraft Combination***
M + 30,534	Payload Separation

*It is noted that the second stage, using the same engine found in the Titan transtage, burns twice; first to circularize the 100 nm parking orbit, and second to provide part of the velocity increment for Hohmann transfer injection. The restart of Stage II will occur at 5.5 revolutions of the parking orbit, at 62.5° east longitude.

** The Stage III/Spacecraft combination will be spun up to 100 rpm by eight spin rockets mounted to the standard spintable for the TE 364-3.

***A yo-yo despin device attached on the spacecraft attach fitting will be used to despin the Stage III/Spacecraft combination to 0 rpm.

8.5 TIME OF LAUNCH

When SCANNAR first reaches its on station position, it is desired to have no eclipse in order that the power systems on the satellite may start operations at full capacity. Thus the vehicle should be launched between April 13 and August 13 or between October 14 and February 10, thus avoiding the maximum eclipse days of March 21 and September 21. These dates provide at least 15 days between apogee motor burnout and the satellite's encounter with even a partial eclipse.

8.6 LAUNCH VEHICLE SYSTEMS

8.6.1 Guidance and Control

The DSV-603 provides a new guidance system called the Douglas Inertial Guidance System (DIGS). This guidance equipment is stored in

the second stage and provides guidance signals for first and second stages during their respective powered flight phases. Guidance signals override the autopilot which is set to command the second stage through a series of ground set turn rates. The launch vehicle-borne guidance unit sends a pulse to ground tracking radar for automatic tracking use and position data generation. An integrating accelerometer system is used on the second stage to control velocity for operation beyond the ground radar horizon.

Control systems for the first and the second stages stabilize the vehicle and initiate sequential functions for trajectory guidance. Attitude control and stabilization damping are also provided by these systems.

The new DIGS provides the following 3-sigma injection accuracies.

Perigee	$\pm$ 10 nm
Apogee	$\pm$ 750 nm
Inclination	$\pm$ 0.7^{o}

8.6.2 Electrical Power Systems

AC and DC systems are used to power first and second stage equipment. AC power is supplied by a three-phase four-wire system with a one point neutral. The DC system is grounded negative.

8.6.3 Telemetry Systems

Both the first and second stages use combinations of pulse duration modulation and frequency modulation.

8.6.4 Range Safety System

The first two stages are both tuned to the same frequency and respond to the same RF modulated ground signal. The second stage contains dual command destruct systems.

8.7 LOADING FACTORS

The maximum axial accelerations on the payload during launch are:

8 g at MECO

2 g at SECO

10 g at third stage burnout

Low frequency sinusoidal excitations are imposed on the spacecraft during various times of flight, but primarily at liftoff, transonic flight, and just prior to first stage main engine cutoff (MECO). To avoid dynamic coupling between the low frequency vehicle and spacecraft modes, the spacecraft structure was designed to produce fundamental frequencies of approximately 45 cps along the thrust axis and 30 cps along the lateral axis.

The maximum sinusoidal vibration accelerations at the above fundamental frequencies are:

Thrust axis	2.4 g (0-peak)
Lateral axis	1.5 g (0-peak)

The maximum sinusoidal vibration accelerations over the entire frequency spectrum are:

Thrust axis	6.0 g (0-peak) at 20 cps
Lateral axis	7.5 g (0-peak) at 250 cps

The maximum angular acceleration during spin-up of third stage/spacecraft combination is 14 rad/sec^2, and has a nominal duration of 30 milliseconds.

8.8 FAIRING

The fairing used is the standard Delta fairing, 224 in long and 65 in in diameter. Assembled, the fairing is a fiberglass structure of circular cross-section, weighing about 535 pounds (see Figure 8.2 and Reference 8.1).

8.9 SPACECRAFT ATTACH FITTING

The spacecraft is supported on the third stage by an attach fitting (see Figure 8.2 and Reference 8.1). A cylindrical aluminum fitting, 18.40 in in diameter and 9.5 in high, weighing 24 lbs and capable of supporting a 1,200 lb spacecraft with a center of gravity located 30 in above the separation plane is used. A yo-yo weight despin system which will despin the third stage/spacecraft combination will be located on the attach fitting.

8.10 APOGEE MOTOR

To circularize the synchronous orbit and to transfer to the equatorial plane, SCANNAR utilizes the United Technology Center's FW-4S solid propellant apogee motor. This motor is built into the satellite, and uses

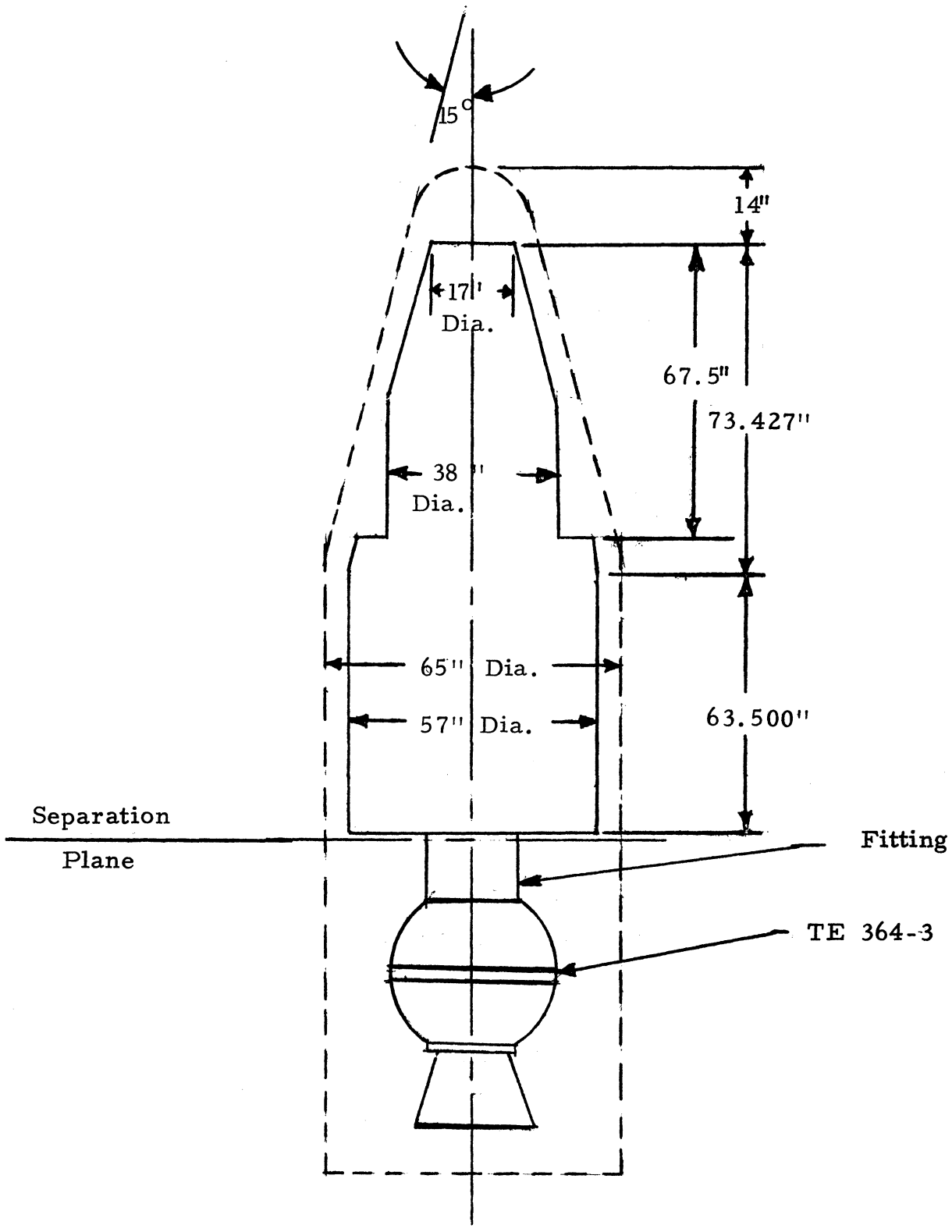

Figure 8.2 Spacecraft Fairing with Attach Fitting & TE 364-3

ammonium perchlorate to oxidize polybutadiene acrylonitrile with aluminum additives. The scaled down version weighs 52 lbs and carries 486 lbs of fuel (see Appendix G).

8.11 USEFUL PAYLOAD

Satellite (including apogee motor)	534 lbs
Apogee Motor Fuel	486 lbs
Spacecraft Attach Fitting	24 lbs
Yo-Yo Despin System	10 lbs
Useful Payload	1054 lbs

REFERENCES

8.1 "Delta Payload Planner's Guide", McDonnell Douglas Astronautics Company, April 1969.

8.2 "Scout Planning Guide", Missiles & Space Division-LTV Aerospace Corporation, October 1968.

* * *

"Atlas Family of Space Launch Vehicles-Configuration and Performance" General Dynamics-Convair Division, October 1969.

"Atlas Family Space Launch Vehicles, USAF Applications", General Dynamics-Convair Division, February 7, 1969.

"Aviation Week & Space Technology", March 10, 1969, p. 172.

"The Burner II", Boeing Company, April 1968.

Carlson, Robert, Personal Correspondence, McDonnell Douglas Astronautics Company, February 1970.

S. F. Iacobellis, V. R. Larson, and R. V. Burry, "Liquid-Propellant Rocket Engines: Their Status and Future", North American Rockwell Corporation-Rocketdyne Division, October 1967.

"Launch Vehicle Estimating Factors", NASA, January 1969.

"MISSAC", University of Michigan, April 1968.

"SLV-3A/Burner II for Synchronous Missions", General Dyanmics-Convair Division, December 1969.

9
ORBITAL ANALYSIS

9.1 TRAJECTORY ANALYSIS

9.1.1 Final Orbit Requirements

The mission requirements of navigation and communications make it necessary to position our satellite at synchronous altitude above the equator midway between North America and Western Europe. An orbit at synchronous altitude is a cirular orbit in the equatorial plane with a period equal to that of the earth's rotation (1 sidereal day) and a theoretical radius of 22,766.90 nm. In reality, certain perturbations caused by the sun and moon and effects of imperfections in the earth's gravitational field alter this theoretical orbit (see Section 9.2). SCANNAR's actual orbit will be at a radius of 22,767.10 nm with an inclination of 0.86° from the equatorial plane.

Since 27.5° west longitude is above the mid-Atlantic and offers minimal drift rate from the nominal position, it is chosen as the final on-station location. Our mode of operation will be to target for a point ahead of the on-station position at an altitude slightly higher than synchronous. This will allow the satellite to drift westward toward the on-station position in a matter of one to two weeks.

Three-sigma errors are used in all orbital error calculations.

9.1.2 Orbital Timing Sequence

The sequence of major operations in SCANNAR's orbital acquisition is given below. The maximum probable timing errors are indicated in parentheses.

Launch	T = 0	
First Perigee Burn Initiation	T = 8 hr 25 min 44 sec	
Second Perigee Burn Initiation	T = 19 hr 11 min 45 sec	(+22 min 43 sec) (-20 min 9 sec)
Apogee Burn Initiation	T = 24 hr 34 min 45 sec	(+22 min 54 sec) (-19 min 58 sec)
Walking Orbit Maneuvers	4 to 14 days, following the apogee burn.	
Rendezvous Maneuvers	Approximately 8 hours, following the conclusion of the walking orbit maneuvers	

9.1.3 Launch Phase

SCANNAR will be launched from the Eastern Test Range into a nominally-circular 100 nm earth parking orbit which is inclined from the equatorial plane at 28.7°. Equatorial crossings of this parking orbit occur as shown in Table 9.1.

Table 9.1 100 Nautical Mile Parking Orbit Equatorial Crossings

Transfer on a Southerly Crossing		Transfer on a Northerly Crossing	
Revolutions	Transfer Longitude	Revolutions	Transfer Longitude
0	4.0° E	$\frac{1}{2}$	173.0° E
1	18.1° W	$1\frac{1}{2}$	150.9° E
2	40.2° W	$2\frac{1}{2}$	128.8° E
3	62.3° W	$3\frac{1}{2}$	106.7° E
4	84.4° W	$4\frac{1}{2}$	84.6° E
5	106.5° W	$5\frac{1}{2}$	62.5° E
6	128.6° W	$6\frac{1}{2}$	40.4° E
7	150.7° W	$7\frac{1}{2}$	18.3° E
8	172.8° W	$8\frac{1}{2}$	3.8° W
9	194.9° W	$9\frac{1}{2}$	26.9° W

9.1.4 Perigee Burn and First Transfer Orbit

The purpose of the first transfer orbit is to place SCANNAR into an elliptic orbit with an apogee radius 422 nm above synchronous. SCANNAR will complete 5 1/2 revolutions of the 100 nm parking orbit before perigee burn. This number of parking orbits is chosen to make the longitudinal position at perigee coincide with that necessary to insure the correct longitudinal position for the final apogee burn. Following are the important parameters before and after the perigee burn:

parking orbit radius	100 nm $\pm$ 10 nm
parking orbit velocity	25568 fps $\pm$ 36 fps
longitude at perigee	62.5° East longitude
perigee burn increment	8109 fps $\pm$ 40 fps

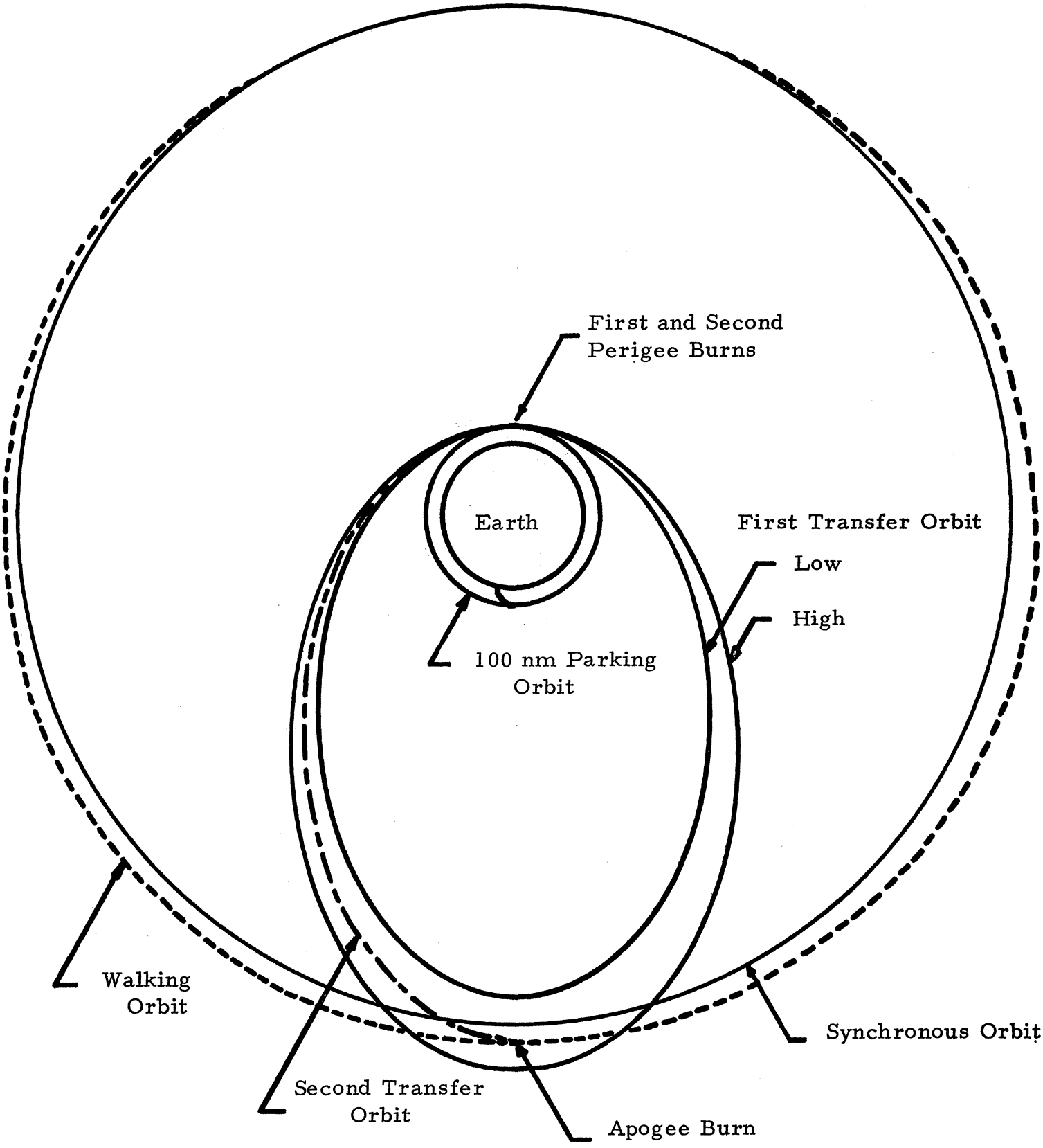

Figure 9.1 Orbital Acquisition

apogee radius	23189 nm $\begin{matrix}(+613\text{ nm})\\(-549\text{ nm})\end{matrix}$
period of transfer orbit	38761 sec $\begin{matrix}(+1363\text{ sec})\\(-1209\text{ sec})\end{matrix}$

The perigee burn will be effected by the second and third stages of the Delta vehicle. After the burn is completed, the vehicle will be de-spun and the booster will be jettisoned. SCANNAR will then complete one cycle of the transfer orbit. Velocity errors when SCANNAR again reaches perigee will be at most 60 fps.

9.1.5 Second Perigee Burn and Second Transfer Ellipse

The purpose of the second perigee burn is to correct any errors in the first transfer ellipse and thus to place the satellite at its nominal apogee position 422 nm above synchronous with small radial errors. This maneuver will be accomplished with the ten-pound hydrazine thrusters and will require from 0 to 60 fps. If SCANNAR was higher than nominal at the apogee of the first transfer ellipse, it will have to be reoriented 180° for the second perigee burn.

Shortly before SCANNAR reaches apogee on the second transfer orbit, its attitude must be changed to orient for the apogee burn and plane change. This orientation will involve a rotation of either 128.3° or, if a reorientation was necessary before perigee, 51.7°. After this maneuver, SCANNAR will be spun to 100 rpm to ensure accuracy and prevent instability in the apogee burn.

9.1.6 Apogee Burn and Plane Change

The purpose of the apogee burn is twofold: to change the plane of the orbit to one that is inclined 0.86° from the equatorial plane and to increase SCANNAR's velocity so that its new orbit will have a nominal perigee at synchronous altitude. This burn is effected by the apogee motor mounted into SCANNAR's structure. The orientation and configuration for apogee burn is shown in Figure 9.2.

The pointing accuracy of SCANNAR's attitude control system is $\pm$ 0.5 degrees and the apogee kick motor delivers its velocity increment with an accuracy of $\pm$ 0.5% of its total burn. These errors, in addition to the radial errors at perigee, lead to the following parameters before and after the apogee burn:

time from second perigee burn to apogee burn	19380 sec $\pm$ 11 sec
radius at apogee of second transfer ellipse	23189 nm $\pm$ 10 nm

velocity at apogee before apogee burn	5146.7 fps $\pm$ 6.3 fps
apogee longitude	0.25^{o} W long. $(+5.2^{o})$ (-5.6^{o})
apogee burn increment	5909 fps $\pm$ 30 fps
velocity after apogee burn	9949 fps $\pm$ 87 fps

The velocity error after apogee burn will be corrected with the hydrazine thrusters at the first apogee of the resulting near-synchronous orbit--this maneuver could require from 0 to 87 fps. The resulting near-synchronous orbit has an apogee as desired 422 nm above synchronous altitude and a perigee altitude equal to the synchronous altitude.

9.1.7 Walking Orbit Maneuvers

The function of a walking orbit is to allow SCANNAR to drift westward until it is reasonably close to its on-station position above 27.5^{o} West longitude. Since the near-synchronous orbit described is always higher than synchronous, it has a longer period of revolution than the synchronous orbit and therefore will drift westward relative to the on-station position. These walking orbit maneuvers are designed to take from four to fourteen days. A plot of drift rate versus apogee altitude above synchronous is given in Figure 9.3 .

It is clear from the plot that lowering the apogee altitude decreases the drift rate. During the drift time, small velocity increments will be employed at the perigee position to gradually lower the apogee altitude so that it becomes synchronous and on-station at the same time (and within the fourteen-day period specified). These walking maneuvers will require no more than 46 fps. When SCANNAR arrives in a region within forty nm of the on-station position, rendezvous maneuvers will begin.

9.1.8 Terminal Phase Rendezvous

The small position errors left at the end of the walking maneuvers will be corrected by the two ten-pound thrusters using a two-burn method of terminal phase rendezvous: a terminal phase initiation maneuver (called TPI), which is a velocity change to effect a rendezvous between target and vehicle in a specified time interval; and a braking maneuver upon coincidence of target and vehicle, which is a velocity increment to make the velocity vector of the rendezvous vehicle exactly match that of the target, thereby setting the rendezvous vehicle in the same orbital path as the target (see Appendix H.4).

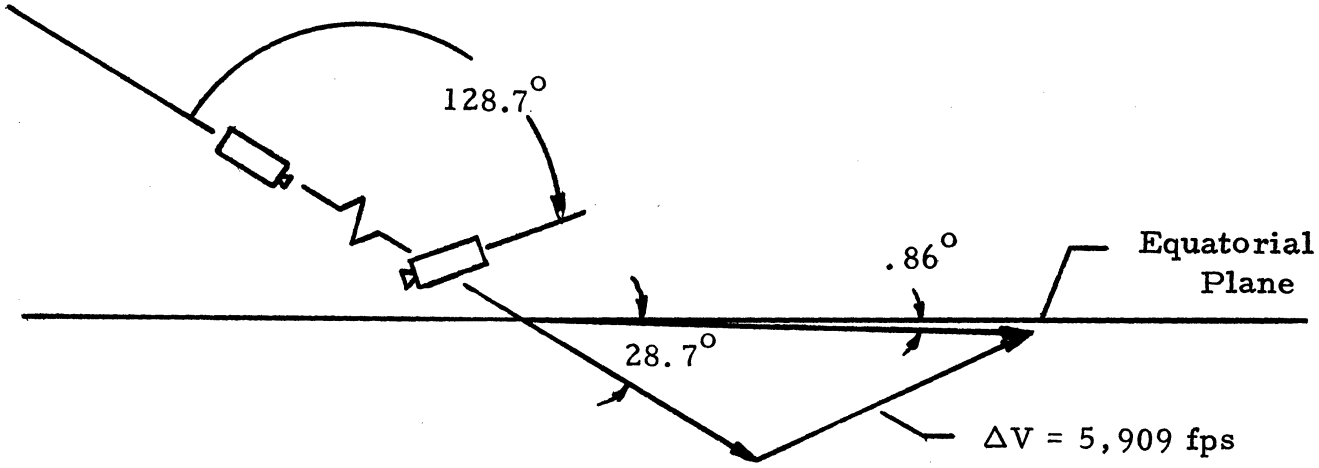

Figure 9.2 Orientation and Configuration for Apogee Burn

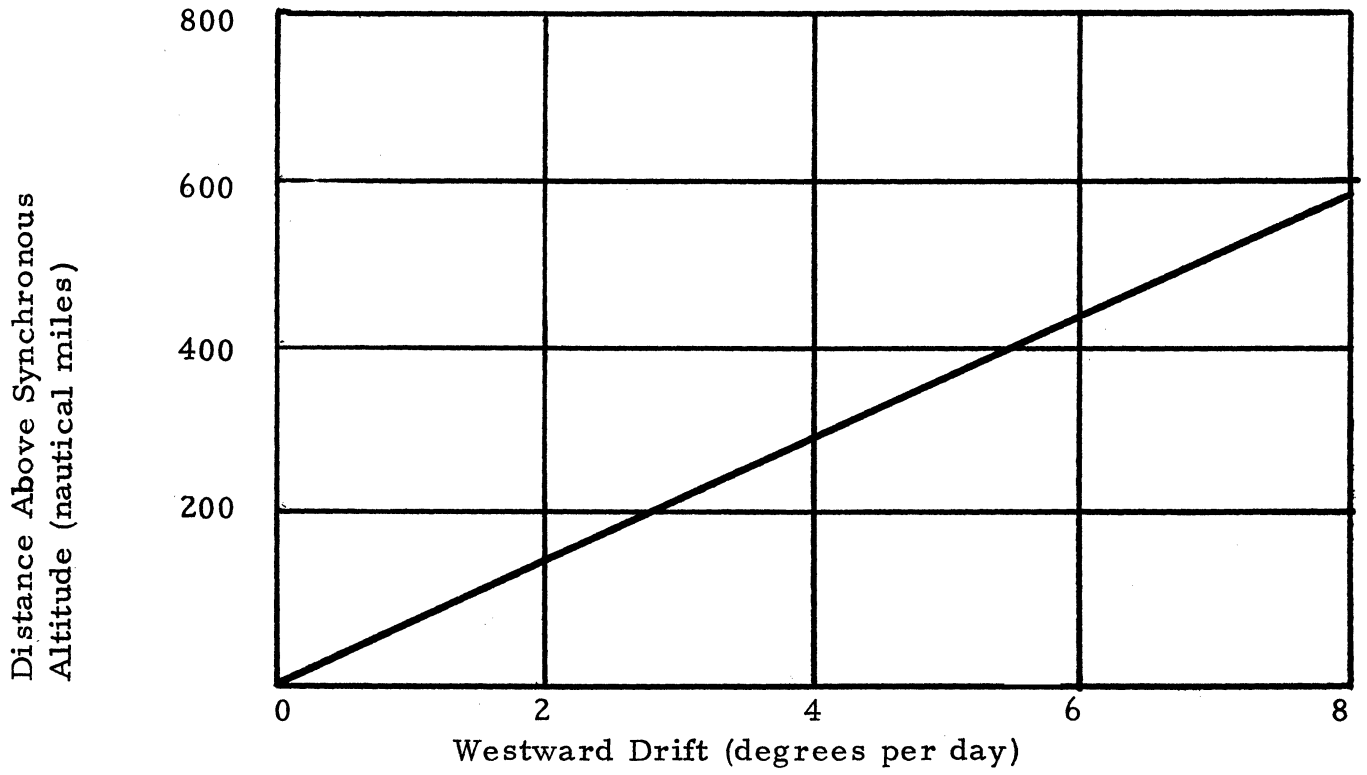

Figure 9.3 Drift Rate versus Altitude Above Synchronous (for calculation of graph see Appendix H.3)

SCANNAR's rendezvous phase may begin any time after it enters a region 40 nm by 40 nm in the second quadrant of the coordinate system shown in Figure 9.4.

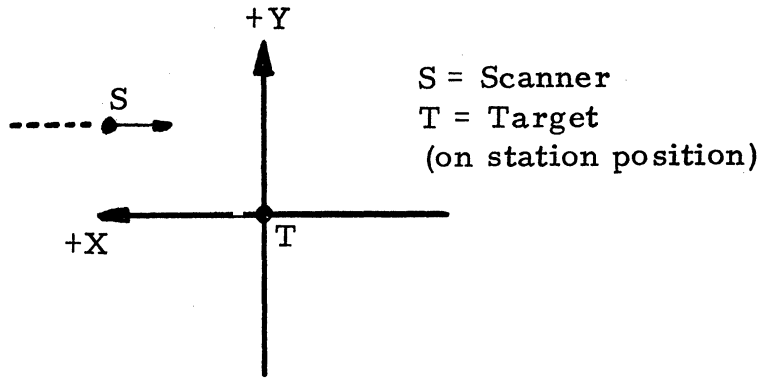

Figure 9.4 Rendezvous Coordinate System

In Figure 9.5, typical required total delta V's are shown for various locations in the 40 by 40 nm region. The location represents the position of the satellite at the time of beginning rendezvous (i.e. at TPI). The time in which rendezvous is to occur is chosen as eight hours (near-optimal for SCANNAR's probable initial conditions). SCANNAR is taken to have local circular X-direction velocity and negligible Y-direction velocity.

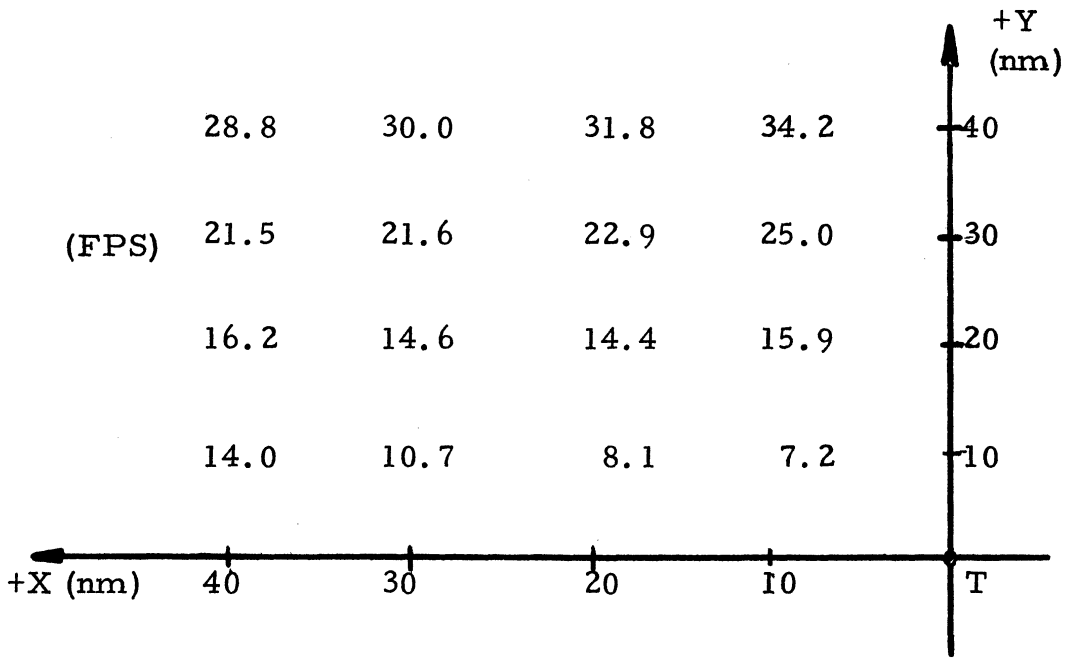

ΔV's are for 8 hour rendezvous

Figure 9.5 Total Rendezvous Velocity Requirements

Based on the values from Figure 9.5, a velocity increment of 30 fps is allotted for the entire rendezvous maneuvers (to be delivered by ten-pound hydrazine thrusters).

9.1.9 Total Hydrazine Thruster Velocity Requirements

The hydrazine velocity requirements of SCANNAR's orbital acquisition are summarized below:

first perigee burn	0 - 60 fps
correction at first apogee of near-synchronous orbit	0 - 87 fps
walking orbit maneuvers	46 fps
rendezvous maneuvers	30 fps
TOTAL REQUIREMENTS	76 - 223 fps

The total hydrazine thruster velocity requirement for orbital acquisition will be between 76 and 223 fps.

9.2 PERTURBATIONS

9.2.1 Introduction

The design of SCANNAR calls for establishing an artificial satellite in a synchronous equatorial orbit. If it is assumed that the mass distribution of the earth is spherically symmetric and that the earth's gravitation is the only force acting on the satellite, the satellite would appear to be fixed relative to the earth. In actual practice, the nonspherical nature of the earth's mass distribution and the gravitational effects of the sun and moon constitute perturbing effects on the motion of the idealized synchronous satellite. The effects of these perturbations must be considered.

9.2.2 Orbital Steady-State Radius

The effect of the earth's equatorial bulge, the oblateness, is to increase the radius of the orbit of the synchronous satellite by 0.20 nm. It is also found that the gravitational attraction of the sun and moon modify the steady-state orbital radius. The magnitude of the correction is a function of the initial geometry of the sun-earth-moon-satellite system, as characterized by certain angles. The corrections of the initial steady-state radius can be included in the initial orbital injection corrections.

9.2.3 In-Plane Perturbations

Due to the triaxiality of the earth, specifically the ellipticity of the equatorial plane, the synchronous satellite will drift eastward along the equator toward an equilibrium position. For our satellite, nominally positioned at 27.5° West longitude, the velocity change per year due to this drift is found to be equal to 3.23 ft/sec/yr. The time to drift a distance of 1° longitude is 43.2 days. Small onboard thrusters will be used to station-keep in compensating for this drift error.

While drifting in such a manner, the synchronous satellite will also experience tangential perturbations due to the sun and moon effects. However, these perturbations are negligible relative to the aforementioned drift error.

A small change in the orbital radius is caused by both the earth's triaxiality and the gravitational effects of the sun and moon. The accumulated amount of radial drift due to the earth's triaxiality, for the maximum longitudinal deviation of 1° is 1.64 nm. The radial deviation due to the sun and moon effects depends on the initial geometry of the sun-earth-moon-satellite system. This has a maximum value of 1.07 nm. The accumulated amount of radial error will be corrected for at the same time as for the angular drift error above.

9.2.4 Out-of-Plane Perturbations

Since the satellite orbit plane forms various angles with the orbit planes of the other bodies, it is subjected to precessional torques which cause its orbit plane to rotate away from the equatorial plane. The effect is a cyclic one with a period of one sidereal day. The amplitude increases linearly with time at the rate of 0.8525° latitude per year. This effect can be halved by biasing the orbit away from the equatorial plane.
The bias inclination is half the maximum unrestrained value expected from Figure 9.6. Figure 9.7 defines the biasing technique. As can be seen, the passive biasing technique can be used and no North-South station keeping is required (Reference 9.2).

Most of the above data has been computed using a Rand Corporation report by Frick and Garber (see Reference 9.1). Later data now in use would show slightly different magnitudes for the computed quantities, (e.g., the time to drift 1° longitude would be slightly longer and the accumulated drift would be slightly smaller).

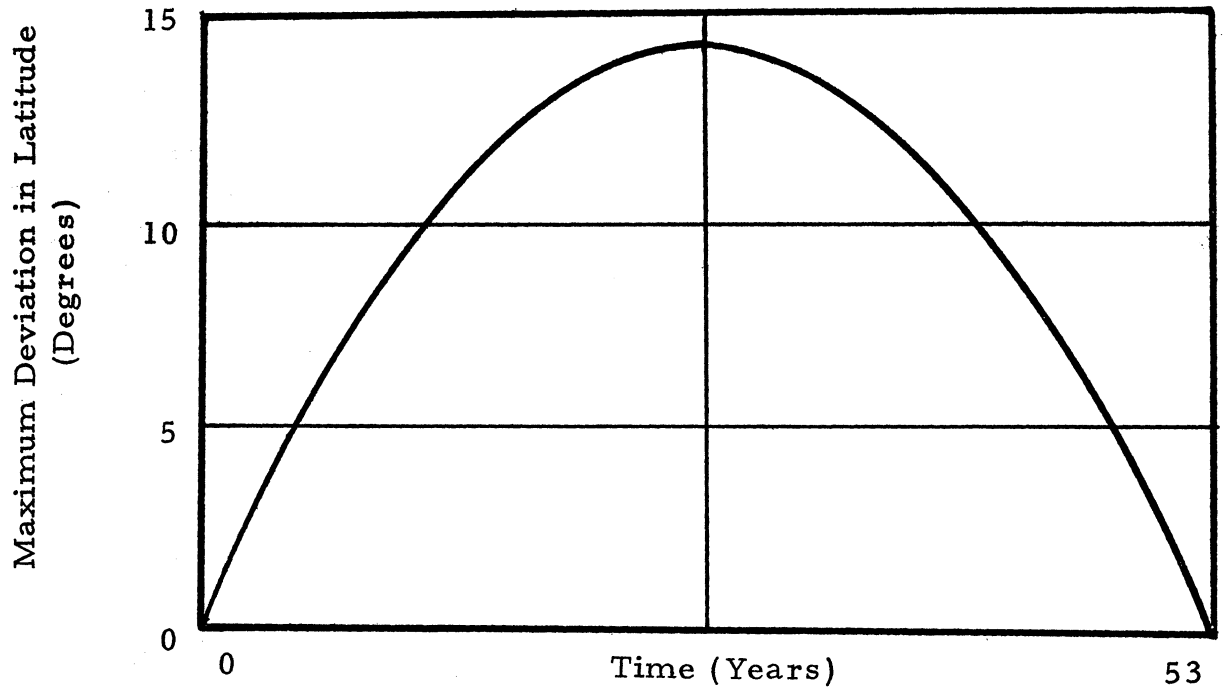

Figure 9.6 Orbital Regression Due to Solar and Lunar Gravitational Attraction.

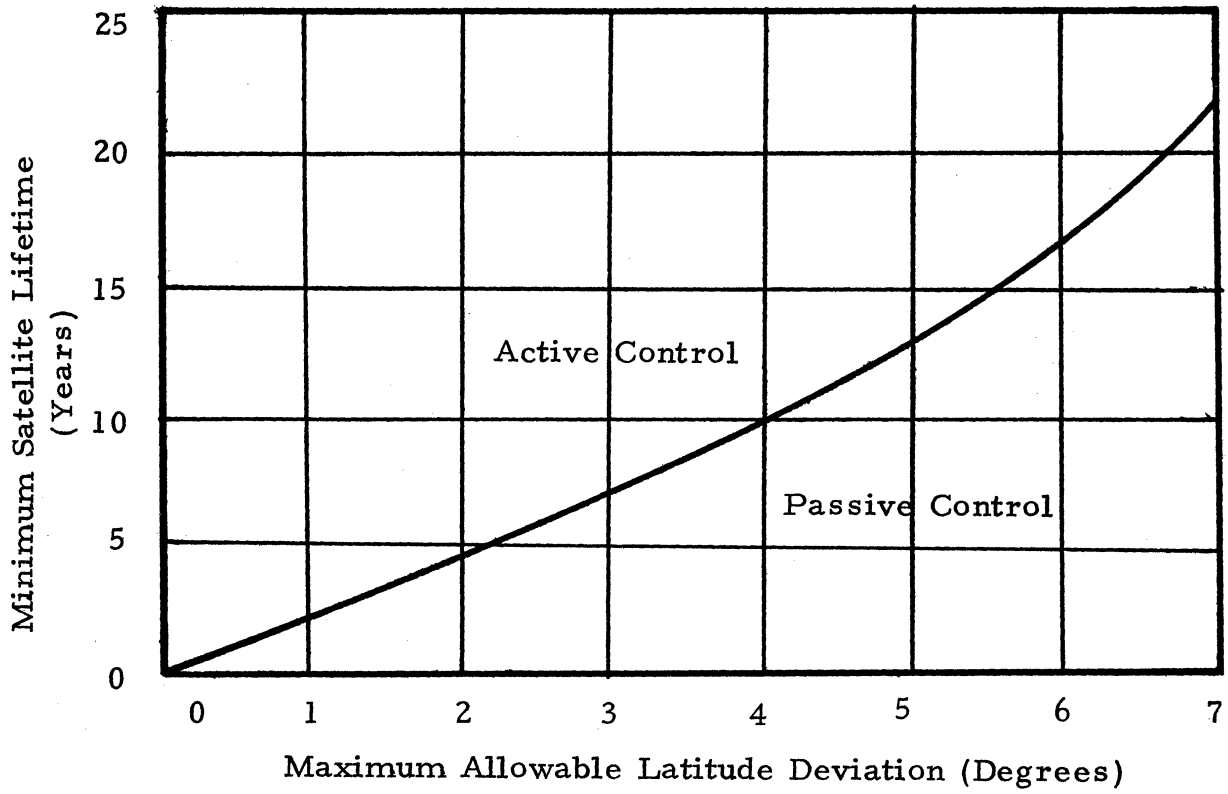

Figure 9.7 Orbital Regression Resulting from Biasing of Synchronous Orbit Away from the Equatorial Plane.

REFERENCES

9.1 Frick, R.H. and Garber, T.B., "Perturbations of a Synchronous Satellite" Rand Report R-399-NASA, May 1962.

9.2 Frick, R.H., "Orbital Regression of Synchronous Satellites Due to the Combined Gravitational Effects of the Sun, the Moon, and the Oblate Earth", Rand Report R-454-NASA, Aug. 1967.

* * *

Wainscott, F.H., "The Syncom III Launch", NASA TN-D-3377, 1966.

Williams, D.D., "Dynamic Analysis and Design of the Synchronous Communications Satellite", Hughes Aircraft Co. TM 649, May 1960.

"Orbital Flight Handbook", NASA SP-33 Parts I, II, and III, 1963.

MISSAC, University of Michigan, Department of Aerospace Engineering design project, April 1968.

10
IMPLEMENTATION

10.1 INTRODUCTION

This section will complete the study of Project SCANNAR with a brief discussion of its implementation. The main topics covered are work scheduling, cost analysis, and testing and reliability.

10.2 WORK SCHEDULING

A work schedule based on a launch in January, 1975 is shown in Table 10.2. The projected launch of ATS-F in 1973 was considered in scheduling design work. ATS-F will include interferometric experiments on its mission and time for gathering and applying this data to Project SCANNAR was allowed before freezing the design. Ample time was also allowed for long lead items such as special processes, tests, and materials.

Two fully tested satellites will be delivered to the Eastern Test Range in October and November of 1974. Launch of SCANNAR I will be in January, 1975. If launch cannot take place before February 10, it will have to be delayed until April 13, 1975 because of the constraint placed on the launch time by power requirements

10.3 COST ANALYSIS

Project SCANNAR is estimated to cost 33 million dollars. This includes all design, fabrication, testing, and delivery of two satellites to the Eastern Test Range. Items not included in this cost are the launch vehicle, launch operations, and operation of the satellite when on station. Table 10.1 shows an overall breakdown of costs. Engineering includes preliminary design; design of structural, thermal, and prototype test models; and a qualification test assembly. Manufacturing includes labor and materials for one qualification test assembly and two flight spacecraft. Testing covers individual component tests; manufacture and testing of structural, thermal, and prototype models; testing of the qualification model; and acceptance test and final plant check out.

Item	Millions of Dollars
Engineering	11.5
Manufacturing	10.0
Testing	9.0
Profit	2.5
Total	33.0

Table 10.1

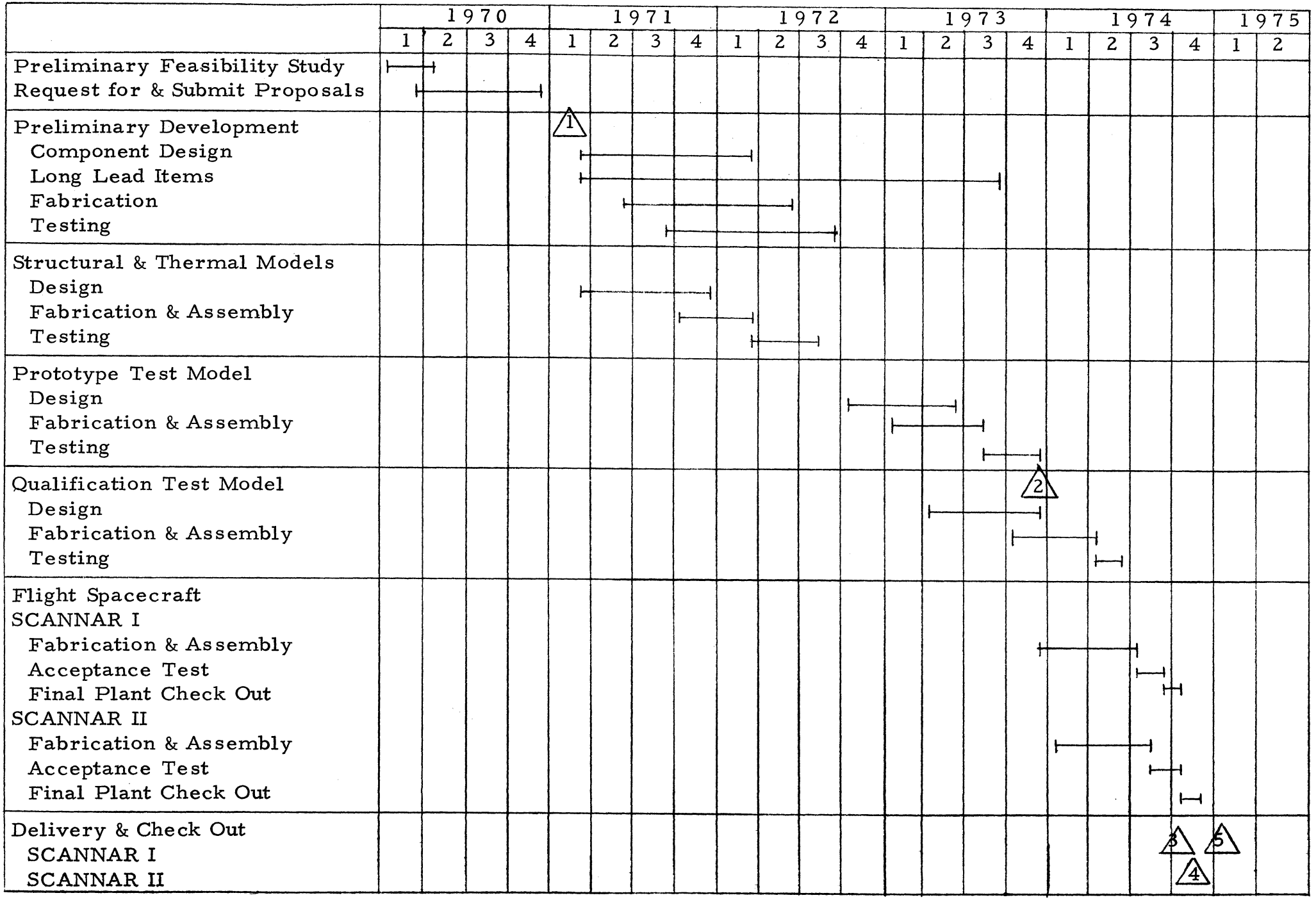

1 Contract Award 2 Design Freeze 3 Deliver SCANNAR I 4 Deliver SCANNAR II 5 Launch SCANNAR I

10.4 TESTING AND RELIABILITY

A high probability of success will be achieved by including a rigorous schedule of testing. Individual components are tested before assembly. Structural and thermal models, a prototype test model, and a qualification model are built and tested beyond design limits. Tests include vibration, acceleration, shock, vacuum, and high and low temperature.

Reliability is also assured by using flight proven items such as the launch vehicle, heat pipes, and reaction wheels, and by a high degree of redundancy in the overall system. Finally, if part of SCANNAR I should fail, it could be used in multiple modes with SCANNAR II to complete the mission. This multiple mode capability could also be used in an operational model to give additional redundancy to the satellite system.

REFERENCES

W. R. Corliss, "Scientific Satellites", NASA SP-133.

University of Michigan, Department of Aerospace Engineering, Project LINUS.

APPENDIX A
NAVIGATION

A.1 ANGLE AMBIGUITIES (Reference 2.3)

SCANNAR's navigation system uses two closely spaced frequencies to resolve the angle measurement ambiguities. In order to determine the nonambiguous space angle (Figure 2.4), the number of ambiguities from the second frequency must be one more or one less than the first frequency. Therefore, if:

$$n = \frac{D}{\lambda_1} \quad \theta_e$$

then $$n - 1 = \frac{D}{\lambda_2} \quad \theta_e$$

where θ_e is the subtended earth angle at synchronous altitude ($\theta_e = 17.3^o$).

Substituting for n,

$$\frac{\lambda_2 - \lambda_1}{\lambda_1 \lambda_2} = \frac{1}{D \theta_e}$$

since $\lambda_2 - \lambda_1 = \Delta\lambda$

$$\frac{\Delta\lambda}{\lambda_2} = \frac{\lambda_1}{D \theta_e} \quad ;$$

$$\frac{\Delta\lambda}{\lambda_1 + \Delta\lambda} = \frac{\lambda_1}{D \theta_e} \simeq \frac{\Delta\lambda}{\lambda_1}$$

therefore,

$$\frac{\Delta\lambda}{\lambda_1} = \frac{1}{149} \times \frac{57.3^o}{17.3^o}$$

$$= 0.023.$$

Since $\lambda = \frac{c}{f}$, $\frac{\Delta\lambda}{\Delta f} = - \frac{c}{f^2}$,

$$\Delta\lambda = - \frac{c}{f^2} \quad \Delta f$$

$$\frac{\Delta\lambda}{\lambda} = -\frac{c}{f^2} \quad \Delta f \quad \frac{f}{c}$$

$$\frac{\Delta\lambda}{\lambda_1} = -\frac{\Delta f}{f_1}$$

therefore,

$$\frac{\Delta f}{f_1} = -0.023$$

For a frequency of 1640 MHz, the separation is:

$$\Delta f = -1640\ (0.023)\ \text{MHz}$$

$$= -36\ \text{MHz}$$

A frequency separation of 36 MHz would resolve all ambiguities, but this does not take into account errors in the angle measurement. The relation between phase and angle for two closely spaced frequencies f_1 and f_2 is shown in Figure A.1. The user vehicle is at angle θ_1. For a worst case error (angle accuracy is $\Delta\theta$), it is possible that θ_2 could be erroneously selected. From the geometry,

$$2\Delta\theta = \frac{\lambda_2}{D} - \frac{\lambda_1}{D}$$

since $\lambda_2 - \lambda_1 = \Delta\lambda$

and $\Delta\lambda = \dfrac{\lambda^2}{D\ \theta_{max}}$

then $\theta_{max} = \dfrac{1}{2\Delta\theta} \quad \left(\dfrac{\lambda}{D}\right)^2$

$$\Delta\theta = 3\Delta\theta_{rms}\ \text{(safety factor)}$$

where $3\Delta\theta_{rms} = 0.02$ milliradians (Appendix A.2)

and safety factor = 4

Therefore,

$$\Delta\theta = (0.02\ \text{milliradians})\ (4)$$

$$= 0.08\ \text{milliradians}$$

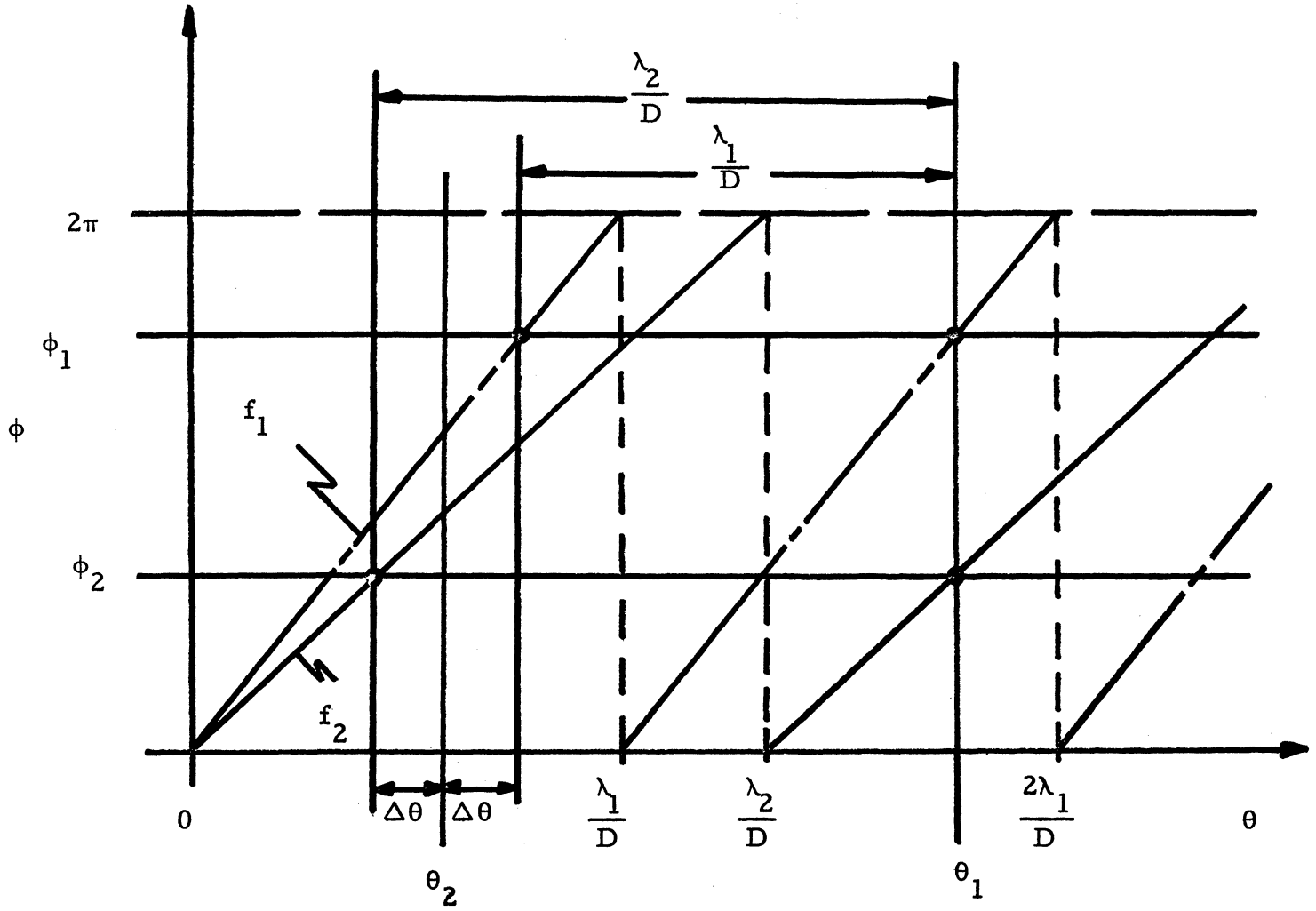

Figure A.1 Effect of Angle Errors on Resolving Ambiguity (Reference 2.2)

Now solving for $\theta_{max} = \frac{1}{2(0.08)} \left(\frac{0.6}{89.5}\right)^2 \times 57.3^\circ$

$= 16.1^\circ$

To resolve all ambiguities, θ_{max} would have to exceed the subtended earth angle of 17.3°. The unresolved angle of 16.1° results in $17.3^\circ/16.1^\circ = 1.08$ ambiguities. This is a spacing at the equator of over 5500 nautical miles.

A.2 ERROR ANALYSIS

The significant error sources discussed are: 1) noise, 2) multipath, 3) propagation medium losses, 4) interferometer boom and antenna errors, and 5) frequency instability.

1) Noise. For a 3.5 millisecond burst of a sinusoidal signal from the aircraft,

$$\sigma_\theta = \frac{\lambda}{2\pi D}\left(\frac{0.33}{\sqrt{S/N}}\right) \quad \text{(Reference 2.3)}$$

For $\frac{D}{\lambda} = 149$ and S/N = 53.5 db (Table 3.7),

$$\sigma_\theta = 1.08\ \mu\text{ rad (rms)}$$

2) Multipath. From a plot of multipath error versus aircraft elevation angle, for a 50,000 foot altitude at 10° elevation (worst case), the uncorrected maximum error is 29 microradians (Reference 2.2, Figure 6.1-52) in space angle. From geometry, the change in path length for the reflected signal is $\Delta\ell = 2h \sin\theta$. For h = 50,000 feet and $\theta = 10^\circ$, $\Delta\ell = 2.86$ nm. Therefore, $\sigma_\theta = 29\ \mu$ rad/2.86 = 10.1 μ rad (max). Since rms 0.29 Δ where $\Delta = 2$ (max),

$$\sigma_\theta = 5.85\ \mu\text{ rad (rms)}$$

3) Propagation Medium Losses. Refraction and other medium losses total:

$$\sigma_\theta = 2.1\ \mu\text{ rad (rms) (Reference 2.3)}$$

4) Interferometer Boom and Antenna Errors

A. Torsion and bending of booms:

$$\sigma_{max} = \frac{E_P}{2\pi(D/\lambda)}\ (1 - \cos\delta) \text{ (Reference 2.2)}$$

where E_p is the angular error in pointing from torsion and bending,
δ is the difference between the aircraft and the calibration station in degrees (9^o maximum).

From Appendix F.3.3, E_p = 2 antennas x 1.6^o/antenna = 3.2^o.

Therefore,

$$\sigma_{max} = \frac{(3.2^o)\,(17.5\ \frac{mrad}{^o})}{2\pi\,(149)}\ (1 - \cos 9^o)$$

$$\sigma_\theta = 0.6\ \mu rad\ (max)$$

$$\sigma_\theta = 0.35\ \mu rad\ (rms)$$

B. Phase Mismatch. This is caused by irregularities in the antenna surface. The calibration error residual could be approximately:

$$\Delta\phi \approx 4\ milliradians\ (max)$$

assuming an improvement in antenna construction since 1964 (Reference 2.3)

$$\sigma_\theta = 4\ \mu rad\ (max)$$

$$\sigma_\theta = 2.32\ \mu rad\ (rms)$$

5) Frequency Instability (Aircraft). Assuming a frequency instability of 2 parts in 10^6. A change in frequency causes a change in wavelength, and therefore a change in D/λ.

Since $\phi = \frac{2\pi D}{\lambda} \sin\theta$

$$\frac{d\phi}{d\lambda} = -\frac{2\pi D}{\lambda^2} \sin\theta$$

$$d\phi = -\frac{2\pi D}{\lambda^2} \sin\theta\, d\lambda.$$

Also $d\phi = \frac{2\pi D}{\lambda} \cos\theta\, d\theta.$

Assume $\cos\theta \approx 1$,

then $d\theta = -\frac{d\lambda}{\lambda} \sin\theta$

or $\Delta\theta = -\frac{\Delta\lambda}{\lambda} \sin\theta.$

From Appendix A.1 ,

$$\Delta\lambda = -\frac{c}{f^2} \quad \Delta f$$

For f of 1640 MHz, the frequency instability is 3280 Hz.

Therefore, $\Delta\lambda = -\frac{9.84 \times 10^8}{(1.64 \times 10^9)^2} \times 3.28 \times 10^3$

$$= 1.2 \times 10^{-6} \text{ feet.}$$

Since $\lambda = 0.61$ ft at 1640 MHz,

and sin $\theta \approx 0.2$,

$$\Delta\theta = \frac{(1.2 \times 10^{-6})}{(0.61)} \quad (0.2)$$

$$\sigma_\theta = 0.39 \text{ μrad (max)}$$

$$\sigma_\theta = 0.23 \text{ μrad (rms)}$$

Total space angle error:

The total angular error, σ_{θ_t}, is given by

$$\sigma_{\theta_t} = (\sum \text{ms})^{1/2} \text{ where ms} = (\text{rms})^2$$

Therefore, $\sigma_{\theta_t} = \left[(1.08)^2 + (5.85)^2 + (2.1)^2 + (0.35)^2 + (2.32)^2 + (0.23)^2 \right]^{1/2}$ μrad (rms)

$$\sigma_{\theta_t} = 6.75 \text{ μ rad (rms)}$$

$$3\sigma_{\theta_t} = 20.25 \text{ μrad (rms)}$$

Phase angle measurement error: $3\sigma_\phi = \frac{2\pi D}{\lambda} (3\sigma_{\theta_t})$ = 18.95 milliradians

= 1.09°

Total ranging error: For the sidetone frequency of 10KHz, the range error is

$$\frac{\Delta\phi}{360^{o}}(\lambda) = \frac{1}{360}\left(\frac{c}{f}\right) = \frac{9.84 \times 10^{4}}{3.60 \times 10^{2}}$$

$$\sigma_{R} = \pm 273 \text{ feet}$$

$$= \pm 0.045 \text{ nautical mile}$$

$$\Delta = 2 \text{ (max)}$$

$$= 2\,(0.045) = 0.09 \text{ nautical mile}$$

$$\sigma_{rms} = (0.29)\,(0.09)$$

$$= 0.035 \text{ nautical mile}$$

$$3\sigma_{rms} = 0.105 \text{ nautical mile}$$

Using spherical geometry, the following relations hold at 70^{o} N latitude (10^{o} elevation): 10μrad space angle at satellite ≡ 1 nm subtended North-South on earth and 50μrad space angle at satellite ≡ 1 nm subtended East-West on earth and the fact that the angular error probability will not change because of a rotation of the interferometer axes, the total position accuracy is as follows:

$$3\sigma_{total} = \left[(3\sigma_{N-S})^{2} + (3\sigma_{E-W})^{2} + (3\sigma_{Range})^{2} \right]^{1/2}$$

$$= \left[(2.03)^{2} + (0.41)^{2} + (0.105)^{2} \right]^{1/2}$$

$$= 2.08 \text{ nautical miles.}$$

Due to uncertainties in the position of SCANNAR, the accuracy of the user aircraft's position will be downgraded. Since tracking will be performed by NASA's STADAN system, the position accuracy of the satellite will be ± 15 meters in range. Using Rosman, N. C. (35^{o} N latitude) as a typical installation, the elevation angle to SCANNAR will be approximately 45^{o}. This will cause an error of ± 11 meters in a lateral and also in a radial direction. The $3\sigma_{rms}$ satellite position error will be:

$$3\sigma_{rms} = 3(.29\Delta) = 3(.29)(22) \text{ meters}$$
$$3\sigma_{rms} = 19 \text{ meters}$$

For such a small error in locating SCANNAR, the accuracy of the aircraft will not change significantly and thus the satellite position uncertainty was not included in the aircraft position error analysis.

APPENDIX B
COMMUNICATIONS

B.1 FREQUENCY ALLOCATIONS

The present L-band frequency usage, as well as possible future expansion, appears in Figure B.1. For the present design several frequencies were chosen to aid in the discussion, concept and calculations of SCANNAR parameters. The actual frequency assignments will depend on many factors. Among these are the number of voice channels desired and the frequency usage at the time of design. The frequency allocations suggested for SCANNAR appear in Figure B.2. The telemetry, tracking and command frequencies will be the standard allocations allotted for these purposes, i.e. 2.2 GHz up and 1.7 GHz down along with 136 MHz for Minitrack.

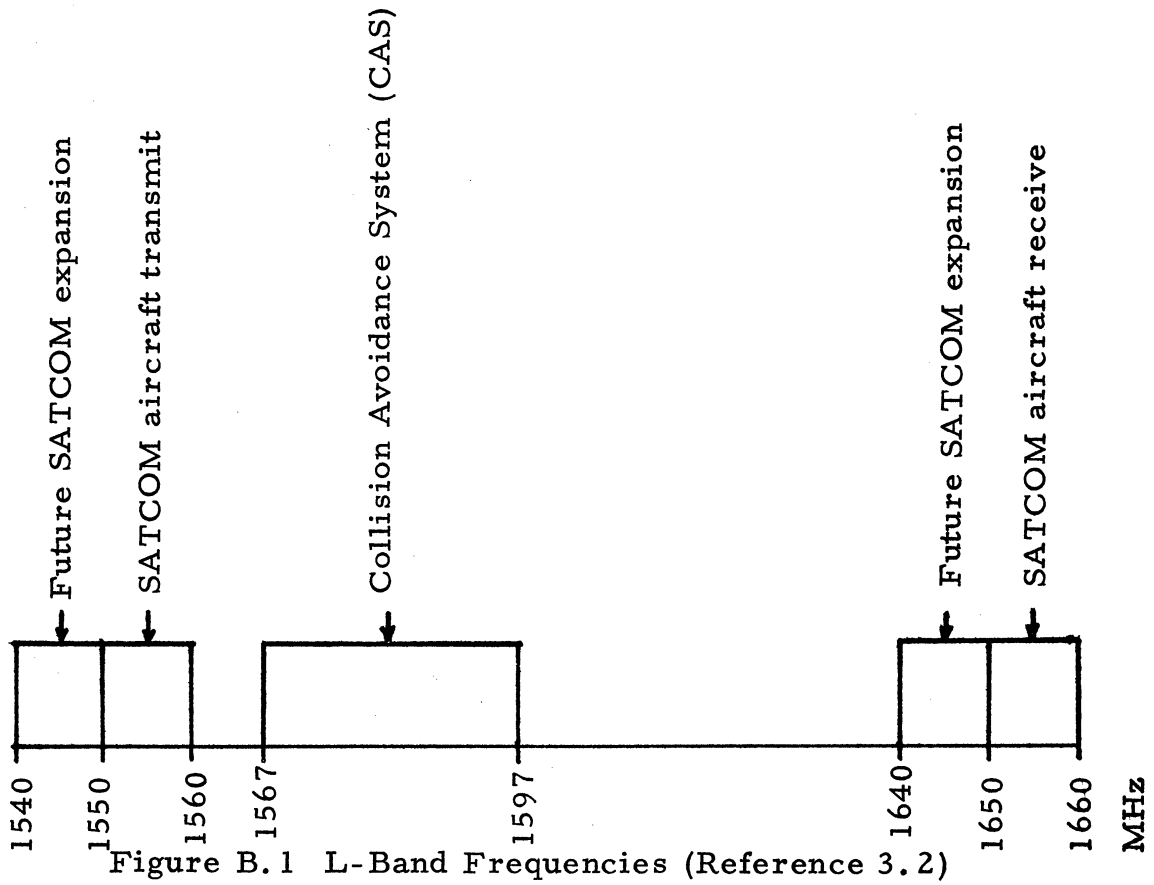

Figure B.1 L-Band Frequencies (Reference 3.2)

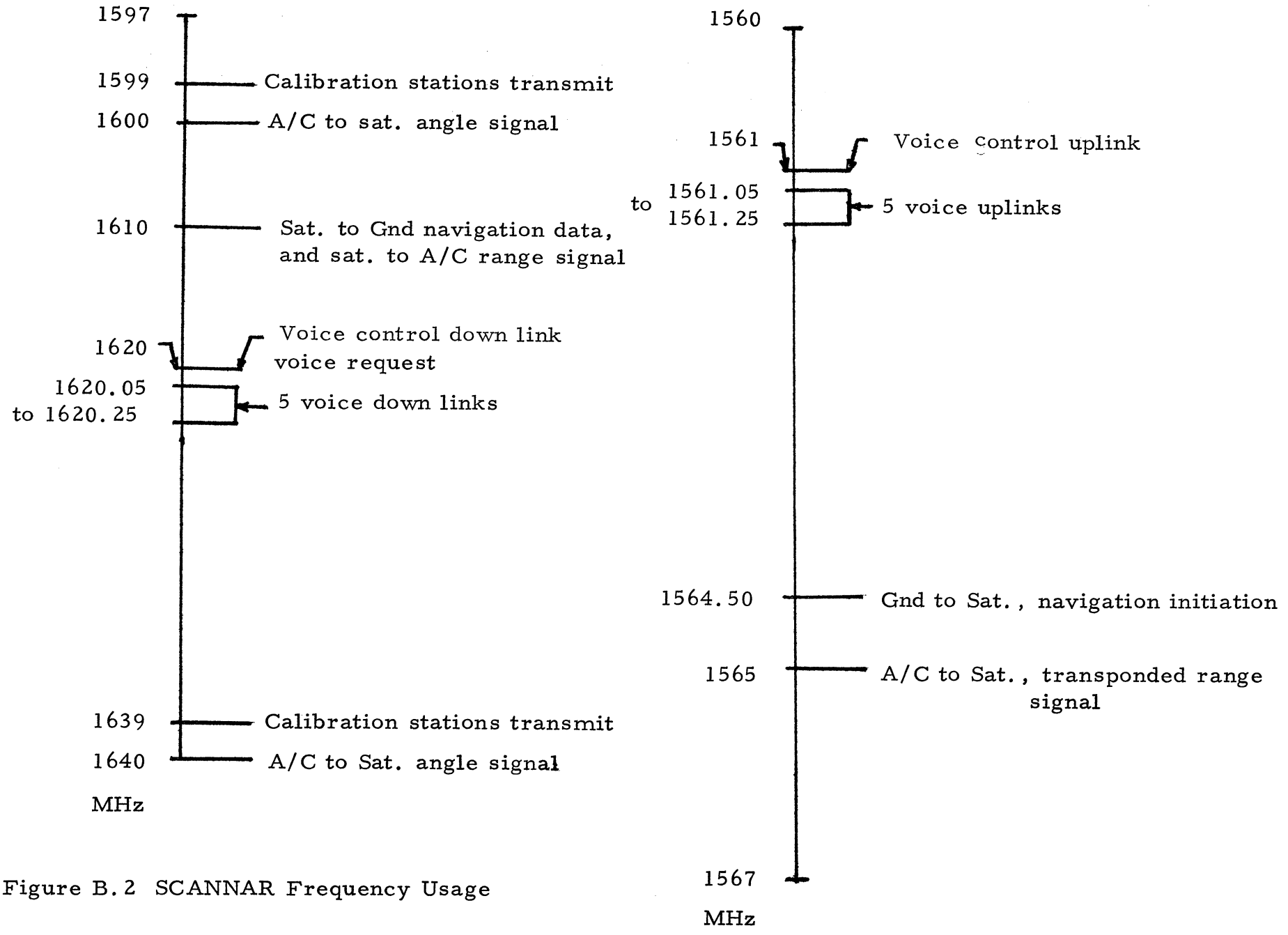

Figure B.2 SCANNAR Frequency Usage

B.2 EQUIPMENT BREAKDOWN

Quantity	Item	Weight (lbs)	Power (Watts)
4	boom antenna	4 (ea)	---
4	boom filters	1 (ea)	---
4	boom preamps	0.5 (ea)	1 (ea)
1	communication antenna	10	---
1	helical antenna	2	---
4	cavity backed spiral antenna	0.75 (ea)	---
1	wire antenna	0.5	---
Telemetry, Tracking, Command:			
1	VHF beacon	1	3
1	S-band transponder	2	4
2	command distributor	2 (ea)	2
2	sub commutator	0.5 (ea)	0.25
2	commutator	0.5 (ea)	0.25
1	clock	0.25	0.25
2	PCM encoder	1 (ea)	1
1	Bi-phase modulator	0.5	0.25
1	S-band transmitter	1	2
2	S-band receiver	4 (ea)	3.5
2	decoder/storage	2 (ea)	1
1	diplexer	0.5	---
1	sub-carrier oscillator	0.3	0.5
Voice:			
1	diplexer	1	---
1	hybrid	1	---
1	frequency translator	14.5	15
6	power amps	0.8 (ea)	100
Navigation:			
1	range transmitter*	1	28
1	range processing	3	3
2	angle processing	8 (ea)	7
1	receiver	4	5
2	multiplexer	4 (ea)	---
1	transmitter*	2	28
Miscellaneous		5	---
		123.35 lbs	180 watts

*Only one of these two is used at any one time.

B.3 NARROWBAND FM PARAMETERS

B_m = message bandwidth
= 3KHz
D = deviation ratio ($\Delta f_c / B_m$)
= 1.0
γ = sideband amplitude level relative to unmodulated carrier amplitude
= 0.1
Δf_c = frequency deviation
Δf_c = (D)(B_m)
= (1) (3KHz) = 3KHz

From Reference 3.3, β = relative bandwidth (2 p B_m) where p is the order of the Bessel function describing the modulated waveform.

β = 4.2
B_{IF} = intermediate frequency bandwidth
= (β) (Δf_c)
= (4.2) (3KHz)
= 12.6KHz = 41 db

Threshold condition:

$(S/N)_{in}$ = signal power to noise power ratio at the demodulator input
$(S/N)_{in,th}$ = threshold condition
$(S/N)_{in,th} = 5 + 5 \log_{10} (B_{IF}/2\ B_m)$ in db
$(S/N)_{in,th}$ = 6.61 db

FM Improvement:

$(S/N)_{out,FM}$ = (S/N) at output of an FM demodulator
$(S/N)_{out,FM} = (3/2)(D)^2(1/B_m)(S/N_o)$ for a bandwidth = $2B_m$

where S/N_o = signal power to noise power density ratio

$$(S/N)_{out,FM}(db) = (S/N_o)_{db} - 33 \text{ db}$$

Link	(S/N_o)	$(S/N)_{out,FM}$
Sat. to A/C	51.5 db	18.5 db
Sat. to ground	86.7 db	53.7 db

B.4 PARAMETERS FOR LINK CALCULATIONS

B.4.1 Transmitter Power

This figure represents the power output of the various system transmitters or power amplifiers. This figure combined with the coupling losses and the antenna gain yields the effective radiated power of the system under consideration.

B.4.2 Coupling Losses

These are the normal losses for transmission links, diplexers, and RF coupling between the antenna and the front end of the receiver. These figures are based on having the RF preamp near the antenna. If the preamps were to be located in the equipment spaces, then the loss in decibels may very well be doubled.

B.4.3 Antenna Gain

The gains of the various antennas are summarized in Appendix B.5. These represent the power gain received at a distance R over that which would be achieved by an isotropic antenna. The gains listed are peak gains which would be achieved at the center of the beam pattern.

B.4.4 Antenna Off-Beam Losses

These losses are representative of the fact that the center of the beam pattern may not be in line with the beam center of the opposing antenna. They are applied to both ends of the particular link. Since the aircraft will be using a phased array antenna as described in Section 2.6 the pointing losses should not exceed one decibel. The ground station will have a highly directional antenna with accurate pointing and thus 0.5 db has been allowed for this loss.

For the satellite antennas, a 3 db pointing loss was allowed for the satellite to ground links since the ground station will be near to the edge of the half-power beamwidth. For the satellite to aircraft links a maximum loss of about 2.8 db will be incurred for aircraft near the periphery of the North Atlantic. The average losses for the nominal flight paths will yield much better results with losses of about 1.5 db. For the purpose of calculations, a worst case situation was chosen and the links were designed to meet these conditions.

B.4.5 Free Space Attenuation

This loss is caused by a spreading out of the wavefront and is inversely proportional to the square of the distance traveled. The free space loss is determined by (Reference 3.4):

$$L_s = 37.8 + 20 \log_{10} R + 20 \log_{10} f \text{ in db}$$

where 37.8 db is the constant of proportionality, R is in nautical miles and f is the frequency in megahertz. For design purposes an average value of 1600 MHz was chosen for the calculations. At the subsatellite point R = 19,328 nm, thus

$$L_s = 37.8 + 20 \log_{10}(19,328) + 20 \log_{10}(1600)$$

$$L_s = 187.6 \text{ db}$$

For an aircraft at 10° elevation, the slant range is approximately 22,000 nm, thus the free space loss increases to about

$$L_s = 188.8 \text{ db}$$

It is this latter value which was used in the link calculations to determine the worst case performance.

B.4.6 Atmospheric Losses (References 3.2 and 3.4)

Reference 3.4 lists the possible losses in a propagation path traversing the earth's ionosphere and troposphere. Table B.1 lists these and a few others along with the effects they cause on the various links. Tropospheric attenuation includes oxygen, water vapor, and precipitation absorption. Faraday rotation is negligible for a path between two circularly polarized antennas. Aurora effects are only prevalent near polar regions. The total values are an estimation since most causes are random. Solar flare phenomena may cause temporary blackouts but these affect all types of communication and are infrequent.

B.4.7 Polarization Losses

The wavefront traveling through the atmosphere is rotated by the Faraday effect and the received power is dependent on relative antenna orientations. For two circularly polarized antennas, this loss is normally 0.5 db.

B.4.8 Boltzman Constant

This factor is a constant of proportionality relating the noise (dbw) per hertz of receiver bandwidth per degree Kelvin. ($k = 1.38 \times 10^{-23}$ joules/$^{\circ}$K.)

Table B.1 Atmospheric Losses

Loss (at L-band)	Sat/Aircraft (db average)	Sat/Gnd (db average)
Tropospheric attenuation	neg	1.0
Ionospheric attenuation	neg	neg
Scintillation	random	random
Birefringence	neg	neg
Faraday rotation	neg	neg
Aurora effects	varies	neg
Luxembourg effect	not known quantitatively	
Scatter (multipath)	varies	neg
Solar flares	<2 db	< 2 db
Totals	1 db	3 db

B.4.9 System Effective Noise Temperature

B.4.9.1 Introduction. The effective system noise temperature is given by

$$T_s = T_a + T_e (\overline{NF} - 1)$$

where, T_a = antenna noise temperature (^oK)

T_e = operating temperature of the components (^oK)

$\overline{NF}$ = receiver front end noise figure

As mentioned in Table 6.1 the average operating temperatures of the various component packages are

Voice: 310 ^oK
Navigation: 300 ^oK
Telemetry: 303 ^oK

For calculation purposes a value of 310^oK will be used for T_e. The antenna temperature will depend on what the antenna is looking at and on what portion of the beam area the noise source takes up. The beamwidths of the various antennas used are summarized in Appendix B.5. The antenna temperature is given by

$$T_a = \alpha_1 T_{sun} + \alpha_2 T_{sky} + \alpha_3 T_{gnd} + \Sigma \alpha_n T_n$$

where the α's are the coefficients relating the effectiveness of the particular noise source.

From Reference 3.5

$$T_{sun} = \frac{(290)(675)}{f} \left[1 + \frac{1}{2.3} \sin 2\pi \frac{\log_{10} 6(f - 0.1)}{2.3} \right]$$

where f is in GHz.

For f = 1.6 GHz

$$T_{sun} = 1.5 \times 10^5 \, ^{o}K$$

The coefficient, α_1, is given by

$$\left(\frac{0.5}{\theta}\right)^2$$

where 0.5^{o} is the angle subtended by the sun and θ is the beamwidth of the antenna under consideration

$$T_{sky} = \lambda^2 (290 \, ^{o}K)$$

where λ is the wavelength in meters.

For f = 1.6 GHz, $\lambda = 0.188$ meters

$$T_{sky} = 10.2^{o}K$$

For all frequencies

$$T_{gnd} = 290^{o}K$$

B.4.9.2 Satellite Antenna.

$$T_a = \alpha_3 T_{gnd}$$

since the earth is in the entire beam, $\alpha_3 = 1.0$

$$T_a = 290^{o}K$$

Assuming a noise figure at the satellite of 4 db (2.5)

$$T_s = T_e (\overline{NF} - 1) + T_a$$

$$T_s = 310^{o}K \, (2.5 - 1) + 290^{o}$$

$$T_s = 755^{o}K = 28.78 \text{ db}$$

B.4.9.3 Aircraft Antenna.

$$T_a = \alpha_1 T_{sun} + \alpha_2 T_{sky}$$

$$\alpha_1 = (0.5/\theta)^2$$

By approximating θ^2 as $(72^o)(10^o)$, the beam pattern of the phased array antenna on the aircraft.

$$\alpha_1 = 3.47 \times 10^{-4}$$

$$\alpha_2 = 1.0$$

$$T_a = (3.47 \times 10^{-4})(1.5 \times 10^{5o}K) + (10.2^oK)$$

$$T_a = 62^oK$$

The contribution from the sun will occur only when the sun is within the beam pattern of the aircraft antenna. Assuming $T_e = 290^oK$ and NF = 5 db (3.16)

$$T_s = 290^oK\,(3.16 - 1) + 62^oK$$

$$T_s = 625^oK + 62^oK$$

$$T_s = 687^oK = 28.4 \text{ db}$$

From the above it can be seen that the effect of the sun (52^oK) is negligible.

B.4.9.4 Ground Antenna.

$$T_s = 100^oK = 20 \text{ db}$$

If the sun comes into the ground antenna's beam the change in system temperature will be:

$$T_a = \alpha_1 T_{sun}$$

$$\alpha_1 = (0.5/\theta)^2$$

For L-band frequencies, a 40 foot parabolic dish would yield a half-power beamwidth of about 1^o. Thus

$$\alpha_1 = 0.25$$

$$T_a = (0.25)(1.5 \times 10^{5o}K)$$

$$T_a = 3.75 \times 10^{4o}K = 45.7 \text{ db}$$

For such a large antenna temperature,

$$T_s \approx T_a = 45.7 \text{ db}$$

From comparison with Table 3.3, this would result in a $(S/N)_{in} = 0$ db. This problem will be short lived and will not occur very often. Since the beamwidth of the ground antenna is only 1^o, the sun will pass through it fairly rapidly as the sun traverses $360^o/24$ hrs, or 1^o per four minutes. Thus the problem will last for approximately 4 minutes when it occurs. This problem could possibly be remedied by using a threshold extender at the ground station. Another solution, which would be very possible and indeed recommended for the operational case, would be to have more than one control center. These could be situated in such a manner as to insure that only one station's antenna would be looking at the sun.

B.5 ANTENNA CHARACTERISTICS

B.5.1 Main Communication Antenna (Parabolic Mesh)

size: 4.38 ft diameter
focus to diameter ratio: approximately 0.4 - 0.5
folded size: 27" long and 10" in diameter
average gain: 24.4 db
beamwidth: 10^o between 3 db points
efficiency: 55%
pointing: 30^o N latitude, 37.5^o W longitude
polarization: circular

B.5.2 Interferometer Antennas (Parabolic reflector)

size: 2.92 ft diameter
focus to diameter ratio: app. 0.4 - 0.5
folded size: 18" long and 5" in daimeter
average gain: 21 db
beamwidth: 15^o between 3 db points
efficiency: 55%
pointing: 30^o N latitude, 37.5^o W longitude
polarization: circular

B.5.3 Telemetry, Tracking, and Command Antennas

B.5.3.1 Enroute to station

1 spiral wire antenna around apogee motor
3 cavity backed spirals spaced 120^o around the satellite body
1 cavity backed spiral located on the side opposite the apogee motor

Cavity backed spiral typical characteristics: (Reference 3.6)

VSWR: 2.0
Gain: 6 db
3 db beamwidth: 70^{o}
polarization: circular
frequency band: 10:1 ratio
size: 5.5" diameter
3.0" deep

B.5.3.2 On Station

type: Helical wire (end-fire)
pitch angle: 12.5^{o}
beamwidth: 17^{o} at 1.7 GHz
11.6^{o} at 2.2 GHz
circumference: 1.2 wavelengths (0.7 ft)
diameter: 0.22 feet
length: 3.72 feet
number of turns: 24
polarization: circular
efficiency: 55%
gain: 18.8 db at 1.7 GHz
22.2 db at 2.2 GHz
transit storage: compressed and deployed on command

RANGE SIGNAL MODULATION

$(\text{Sidetone})_1 = 100$ Hz

$(\text{Sidetone})_2 = 10$ KHz

"Message" bandwidth = $B_m = 10.1$ KHz

$D = 2$

$\gamma = 0.1$

From Reference 3.3, $\beta = 3.1$

$\Delta f_c = 2B_m = 20.2$ KHz

$B_{IF} = 62.6$ KHz

allowing 4.40 KHz for Doppler shift and frequency instability (Doppler $\approx$ 1.5 KHz, frequency $\approx$ 1 part in 10^6)

$$B_{IF} = 67 \text{ KHz} = 48.3 \text{ db}$$

Threshold condition:

$$(S/N)_{in,th} = 5 + 5 \log_{10} (B_{IF}/2B_m) \text{ in db}$$

$$(S/N)_{in,th} = 7.6 \text{ db}$$

B.7 NAVIGATIONAL DATA MULTIPLEXING

B.7.1 Range data

Before transmission the range signals are taken down to an IF frequency of 200 KHz. From Appendix B.6 the IF bandwidth is 67 KHz. Along with the transponded range tones, the reference tones will also be multiplexed. The message bandwidth will thus be about 275 KHz (54.4 db) allowing for sufficient guard band. Using a deviation ratio of two, the IF bandwidth becomes

$$\Delta f_c = 2B_m = 550 \text{ KHz}$$

$$B_{IF} = \beta \Delta f_c = 3.1 \text{ (550 KHz)}$$

$$B_{IF} = 1.705 \text{ MHz (62.3 db)}$$

Threshold condition

$$(S/N)_{in,th} = 5 + 5 \log_{10} (B_{IF}/2B_m)$$

$$(S/N)_{in,th} = 7.45 \text{ db}$$

B.7.2 Angle Data

As stated in Section 2.5 , the two angle signals are mixed to give a difference frequency of 3 KHz. The signals from both interferometers plus the reference signal will need to be multiplexed. Each of the three signals will be modulated onto a subcarrier prior to multiplexing. These subcarriers will be spaced 50 KHz apart yielding a message bandwidth (plus guard bands) of 125 KHz. Using a deviation ratio of two

$$B_m = 125 \text{ KHz}$$

$$D = 2$$

$$\Delta f_c = 250 \text{ KHz}$$

$$B_{IF} = (3.1)\ (250\ KHz)$$

$$B_{IF} = 775\ KHz = (58.9\ db)$$

Threshold Condition:

$$(S/N)_{in,th} = 5 + 5 \log_{10}(B_{IF}/2B_m)\ in\ db$$

$$(S/N)_{in,th} = 7.45\ db$$

B.8 TELEMETRY, TRACKING AND COMMAND

B.8.1 Telemetry

A block diagram of the telemetry and command subsystem appears in Figure B.3. An S-band helical antenna will be used to transmit and receive the PCM/FM signals. To provide redundancy, the receiver portion of the S-band tracking transponder may be designed to receive the command signals should both of the two telemetry command receivers fail.

The prime commutator will contain 16 channels with 2 of these being used for redundancy. The redundant channels will be designed for a dual mode capability. The first mode will serve as a backup for any of the other prime channels should one of them fail. The second mode of operation will be initiated on command from ground if one of the inputs to the subcommutator begins to vary away from normal. In this manner, any one of the subcommutator channels can be inspected much more frequently. The prime commutator channels are shown in Table B.2. A second prime commutator is supplied for redundancy.

The subcommutators (one redundant) sample 20 channels with one channel unassigned. The channel assignments are listed in Table B.3. These channels are used for slowly varying functions. In addition to the telemetering of housekeeping functions, all commands will also be telemetered as a check. These are not required to go through the commutators as they are already coded.

The subcommutator will sample at a rate of 0.1 samples/sec while the prime commutator will sample at a rate of 2 samples/sec. Since each channel contains 8 bits per sample, the prime data rate will be

$$(8\ bits/sample)\left(\frac{2\ samples/sec}{channel}\right)\ (16\ channels)$$

or

256 bits per second (bps)

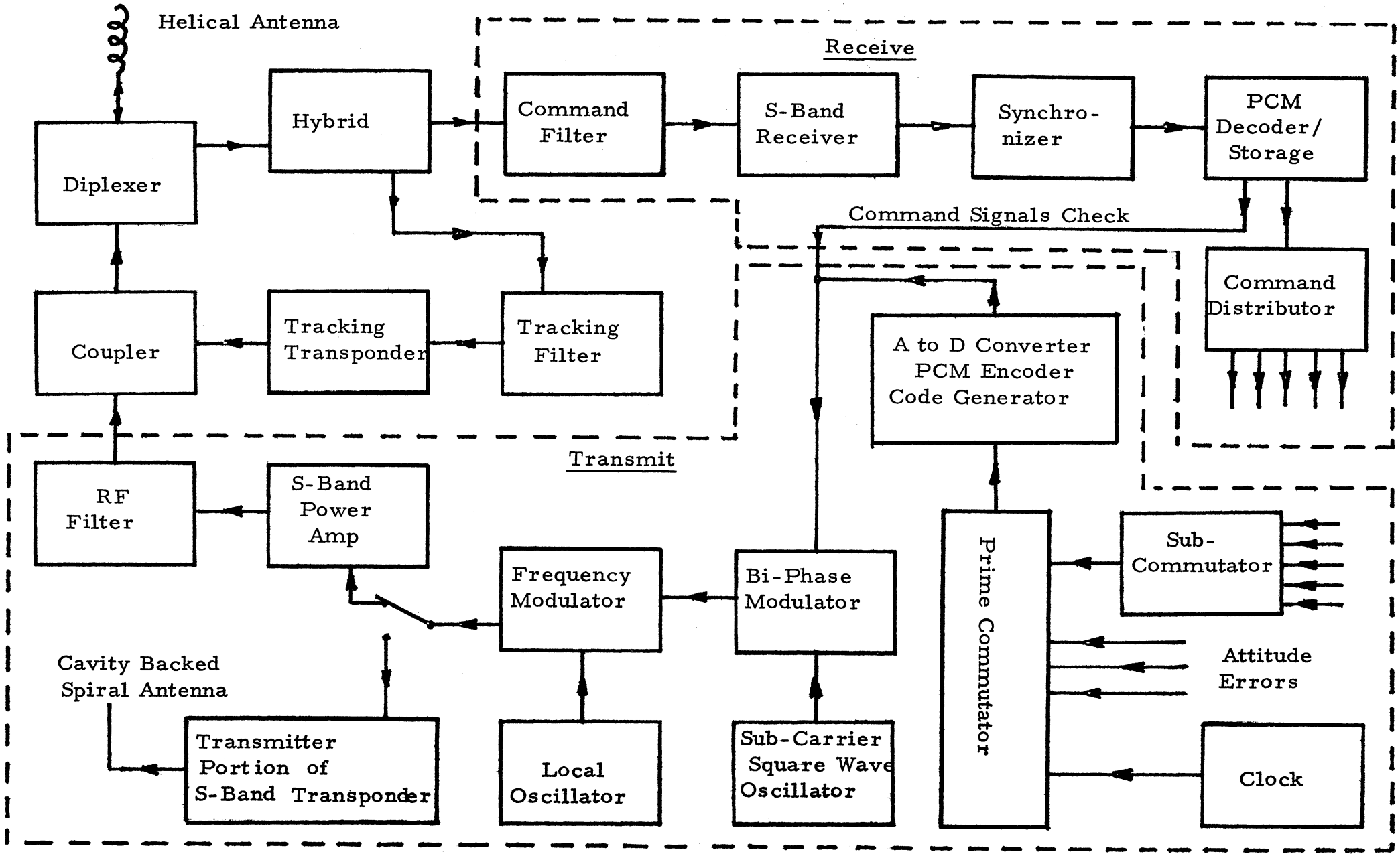

Figure B.3 Telemetry, Tracking and Command Subsystem

Table B.2 Prime Channels

Channel	Function
1	subcommutator
2	time signals
3-9	yaw, roll and pitch errors
10-13	attitude & control computer outputs
14	synchronization

Table B.3 Sub-Commutator Channels

Channel	Function
1-2	battery voltage and temperature
3-6	solar array voltage and angle
7-10	fuel pressure and temperature
11-13	yaw, roll and pitch wheel RPM's
14	communication antenna feed position
15-18	thruster status (0.05 lb)
19	thruster status (10 lb)

The encoding technique has not been specified. A sufficient encoding technique should be used to allow for error detection and correction in the data bits. A possible technique is the one-half convolution code. In order to perform the link calculations, a bit rate of 512 bps was selected as supplying sufficient room for the encoding technique to be inserted with the prime data rate of 256 bps.

The coding of the composite (prime data plus error detecting and correcting code) signal will be performed by a Bi-Phase technique. This technique performs a polarity ("1" or "-1") change at the beginning of each bit and also in the middle of the bit if the bit is a "one". An example is shown in Figure B.4

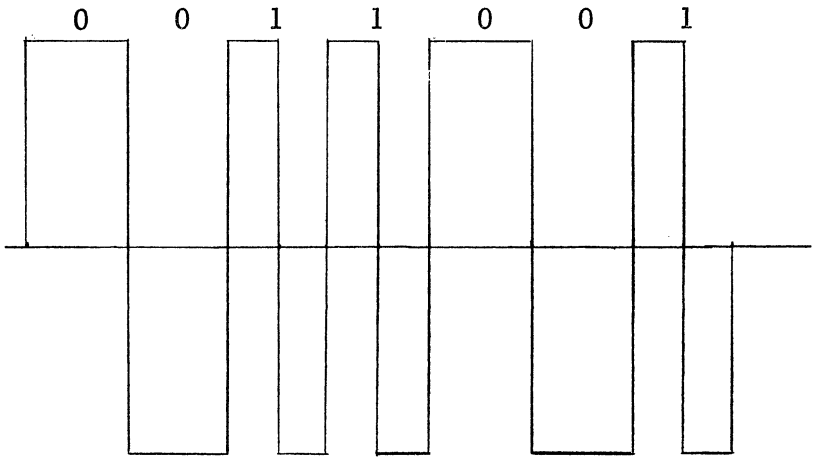

Figure B.4 Digital Stream with Bi-phase Code

From Reference 3.7, p 246, the IRIG recommended RF bandwidth is 1.5 to 3.0 times the bit rate for PCM/FM systems. Selecting a message bandwidth of one half the bit rate results in a bandwidth of 256 Hz. Using a deviation ratio of 0.71 the IF bandwidth becomes 1.46 KHz (approximately 3 times the bit rate). For a bit error requirement of one bit in 10^6 bits, the required S/N_o is 40.1 db. The FM receiving $(S/N)_{in}$ at threshold is 7.3 db. The above parameters are determined in Appendix B.9. The link calculations appear in Appendix B.10 and from them it is evident that the 1 watt RF output of the telemetry transmitter will be sufficient for the desired bit error.

Redundancy is accomplished by supplying a backup for vital components. The redundant parts can be identified by a quick glance at Appendix B.2 (telemetry section). Redundancy has also been introduced as discussed in the various operational modes above.

B.8.2 Tracking

Tracking will be performed as mentioned in section 3.4. Both the VHF beacon and the S-band transponder will provide 1 watt RF output power. The link calculations in Appendix B.10 show that this is enough power to provide an adequate S/N for tracking as well as for telemetry. Prior to the on station operation a power divider will be used to relay the signals to the various tracking transponder antennas. To save power, the incoming tracking signal could be used to trigger a circuit which will supply the transponded signal to the antenna which is facing the earth at that time. Since the delay through the satellite is on the order of several microseconds, the rotation of the satellite will not be so great as to cause an error in transmitting via the wrong antenna.

The tracking prior to on station will employ the use of four cavity backed spiral antennas, three spaced 120° around the satellite body and one on the end opposite the apogee motor, and a conical wire wrapped around the apogee motor. This antenna configuration should provide adequate coverage no matter what configuration the satellite may be in relative to ground. Since nulls may occur, a 10 db loss was included in the link calculation. The antennas are described in Appendix B.5, and a diagram of a typical tracking transponder is shown in Figure B.5.

B.8.3 Command

Commands will be given in a three step format to insure that spurious signals do not trigger one of the command circuits. This format uses an enabling command to prepare the system for the command, an operational command, and an execute command which unlocks the decoder to allow the command to be executed. Prior to ground transmission of the operational and the execute commands, the satellite telemetry system will transmit the previous signal as a verification that it has received the correct command. Upon verification that the satellite has received the correct signal, the ground station will transmit the next format sequence until the execute command is given. This mode of operation requires an onboard storage capability which has been provided. The various command signals are summarized in Table B.4.

Table B.4 Command Signals

enable

execute

reset gyros

computer on

thrusters on-off

boom deploy

solar panel deploy

antenna deploy

communication subsystem on

activate inertia wheels

communication antenna steering

redundant components on

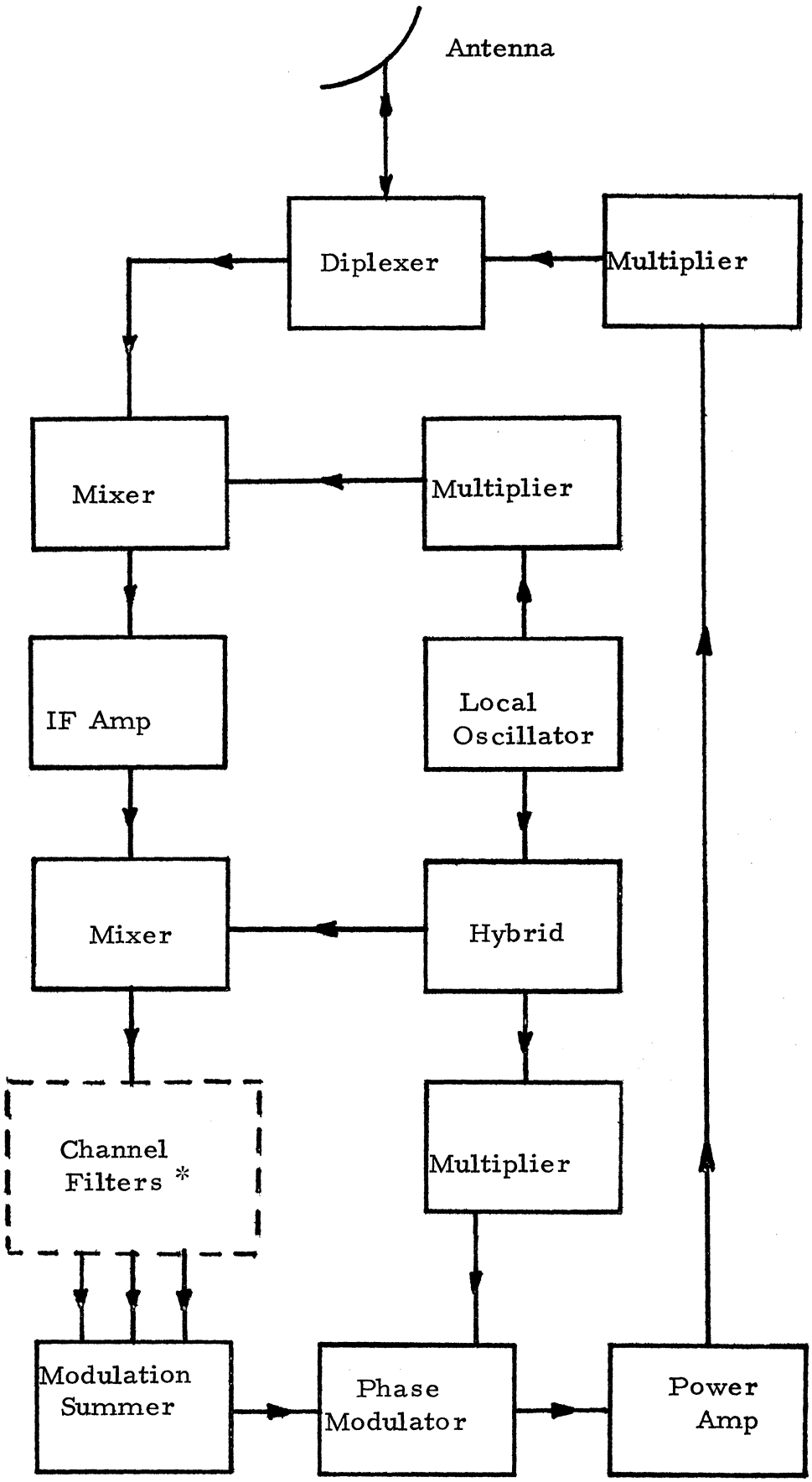

*One filter for each tracking station frequency

Figure B.5 Satellite Tracking Transponder

B.9 PCM/FM PARAMETERS

$$B_m = 1/2\ R_b$$

where B_m = message bandwidth

R_b = bit rate

$$B_m = \frac{1}{2}(512 \text{ bps})$$

$$B_m = 256 \text{ Hz}$$

From Reference 3.8 the optimum detection occurs for a deviation ratio of 0.71. Choosing $\gamma = 0.01$, from Reference 3.3

$$\beta = 8$$

$$\Delta f_c = (D)(B_m)$$

$$\Delta f_c = (0.71)(256 \text{ Hz})$$

$$\Delta f_c = 182 \text{ Hz}$$

$$B_{IF} = \beta\ \Delta f_c$$

$$B_{IF} = 8(182 \text{ Hz})$$

$$B_{IF} = 1.46 \text{ KHz} = 31.6 \text{ db} \quad (B_{IF} = 2.8\ R_b)$$

Threshold condition

$$(S/N)_{in,th} = 5 + 5 \log_{10} (B_{IF}/2B_m) \text{ in db}$$

$$(S/N)_{in,th} = 7.3 \text{ db}$$

From reference 3.8, for a bit error of one bit in 10^6 bits,

$$10 \log_{10}(E_b/N_o) = 13 \text{ db}$$

where E_b = received energy per bit

N_o = noise power density

$$S/N_o = (E_b/N_o)\ R_b$$

$$S/N_o = 13 \text{ db} + 10 \log_{10} R_b$$

$$S/N_o = 13 \text{ db} + 10 \log_{10}(512)$$

$$S/N_o = 40.1 \text{ db}$$

B.10 TELEMETRY LINK CALCULATIONS

	db
sat. transmitter power	0 (1 watt)
sat. antenna coupling loss	-1
sat. antenna gain (transmit)	+18.8
sat. off-beam losses	-1.5
free space attenuation	-190.0
atmospheric attenuation	-3.0
polarization loss	-0.5
gnd. antenna gain (40' parabolic dish)	+43
gnd. off-beam loss	-0.5
gnd. coupling loss	-0.5
gnd. effective system temperature	-20
Boltzman constant	+228.6 db/^{o}KHz
other system losses	-2

S/N_o = 71.4 db-Hz (on station)

$(S/N)_{in}$ = 39.8 db

Prior to on station operation, the gain of the cavity backed spiral antennas is 6 db and off-beam losses due to nulls may amount to 10 db, thus

S/N_o = 50.1 db-Hz

$(S/N)_{in}$ = 18.5 db

APPENDIX C
ATTITUDE AND CONTROL

C.1 CONSOLIDATED DESCRIPTION OF SYSTEM MODES

Launch Mode

1) Spin-up of body-mounted position gyros
2) Launch
3) Removal of fairing
4) Third-stage burn at perigee
5) Despin of third-stage and satellite using yo-yo despin mechanism
6) Separation of satellite from third stage
7) Attitude determination using data from sun sensors, reduced by onboard computer
8) Reset gyros
9) Attitude corrections made for second perigee burn using 0.05 lb thrusters
10) Second perigee burn by firing pair of 10 lb thrusters
11) Attitude determination using sun sensors
12) Reset gyros
13) Attitude corrections made for apogee burn using the 0.05 lb thrusters
14) Spin-up of satellite using 0.05 lb thrusters
15) Apogee burn using solid propellant apogee motor

Rendezvous Mode

16) Despin satellite using 0.05 lb thrusters
17) Attitude determination using sun sensors
18) Reset gyros
19) Attitude corrections made for rendezvous burn by using 0.05 lb thrusters
20) Rendezvous by firing pair of 10 lb thrusters
21) Arrival on station

Initial Stabilization Mode

22) Acquisition of Earth by planar scanner using gyro and sun sensor information fed into the onboard computer which would fire appropriate 0.05 lb thrusters
23) All rotational errors corrected by activating appropriate reaction wheels
24) Deployment of booms and solar panels

On Station Mode

25) Continual pitch and roll attitude sensing by planar scanner. Yaw sensing and redundant pitch and roll sensing through sun sensors and position gyros

26) Resetting of gyros using planar scanner and sun sensor information.
27) Attitude control maintained by feeding sensing information into the onboard computer. Any errors would activate appropriate reaction wheels in conjunction with the 0.05 lb thrusters for unloading of the wheels.
28) All firing signals sent to the thrusters will be in a square wave pattern, resulting in pulses which allow higher accuracies since inherent system inaccuracies will, in this way, be accounted for by proper 'tuning' of thruster firing time.

Station-Keeping Mode

29) All translational position fixes will be made by ground tracking stations. Drift corrections will be computed on the ground, telemetered to the satellite, and stored in the onboard computer for future execution.

Back-Up System Mode

30) The telemetry link will provide the means to overcome two possible failure modes:
A. Onboard computer failure: All sensing information telemetered to ground where it is processed. Error signals telemetered back to satellite to activate appropriate reaction wheels and thrusters.
B. Failure of all sensors: Ground determination of attitude by measuring phase differences in interferometer signals using fixed position transmitters on Earth. Information then telemetered to satellite.

C.2 ATTITUDE AND CONTROL COMPONENT SPECIFICATIONS

Component	Weight	Power
Hydrazine fuel	30.00 lbs	None
Pressurization system	30.00 lbs	None
Sixteen 0.05 lb thrusters	2.24 lbs	6 watts
Two 10 lb thrusters	1.40 lbs	
Three reaction wheels	30.30 lbs	13.8 watts
Three position gyros	10.00 lbs	5.2 watts
One planar scanner	3.00 lbs	4 watts
Five sun sensors	3.12 lbs	3 watts
Sensor electronics	3.50 lbs	
Computer	4.00 lbs	8 watts
TOTALS	117.56 lbs	40 watts

C.3 CALCULATION OF DISTURBING TORQUES ON STATION

A. Solar Pressure

$$\tau = A \cdot M \cdot P$$

where τ = Torque due to solar pressure
A = Area of Satellite
M = C.P. - C.M. offset
P = Radiation pressure constant for a totally reflective surface
C.M. - C.P. offset along satellite centerline (Max) = 0.198 ft
A(Max) = 72.5 ft^2
P = 1.865×10^{-7} lb-ft^2

Hence

$$\tau(\text{Max}) = (1.865 \times 10^{-7})(72.5)(0.198)$$

$$\tau(\text{Max}) = 26.7 \times 10^{-7} \text{ ft-lbs}$$

This torque is cyclic each day as shown

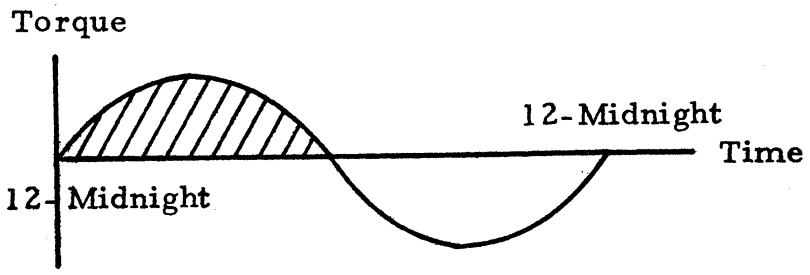

Total momentum absorbed in one 12 hr period is:

$$M\ (\text{Max}) = 2.67 \times 10^{-6} \text{ ft-lb } (4.32 \times 10^{4} \text{ sec})\ (2/\pi)$$

which is the area under the above sine curve for a 12 hr period.

$$M\ (\text{Max}) = .0735 \text{ ft-lb-sec/12 hr}$$

This is cancelled out during the next 12 hr period.

B. RF Radiation Pressure

One kilowatt of transmitted power yields

$$7.5 \times 10^{-7} \text{ lbs of force.}$$

$$\tau(\text{Max}) = M\ (7.5 \times 10^{-7} \text{ lbs/kilowatt}) \cdot P$$

where P = Transmitted power = 0.08 kilowatts
M = Offset of antenna dish from C.M. = .5 ft.

Hence

$$\tau \text{ (Max)} = (0.08)(7.5 \times 10^{-7})(0.94) = .3 \times 10^{-7} \text{ ft-lbs.}$$

This torque acts along the negative pitch axis. For a two-year period, this results in a momentum of $M = (.3 \times 10^{-7})(6.3072 \times 10^{7}) = 1.91$ ft-lb-sec.

C. Gravity Gradient

$$\tau_P = 1.5\ \omega_o^2 (I_R - I_Y) \sin 2\theta_P$$

$$\tau_R = 2\ \omega_o^2 (I_P - I_Y) \sin 2\theta_R$$

$$\tau_Y = 2\omega_o^2 (I_P - I_R) \sin 2\theta_Y$$

The above equations ignore second-order cross coupling effects.

τ_P = Pitch torque

τ_Y = Yaw torque

τ_R = Roll torque

ω_o = Orbital rate

I = Moments of inertia around respective axes

θ - Error from desired orientation

$\omega_o = 0.728 \times 10^{-4}$ rad/sec

$\theta_R = \theta_P = \theta_Y = \pm 1^{\circ}$ Max

$I_R = 923$ ft^2-slug

$I_P = 840$ ft^2-slug

$I_Y = 1250$ ft^2-slug

$\sin 2\theta = \sin (\pm 2^{\circ}) = \pm 0.035$

Hence

$$\tau_P = \overline{+}\ 9.1 \times 10^{-8} \text{ ft-lbs}$$

$$\tau_R = \overline{+}\ 15.25 \times 10^{-8} \text{ ft-lbs}$$

$$\tau_Y = \overline{+}\ 0.767 \times 10^{-8} \text{ ft-lbs}$$

D. Thruster Misalignment

During a translational dirft correction, a torque could be exerted on the satellite due to misalignment of the translational thrust vectors. The magnitude of this torque and the resulting momentum is calculated for an assumed misalignment of 0.1 inches.

Torque = Thrust x Misalignment

$$\tau = 2\ (0.05\ \text{lb})(0.1\ \text{in})(1\ \text{ft}/12\ \text{in})$$

$$\tau = 8.35 \times 10^{-4}\ \text{ft-lbs}$$

Momentum = Torque x Duration of thrust

$$M = \tau\ \Delta\ t$$

From $F = ma = m_s \frac{\Delta V}{\Delta t}$

where m_s = satellite weight

$$\Delta t = \frac{m_s \Delta V}{F}$$

For a two-year period, $\Delta V = 6.46$ ft/sec for drift corrections.

$$m_s = 521\ \text{lbs}$$

$$F = 2\ (0.05) = 0.10\ \text{lbs}$$

Hence

$$M = \frac{m_s \Delta V}{F} = (8.35 \times 10^{-4})\ \frac{(521)\ (6.46)}{(32.174)(0.1)}$$

$$M = 0.875\ \text{ft-lb-sec}/2\ \text{yrs}$$

C.4 REACTION WHEEL UNLOAD CALCULATIONS

For a 12 hr period, the momentum imparted to the satellite due to solar pressure is 0.0735 ft-lb-sec (Appendix C. 3. A). Since the reaction wheels can absorb 1.456 ft-lb-sec, they will not have to be unloaded during this 12 hour period. During the next 12 hours, the second half of the solar pressure cycle is reversed, resulting in a net momentum of zero without having to unload the reaction wheels. This cycle is continuous during the two-year operational life of the satellite.

The momentum resulting from RF radiation pressure and thruster misalignment totals 2.785 ft-lb-sec for the full two-year period (Appendix C. 3. B and D), which would require only two unloadings.

The gravity gradient torque acts only when there is an excessive rotation in the attitude of the satellite. Sufficient capability to counterbalance these torques is allowed for in the fuel contingency factor.

The time and fuel required to perform a reaction wheel unloading is calculated below:

Since $M = \tau \Delta t$ $\qquad \Delta t = \frac{M}{\tau}$

where M = Momentum to be unloaded
τ = Torque produced by thrusters during unloading

Using the minimum torque in order to find the maximum fuel required:

$$\tau = 0.1917 \text{ ft-lb}$$

And since

$$M = 1.456 \text{ ft-lb-sec per unloading}$$

$$\Delta t = \frac{1.456}{.1917} = 7.6 \text{ sec.}$$

Also, since

$$\frac{F\Delta t}{I_{sp}} = m_e$$

where F = 0.10 lbs
m_e = lbs of fuel required
I_{sp} = 150 sec

$$m_e = \frac{(.10)(7.6)}{150} = 0.00506 \text{ lbs per unloading}$$

C.5 MISALIGNMENT TORQUE OF THE TEN POUND THRUSTERS

The 10 lb thrust rocket motors are fired only while the satellite is in a folded configuration. They are used in a non-spinning mode both before and after apogee burn. For this type of firing mode, a possible 0.25° thrust vector misalignment is assumed.

Before apogee burn, the center of gravity is located as shown:

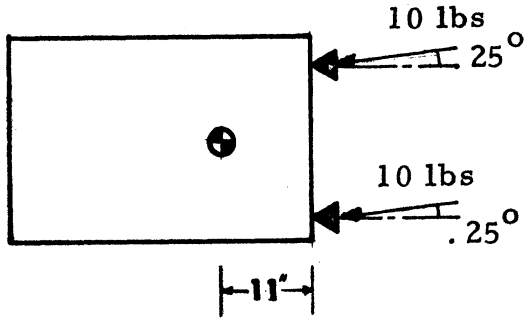

$$\text{Misalignment torque} = \tau = 2(10 \text{ lbs})\left(\frac{11}{12} \text{ ft}\right)(\sin .25^{\circ})$$

$$\tau = 20\ (.004)$$

$$\tau = 0.08 \text{ ft-lbs}$$

The duration of action of this torque is also the firing time of the 10 lb thrusters for a ΔV of 60 fps before apogee burn.

$$\Delta t = \frac{m_s \Delta V}{F}$$

where m_s = satellite weight = $\frac{1020}{32.174}$ = 31.7 slugs

F = 20 lbs

ΔV = 60 fps

$$\Delta t = \frac{(31.7)(60)}{20} = 95.1 \text{ sec} = 1.59 \text{ min}$$

The momentum due to this misalignment torque is given by:

$$M = \tau \Delta t$$

$$M = (.08)(95.1) = 7.61 \text{ ft-lb-sec.}$$

To counteract this torque and resulting momentum, a torque of 0.1917 ft-lbs is available for roll, and a torque of 0.2333 ft-lbs for pitch and yaw by using the 0.05 lb thrusters. The minimum torque is used in the following calculations to determine the maximum amount of fuel required for counterbalancing the misalignment torque.

$$t = \frac{M}{\tau} = \frac{7.61}{0.1917} = 39.8 \text{ sec total firing}$$

time, pulsed during firing of the 10 lb thruster. The fuel required is given by:

$$m_e = \frac{F \Delta t}{I_{sp}}$$

where F = 0.10 lbs

I_{sp} = 150 sec

$$m_e = \frac{(0.10)(39.8)}{150} = 0.0265 \text{ lbs}$$

After apogee burn, but still in the folded state, the satellite c.g. is located as shown:

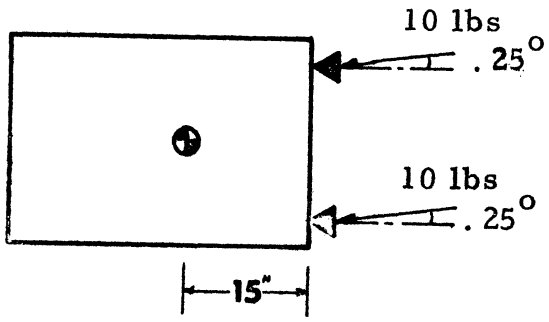

Misalignment torque = $\tau = 2(10\ \text{lb})(15/12)(\sin .25^{\circ})\text{ft}$. The duration of action of this torque is the firing time of the 10 lb thrusters for a ΔV of 163 fps after apogee burn.

$$\Delta t = \frac{m_s \Delta V}{F}$$

where $m_s = \frac{521}{32.174} = 16.2$ slugs

$F = 20$ lbs

$V = 163$ fps

$$\Delta t = \frac{m_s \Delta V}{F} = \frac{(16.2)(163)}{20} = 132 \text{ sec} = 2.2 \text{ min.}$$

The momentum due to this torque is $M = \tau \Delta t$

$$M = (0.1090)(132) = 14.4 \text{ ft-lb-sec.}$$

Again, the minimum restoring torque available is used to determine the maximum amount of fuel necessary to counterbalance the misalignment torque:

$$\Delta t = \frac{M}{\tau} = \frac{14.40}{0.1917} = 75.2 \text{ sec, again pulsed during the 10 lb}$$

thruster firing time of 132 sec. The fuel required is:

$$m_e = \frac{F \Delta t}{I_{sp}} = \frac{(0.10)(75.2)}{150} = 0.0501 \text{ lbs.}$$

C.6 CALCULATIONS FOR ORIENTATION MANEUVERS

The time required to rotate the satellite by an amount θ_t (assuming zero initial spin rates) is given by:

$$\Delta t = \sqrt{\frac{2 I_y \theta_t}{\tau}}$$

The total fuel weight required for two reaction jets working in conjunction to effect a rotation of θ_t is given by (Reference 4.3)

$$m_e = \frac{4 I_y \theta_t}{I_{sp} \ell \Delta t}$$

where ℓ = separation distance between thrusters

The effective torques and thruster separation distances (from Figure 4.8.1) are:

$\tau_x = 0.1917$ ft-lbs $\quad\quad \ell_x = 46$ in $= 3.83$ ft

$\tau_y = 0.2333$ ft-lbs $\quad\quad \ell_y = 56$ in $= 4.66$ ft

$\tau_z = 0.2333$ ft-lbs $\quad\quad \ell_z = 56$ in $- 4.66$ ft

$I_{sp} = 150$ sec.

In calculating the burn time and fuel required for 360° rotational maneuvers about each axis before apogee burn, the appropriate values of the moments of inertia are:

$I_{xx} = 44$ ft^2-slug

$I_{yy} = 41.5$ ft^2-slug

$I_{zz} = 31.4$ ft^2-slug

Using the above equations, the results are:

For 360° about X, roll, axis

$m_e = 0.0359$ lbs

$\Delta t = 53.85$ sec.

For 360° about the Y, pitch, axis

$m_e = 0.0316$ lbs

$\Delta t = 47.40$ sec.

For 360° about the Z, yaw, axis

$m_e = 0.0275$ lbs

$\Delta t = 41.25$ sec.

In calculating the burn time and fuel required for 360^{o} rotational maneuvers about each axis after apogee burn, the values for the moments of inertia are changed to:

$$I_{xx} = 39.8 \text{ ft}^2\text{-slug}$$
$$I_{yy} = 34.6 \text{ ft}^2\text{-slug}$$
$$I_{zz} = 27.0 \text{ ft}^2\text{-slug}$$

Now, after apogee burn

For 360^{o} about X, roll, axis

$$m_e = 0.0341 \text{ lbs}$$
$$\Delta t = 51.1 \text{ sec.}$$

For 360^{o} about Y, pitch, axis

$$m_e = 0.0288 \text{ lbs}$$
$$\Delta t = 43.2 \text{ sec.}$$

For 360^{o} about Z, yaw, axis

$$m_e = 0.0255 \text{ lbs}$$
$$\Delta t = 383. \text{ sec.}$$

C.7 SPIN-UP AND DESPIN USING THRUSTERS

Before apogee, the satellite is spun-up around the Z-axis to achieve $\omega_z = 100 \text{ rpm} = 10.47 \text{ rad/sec}$

while $\omega_y = 0$

$\omega_x = 0$

The governing equation is $\tau_z = I_{zz}\dot{\omega}_z + \omega_x \omega_y (I_{yy} - I_{xx})$

where $\tau_z = 0.2333 \text{ ft-lbs}$

$I_{zz} = 31.4 \text{ ft}^2\text{-slug}$

$$\dot{\omega}_z = \frac{\tau_z}{I_{zz}} = \frac{.2333}{31.4} = 7.43 \times 10^{-3} \text{ sec}^{-2}$$

$$\dot{\omega}_z \Delta t = \omega_z$$

$$\Delta t = \frac{\omega_z}{\dot{\omega}_z} = \frac{10.47}{7.43 \times 10^{-3}} = 1.410 \times 10^{3} \text{ sec} = 23.50 \text{ min}$$

$$m_e = \frac{F\Delta t}{I_{sp}} = \frac{(.1)(1410)}{150} = 0.939 \text{ lbs.}$$

To despin the satellite, ω_z must be equal to but in the opposite direction of the existing spin, bringing the final spin rate to zero. After apogee burn, I_{zz} has changed to $I_{zz} = 27.0$ ft^2-slug.

$$\Delta t = \frac{\omega_z}{\dot{\omega}_z} = \frac{\omega_z I_{zz}}{\tau_z} = \frac{10.47\ (27.0)}{0.2333}$$

$$\Delta t = 1.21 \times 10^3 \text{ sec} = 20.15 \text{ min}$$

$$m_e = \frac{F\Delta t}{I_{sp}} \quad \frac{(0.1)(1210)}{150} = 0.806 \text{ lbs}$$

C.8 YO-YO DESPIN CALCULATIONS

Definition of Symbols:

I - moment of inertia about spin axis (I_{zz})
a - radius of attach fitting
L - length of one yo-yo cable ($8\pi a$)
R_i - initial spin rate
T_{max} - maximum tension in cable
M - mass of one end weight

$$M = \frac{I}{(L+a)^2 - a^2} \qquad \text{(Reference 4.4)}$$

$$M = \frac{45.246}{(19.59)^2 - (0.75)^2}$$

$$M = 3.79 \text{ lb}$$

$$T_{max} = \frac{3IR_i^2}{4} \quad \frac{3M}{2(I + 2Ma^2)}^{1/2}$$

$$T_{max} = \frac{3(10.46)^2(45.246)}{4} \left[\frac{3(0.117)}{2(45.246) + 4(0.117)(0.75)^2} \right]^{\frac{1}{2}}$$

$$T_{max} = 229 \text{ lb.}$$

APPENDIX D

POWER

D.1 LOSS FACTORS FOR SOLAR PANELS

Current:	Transmission loss, cell mismatch	0.93
	Solar constant variation	0.95
	23.5 degree maximum sun angle	0.92
Voltage:	Diode and line loss	0.95
Power :	Power conversion efficiency	0.85
	15% allowance for cell degradation	0.85

D.2 SIZE OF SOLAR PANELS

Power necessary from solar panels at beginning of life to supply required power level.

$$P_{Panel} = \frac{238 \text{ watts}}{(0.85)(0.85)} = 330 \text{ watts}$$

Current necessary from panels to supply 330 watts at 28 volts.

$$I_{Panel} = \frac{330 \text{ watts}}{(28 \text{ volts})(0.93)(0.95)(0.92)} = 14.5 \text{ amps}$$

Voltage necessary to deliver 28 volts.

$$V_{Panel} = \frac{28 \text{ volts}}{(0.95)} = 29.5 \text{ volts}$$

Number of cells per series string.

$$\#\text{Cells/string} = \frac{29.5 \text{ volts}}{0.41 \text{ volts/cell}} = 72 \text{ cells}$$

Number of cells in parallel to supply current.

$$\#\text{ Parallel cells} = \frac{14.5 \text{ amps}}{0.130 \text{ amps/cell}} = 112 \text{ cells}$$

Total number of solar cells on panels.

$$\#\text{Cells} = (72)(112) = 8064 \text{ cells}$$

D.3 BATTERY DISCHARGE

The capacity of an 18 amp-hour battery system at 28.6 volts is 515 watt hours.

$$\text{Max. depth of discharge} = \frac{311 \text{ watt-hours}}{515 \text{ watt-hours}} = 60\%$$

D.4 SYSTEM WEIGHT AND POWER SUMMARY

Battery system and case	24 lbs
Solar cells on panels	16
Aluminum panels and support	30
Drive motors (2)	4
Solar cells on body	8
Voltage Regulator (2)	12
Battery Regulator (2)	8
Power Control Unit (2)	6
Filter	2
Misc. wiring, connectors	5
Total System Weight	115 lbs

The power system requires a maximum of 18 watts used for solar panel orientation and battery charging.

APPENDIX E
THERMAL CONTROL

E.1 SYMBOLS

q_s = heat from solar radiation
q_e = heat from planet emitted radiation = 0
q_r = heat from planet reflected radiation = 0
q_{int} = heat from internal equipment
q_c = heat from conduction
q_R = heat radiated
F = shape factor = 1.0
A_R = radiating area
ϵ = emittance coefficient
σ = Stefan-Boltzman constant = 5×10^{-10} w/ft^2 $^oR^4$
T = temperature
A_p = projected area facing the sun
α_s = absorptance coefficient
S = solar constant = 130 watts/ft^2 at 1 A. U.
C_{th} = thermal capacity of segment
R = resistivity to heat flow
L = average length heat flows
k = conductance of material
A = cross-sectional area
C_p = specific heat of material
m = mass
t = time

The instantaneous heat balance equation used to determine the thermal control system is:

$$q_s + q_e + q_{int} + q_c + q_r - q_{rad} = C_{th} \frac{dT}{dt} \qquad \text{(E1)}$$

SCANNAR's internal temperatures vary slowly enough so that a simpler form of this equation may be used for the analysis with good accuracy.

$$q_{rad} = q_s + q_{int} \qquad \text{(E2)}$$

$$q_s = A_p \alpha_s S \qquad \text{(E3)}$$

$$q_R = F A_R \epsilon \sigma T^4 \qquad \text{(E4)}$$

An iteration process is used to determine the radiating areas and the temperature of the components desired. The following equations for conduction are used in the iteration process.

$$q_c = \frac{\Delta T}{R} \tag{E5}$$

$$R = \frac{L}{KA} \tag{E6}$$

The iteration process is as follows: a radiation area is assumed. q_s is computed and added to q_{int} to determine q_R. The radiating surface temperature may then be computed from equation E4. The temperature of the component, T_{comp}, is defined by the following equation:

$$T_{comp} = T_R + \Delta T \tag{E7}$$

ΔT is obtained from equation E5. If T_{comp} is too high or low, a new radiating area and/or a new R may be assumed to determine T_{comp}.

E. 2 CALCULATION OF RADIATING AREA AT $32^{\circ}F$

E.2.1. $q_{s\ max.} = (A_R/2)\ (0.2)\ (\sin 25^{\circ})\ (130\ w/ft^2)$

$= A_R\ (5.5)\ watts/ft^2$

$q_{int} = 245\ watts$

σT^4 at $32^{\circ}F = 29.41\ w/ft^2$

$(A_R)(5.5 w/ft^2) + 245w = A_R\ (0.9)(29.41\ w/ft^2)$

$A_R = 11.7\ ft^2$

E. 2. 2 T_R when $q_s = 0$ (during eclipse)

$q_{int} = 245\ w$

$A_R = 11.7\ ft^2$

$$\sigma T^4 = \frac{245\ w}{(11.7\ ft^2)\ (0.9)} = 23.3\ w/ft^2$$

$T_{low} = 4^{\circ}F$

E. 3 COMPONENT TEMPERATURES

As an illustration, the battery and computer temperatures are calculated.

E. 3. 1 Batteries when Discharging

$$R = \frac{L}{KA} = \frac{(2.62 \text{ in})\ (12 \text{ in/ft})}{(37.6 \text{ w/ft}^{\circ}\text{F})\ (0.08 \text{ in})\ (7.5 \text{ in})}$$

$$R = 1.4^{\circ}\text{F/w}$$

$$\Delta T = T_{comp} - T_R = q_{comp}\ R = (60\text{w})(1.4^{\circ}\text{F/w}) = 84^{\circ}\text{F}$$

$$T_{comp} = 84^{\circ}\text{F} + 4^{\circ}\text{F}^{*} = 88^{\circ}\text{F}$$

*Batteries will discharge when $T_R = 4^{\circ}\text{F}$ only.

E.3.2 Computer

This calculation illustrates the technique used when a component is behind another heat dissipating component with respect to the radiating surface. ΔT_{tot} will equal the ΔT between the computer and the voice communications package plus the ΔT for the voice communications package itself.

$$R = \frac{L}{KA} = \frac{(6.0 \text{ in})(12 \text{ in/ft})}{(37.6 \text{ w/ft}^{\circ}\text{F})(0.08 \text{ in})(5.0 \text{ in})}$$

$$R = 4.8^{\circ}\text{F/w}$$

$$T = (8\text{w})(4.8^{\circ}\text{F/w}) = 38.3^{\circ}\text{F}$$

Now, the ΔT of the voice communications package must be considered.

$$R = \frac{L}{KA} = \frac{(2.0 \text{ in})(12 \text{ in/ft})}{(37.6 \text{ w/ft}^{\circ}\text{F})(0.08 \text{ in})(9 \text{ in})}$$

$$R = 0.887^{\circ}\text{F/w}$$

$$T = (83\text{w} + 8\text{w})(0.887^{\circ}\text{F/w}) = 80.7^{\circ}\text{F}$$

$$T_{tot} = 80.7^{\circ}\text{F} + 38.3^{\circ}\text{F} = 119^{\circ}\text{F}$$

$$T_{comp_{max}} = 32^{\circ}\text{F} + 119^{\circ}\text{F} = 151^{\circ}\text{F}$$

$$T_{comp_{min}} = 4^{\circ}\text{F} + 119^{\circ}\text{F} = 123^{\circ}\text{F}$$

E.4 TEMPERATURE VARIATION OF BOOMS

This calculation gives the ΔT for the interferometric booms. The amount of solar input to the booms is first calculated. It is assumed that a certain amount of this heat (q_2) is conducted to the dark half of the boom. This establishes a ΔT for the boom.

An iteration process follows to determine whether the actual amount of heat conducted to the dark side is equal to the amount assumed. Knowing the values K, L, and A, and assuming an initial q_2, we can determine $\Delta T'$ from equations E5 and E6. If $\Delta T'$ does not equal ΔT, we must assume a new value for q_2.

$$\sigma T^4 = \frac{S\alpha}{F\epsilon} \quad \frac{A_P}{A_R} = \frac{(130 \text{ w/ft}^2)(0.1)}{(1.0)(0.8)} \quad (0.212) = 3.44 \text{ w/ft}^2$$

$$L = \frac{\pi r}{2} = \frac{\pi(0.75 \text{ in})}{2(12 \text{ in/ft})} = 0.0982 \text{ ft}$$

$$K = 2.48 \text{ w/ft}^{\circ}\text{F}$$

$$A = (45 \text{ ft})(0.005 \text{ in})(1 \text{ ft}/12 \text{ in}) = 1.88 \times 10^{-2}$$

1st Iteration:

$$q_2 = 1.00 \text{ w/ft}^2$$

$$q_1 = 2.44 \text{ w/ft}^2$$

Therefore,

$$T_2 = -249^{\circ}\text{F}$$

$$T_1 = -196^{\circ}\text{F}$$

$$\Delta T = 53^{\circ}\text{F}$$

$$\Delta T' = \frac{L}{KA} \quad q$$

In order to get $\Delta T'$ in the correct form, we multiply by the total area affected by the solar input which is 8.85 ft^2.

$$\Delta T' = \frac{(8.85 \text{ ft}^2)(0.0982 \text{ ft})\,(q)}{(2.48 \text{ w/ft}^{\circ}\text{F}(1.88 \times 10^{-2} \text{ft}^2)}$$

$$\Delta T' = (18.6^{\circ}F\ ft^2/w)(1.00\ w/ft^2) = 18.6^{\circ}F$$

$$\Delta T' \neq \Delta T$$

2nd Iteration

$$q_2 = 1.40\ w/ft^2$$

$$q_1 = 2.04\ w/ft^2$$

Therefore,

$$T_2 = -230^{\circ}F$$

$$T_1 = -207^{\circ}F$$

$$\Delta T = 23^{\circ}F$$

$$\Delta T' = (18.6^{\circ}F\ ft^2/w)(1.40\ w/ft^2) = 26^{\circ}F$$

We see that these values are in fairly close agreement. Therefore, we can conclude that the ΔT for the booms is approximately $25^{\circ}F$.

E.5 THERMAL TIME CONSTANT

Temperature calculations made represent maximum and minimum values only. To determine the time it takes for a component's temperature to change, the thermal time constant must be computed. The following equation will determine this constant:

$$q = C_p\, m \frac{\Delta T}{\Delta T}$$

Solving for $\frac{\Delta T}{\Delta t}$:

$$\frac{\Delta T}{\Delta t} = \frac{q}{C_p m} = \frac{(245w)(3.413\ BTU/w\text{-}hr)}{(.23\ BTU/lb^{\circ}F)(521\ lb)} = 6.96^{\circ}F/hr.$$

This is SCANNAR's thermal time constant. The same equation is used to determine the thermal time constant for each component.

APPENDIX F
STRUCTURES

The following symbols are used in the calculations of Appendix F.

α	coefficient of thermal expansion
A	area
d	diameter
E	modulus of elasticity
G	acceleration, in g's
$\underline{G}$	shear modulus
I	area moment of inertia
J	polar moment of inertia
L	length
M	bending moment
P	load
r	radius
r_a	average radius
S^a	safety factor
σ_a	total applied stress
σ_b	stress due to bending
σ_c	compressive stress
σ_{cr}	critical stress
σ_y	yield stress
t^y	thickness
T	temperature difference across a boom
W	weight
X	boom deflection parallel to boom axis
Y	boom deflection perpendicular to the boom axis
θ	angle of twist per unit length
θ_{max}	maximum angle of twist
ϕ^{max}	angle due to bending

F.1 SUPPORT TUBE ANALYSIS

The support tube is designed to support the satellite weight without buckling. If it is assumed to be a cylindrical shell bearing an axial load the correct formula for the buckling analysis is (Reference 7.1):

$$\sigma_{cr} = E \frac{.6t/r_a - 10^{-7} r_{a/t}}{1 + 0.004\ E/\sigma_y}$$

$E = 10^7$ psi
$\sigma_y = 70,000$ psi
$r^a = 11$ in
$t = .03$ in

$$\sigma_{cr} = 10^7 \quad \frac{\frac{(.6)(0.03)}{11} - \frac{(10^{-7})(11)}{0.03}}{1 + \frac{0.004\ (10^7)}{70,000}}$$

$$\sigma_{cr} = 10,600 \text{ psi}$$

The total stress is the sum of the compressive stress and stress due to a bending moment.

$$\sigma_a = \sigma_c + \sigma_b$$

$$\sigma_a = \frac{WG}{A} + \frac{Mr_a}{I}$$

W = 525 lbs
G = 16
A = 2.075 in
M = 11,020 in-lbs (16)
I = 152 in
r_a = 11 in

$$\sigma_a = \frac{(525)(16)}{2.075} + \frac{11,020\ (11)(16)}{152}$$

$$\sigma_a = 5,000 \text{ psi}$$

The safety factor is defined as:

$$S = \frac{\sigma_{cr}}{\sigma_a}$$

$$S = \frac{10,600}{5,000} = 2.21$$

F.2 LAUNCH RING ANALYSIS

The analysis for the launch ring follows exactly the analysis for the support tube.

For the launch ring:

E = 10^7 psi
σ_y = 70,000 psi
r_a = 10 in
t = 0.035 in

$$\sigma_{cr} = \frac{\frac{(0.6)(0.035)}{10} - (10^{-7})\frac{(10)}{(0.035)}}{1 + \frac{0.004\,(10^{7})}{70,000}}$$

$$\sigma_{cr} = 14,850 \text{ psi}$$

W = 1021 lbs
G = 16
M = (16)(1021)(115) in-lbs
A = 1.98 in^2
I = 160 in^4

$$\sigma_a = \frac{1021(16)}{1.98} + \frac{1021(16)(15)}{160}$$

$$\sigma_a = 10,010 \text{ psi}$$

$$S = \frac{14,850}{10,010}$$

$$S = 1.48$$

F. 3 BOOM DEFLECTIONS

The antenna booms are subject to solar pressure, satellite dynamics, and thermal warping. These forces can cause both torsional and bending deflections. The dynamic response of the booms is not critical to angle measurement as long as maximum deflections do not exceed $\pm 2^{o}$ which could happen if a resonant driving force was applied. The boom's damping ratio is quite small, as well as is its fundamental frequency, and care must be taken to avoid resonant modes. The only forces affecting the booms near resonant frequency are satellite dynamics arising from attitude controllers. To avoid coupling of satellite and boom dynamics the control circuit will be designed to operate at frequencies below the booms natural frequency.

Static deflections serve as upper limits for dynamic response, if resonance is neglected. These are calculated using boom characteristics (Reference 7.2).

For the booms:

EI = 6×10^{5} psi
t = 0.005 in
d = 1.5 in
$\underline{G} = 11.5 \times 10^{6}$ psi
$\Delta T = 25^{o}F$

Critical bending moment = 150 ft-lbs
Critical torque = 10 in-lbs
Damping ratio = 0.02
First cantilever frequency = 0.008 cps
L = 45 ft

F. 3.1 Torsional deflections

$$\theta = \frac{\text{Torque}}{G\ J}$$

$$J = \frac{\pi d^3 t}{4}$$

$$J = 0.01327 \text{ in}^4$$

$$\text{Torque} = 0.25 \text{ ft-lbs}$$

$$\theta = \frac{(0.25)(12)}{(11.5 \times 10^6)(0.01327)}$$

$$\theta = 2.01 \times 10^{-5} \text{ rad/in}$$

$$\theta_{max} = \theta L$$

$$= (2.01 \times 10^{-5})(45)(12)$$

$$= 0.012 \text{ rad}$$

$$= 0.69^o$$

F. 3.2 Bending Deflections

Bending deflections are due to temperature differences across the boom and to satellite dynamics. Deflections due to solar pressure are six orders of magnitude smaller than those for temperature differences or thrust loads and are thus neglected.

For a cantilever beam experiencing an end load the maximum deflection is given by (Reference 7. 3);

$$\phi_{max} = \frac{PL^2}{2EI}$$

For P = .1

$$\phi_{max} = \frac{0.1\ (45)^2(12)^2}{(2)(6 \times 10^5)}$$

$$\phi_{max} = 0.0194 \text{ radians}$$

$$\phi_{max} = 1.04^{o}$$

For the temperature difference the deflection in the direction of the boom axis is given by (Reference 7.4):

$$X = \frac{2}{3} \left[\frac{\alpha \Delta T}{d}\right]^{2} L^{3}$$

$$X = \frac{2}{3} \left[\frac{(8.5 \times 10^{-6})(25)}{\frac{1.5}{12}}\right]^{2} (45)^{3}$$

$$X = 0.173 \text{ ft.}$$

The deflection perpendicular to the boom axis is given by (Reference 7.4)

$$Y = \frac{\alpha \Delta T}{d} L^{2}$$

$$Y = \frac{(8.5 \times 10^{-6})(25)}{\frac{1.5}{12}} (45)^{2}$$

$$Y = 0.345 \text{ ft}$$

$$\phi = \text{Tan}^{-1} \left(\frac{0.345}{45}\right)$$

$$\phi = 0.44^{o}$$

Total $\phi = 1.04^{o} + 0.44^{o}$

$= 1.48^{o}$

F.3.3 Total Deflection

$$\text{Total Deflection} = \sqrt{\phi^{2} + \theta^{2}}$$

$$= \sqrt{(1.48)^{2} + (.69)^{2}}$$

$$= 1.635^{o}$$

F.4 WEIGHT BUDGET

Attitude Control and Propulsion

Apogee Motor	52
Fuel	486
Attach Fitting and Yo-Yo Despin	34
Hydrazine Thruster System	33.64
Hydrazine Fuel	30
Sensors and Electronics	13.62
Position Gyroscopes	10
Reaction Wheels	30.3
System Total	689.56 lbs

Structures and Thermal

Heat Pipes and Insulation	6.2
Booms and Boom Mechanisms	28.8
Platforms and Cover Plate	33.05
Side Panels and Stringers	22.4
Support Tube, Struts, Pins and Brackets	29.64
Hardware	6.0
System Total	126.09 lbs

Communication and Navigation

Boom Antennas	16
Communication Antenna	10
Telemetry Antennas	5.5
Voice Equipment	21.3
Navigation Equipment	45
Telemetry, Tracking and Command Equipment	25.55
System Total	123.35 lbs

Power

Batteries	24
Control System	28
Solar Panels	50
Body Cells and Wiring	13
System Total	115 lbs

TOTAL 1054 lbs

APPENDIX G

LAUNCH VEHICLE

The apogee motor chosen is a scaled down FW-4S manufactured by United Technology Center, Sunnyvale, California, a division of United Aircraft Corporation. This rocket motor uses the solid propellant PBAN (polybutadiene acrylic acid-Acrilonitrile).

Specific Impulse (I_{sp}) . . . . . 284.07 sec
Thrust, avg.-vacuum . . . . . 5,857 lbs

To obtain the amount of fuel needed, use:

$$\Delta V = I_{sp} g_o \ln \frac{(M_b + M_f)}{M_b}$$

M_f . . . . Fuel weight (lbs)

M_b . . . . Burn-out weight (534 lbs)

ΔV . . . . 5,909.173 ft/sec

And obtain,

M_f = 486 lbs.

Scaling down of FW-4S motor:

The full scale FW-4S carries 606.3 lbs of fuel, has a burning chamber length of 31.2 in, and a total length of 58.43 in (Reference 8.2). The burning chamber is scaled down linearly along the thrust axis.

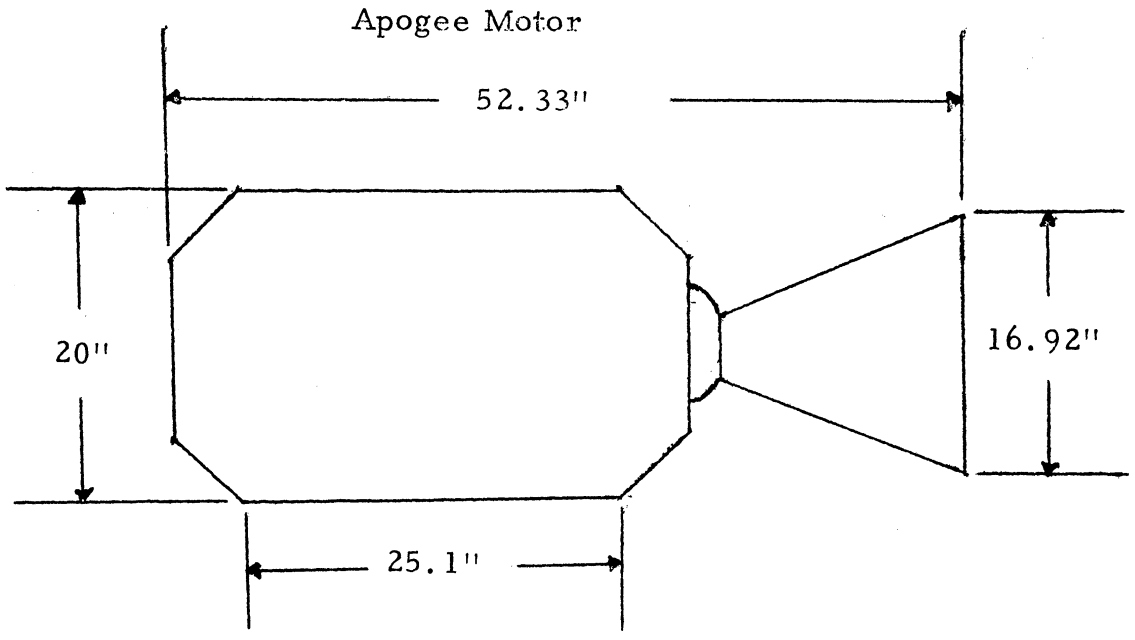

Figure G.1

Letting L_{sd} be the scaled down burning chamber length:

$$L_{sd} = 31.2 \frac{486}{606.3} \text{ in} = 25.1 \text{ in.}$$

Burning time:

$$\text{Thrust} = \frac{M_f I_{sp} g_o}{t_b g_0}$$, where t_b is the burning time in seconds.

Thus, $t_b = 23.6$ sec.

The scaled down weight of the apogee motor is 52 lbs.

Apogee motor accuracies:

The FW-4S is a solid fuel motor and the nominal accuracy given by industry is a $\pm$ 0.5% deviation in the given value I_{sp} for the fuel. Because ΔV is directly proportional to I_{sp}, the apogee burn accuracies are:

$\Delta V = \pm 0.005 (5,909.173)$ ft/sec $= \pm 29.55$ ft/sec.

APPENDIX H
ORBITAL ANALYSIS

H.1 BASIC KEPLERIAN ORBIT PARAMETERS

A. Physical Constants

$\mu = 1.40765392 \times 10^{16}$ ft^3/sec^2

ω_E = 2π radians/sidereal day

$= 7.2921 \times 10^{-5}$ radians/sec

τ_E = 1 sidereal day = 86164.09 sec

r_E = earth radius = 3443.9367 nm

$= 2.09257 \times 10^{7}$ ft

1 nautical mile (International) = 6076.11 feet

B. Circular Parking Orbit Parameters

r_{pkg} = 3543.9367 nm

$V_{lc_{pkg}}$ = 25,567.7 ft/sec (circular velocity)

τ_{pkg} = 88 min 11 sec

C. Synchronous Circular Orbit Parameters

$\tau_{syn} = \tau_E$ = 86164.09 sec

$\omega_{syn} = \omega_E = 7.2921 \times 10^{-5}$ rad/sec

r_{syn} = 22,766.90 nm $= 1.3833421 \times 10^{8}$ ft

$V_{lc_{syn}}$ = 10,087.5 ft/sec (circular velocity)

h_{syn} = 19,322.97 nm $= 1.17408 \times 10^{8}$ ft

D. Keplerian Orbit Equations

Most of SCANNAR's trajectory analysis was made using these Keplerian orbital equations:

(1) $r_a V_a = r_p V_p$

(2) $2a = r_a + r_p$

(3) $V_{lc} = \sqrt{\frac{\mu}{r}}$ (circular velocity)

(4) $V = V_{lc} \sqrt{2 - \frac{r}{a}}$

(5) $\tau = \frac{2\pi a^{3/2}}{\sqrt{\mu}}$ (orbital period)

where: subscript a refers to apogee
subscript p refers to perigee
a refers to the orbit semi-major axis

H.2 CALCULATION OF THE LOCATION OF APOGEE LONGITUDE FOR NOMINAL AND OFF-NOMINAL CONDITIONS

From Table 9.1, ignition for first transfer orbit after 5 1/2 parking orbits sets the first perigee longitude at 62.5° E longitude. Figure H.1 below, shows a typical complete transfer to synchronous altitude.

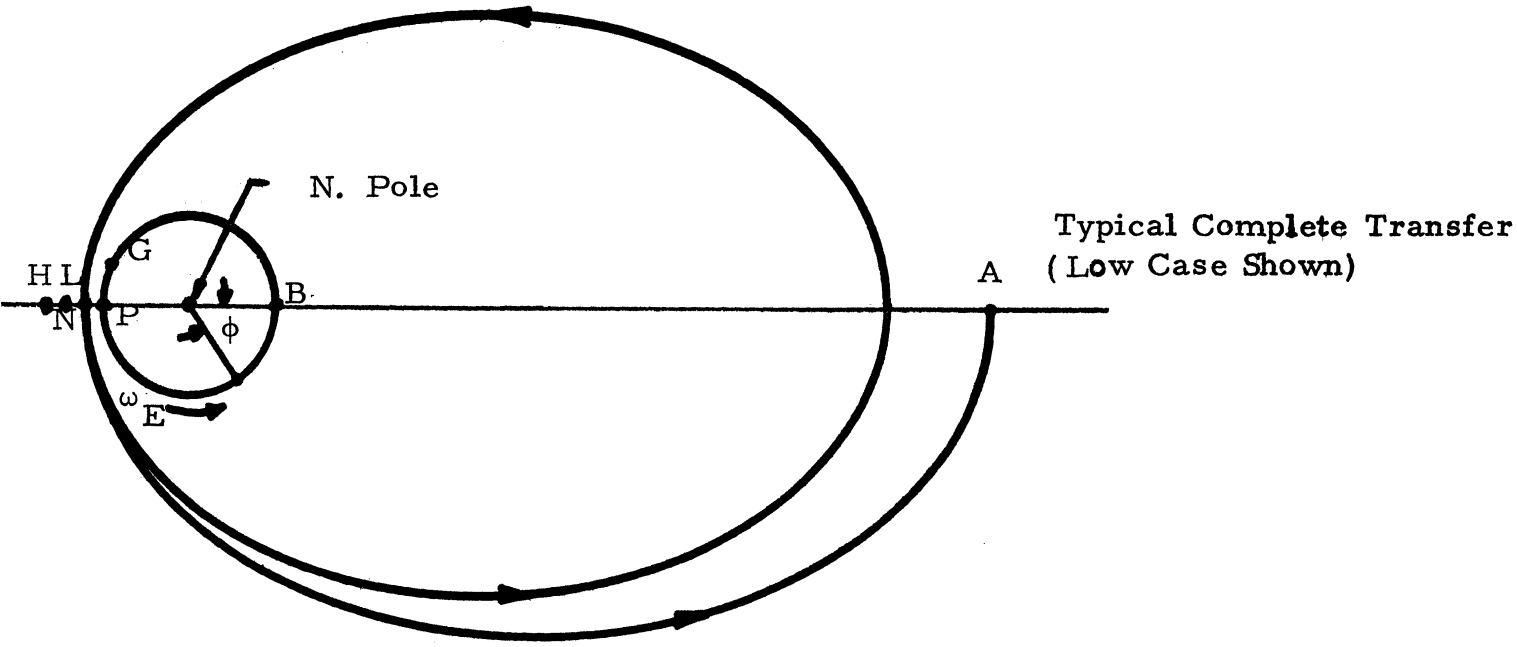

Figure H.1

where: N represents nominal orbit (100 nm)
L represents low orbit (90 nm altitude)
H represents high orbit (110 nm)
G represents the meridian of Greenwich
A represents the longitude of apogee of the second transfer ellipse
ϕ represents the angular rotation of the earth during the transfer
P represents the longitude of first perigee
B represents a point 180 degrees opposed from point P

At the time of the first perigee burn:

P is at 62.5° E so B is at 117.5° W

The earth is considered to rotate eastward at a rate of

360° per 24 hours

It is understood that the transfer from N represents the nominal transfer; and that transfer from L (low) and H (high) represent cases of worst probable error (based on booster and system inaccuracies).

A calculation of the amount of rotation of point B during transfer is made for each of the transfers from points H, N, L.

Times of transfer:

H: 59,515 seconds or 16.5319 hours
N: 58,141 seconds or 16.1503 hours
L: 56,921 seconds or 15.8114 hours

The earth's rotation, then, is given by, ϕ:

H: $\phi_H = 16.5319 \times 360^o/24 = 247.98^o$
N: $\phi_N = 16.1503 \times 360^o/24 = 242.25^o$
L: $\phi_L = 15.8114 \times 360^o/24 = 237.17^o$

Therefore, the apogee altitude will occur at longitude:

H: $B + \phi_H = 5.48^o$ W
N: $B + \phi_N = .25^o$ W
L: $B + \phi_L = 5.33^o$ E

Our nominal initial target location occurs almost directly above the prime meridian, and necessitates a drift range of 27.25^o (to arrive at 27.5^o W: the on-station location). The actual apogee will occur at a longitude between 5.33^o E and 5.48^o W longitude and could, therefore, require a maximum drift range of 32.83^o or a minimum drift range of 22.02^o.

H. 3 WALKING ORBIT DRIFT RATES

The near-synchronous orbit which SCANNAR enters after apogee burn is always higher than the synchronous orbit. Therefore, its period will always be longer than that of the synchronous orbit, causing SCANNAR to drift westward toward the on-station location at 27.5^o W. The rate of drift is dependent on the difference in orbital periods and so is given by the following equation:

$$\text{Drift Rate} = \frac{1}{\tau_{syn}} - \frac{1}{\tau_{w.o.}}$$

where: $\tau_{syn} = \tau_E = 86164.09$ sec

$$\tau_{w.o.} = \frac{2\pi}{\sqrt{\mu}} (a_{w.o.})^{3/2}$$

$a_{w.o.}$ is the semi-major axis of the walking orbit

A plot of walking orbit apogee height versus mean drift rate is given in the text as Figure 9.3.

H.4 RENDEZVOUS WITH FINAL ON STATION LOCATION

Figure H.2 shows SCANNAR in a coordinate system fixed to the on-station point or target (located at synchronous altitude and 27.5 degrees west longitude).

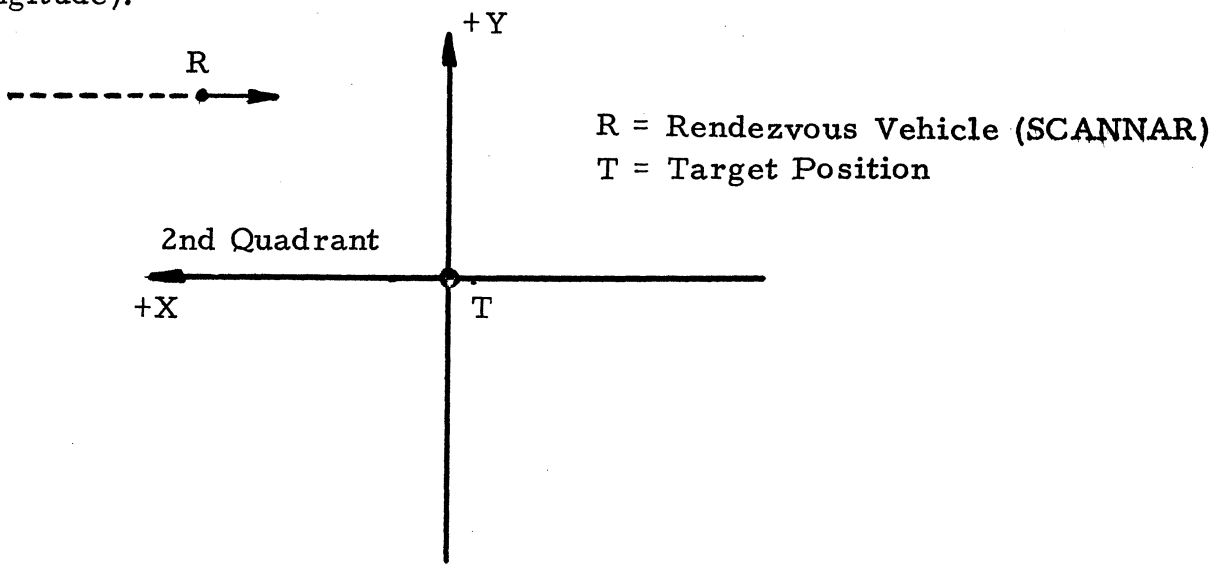

Figure H.2 Rendezvous Coordinate System

Because of SCANNAR's carefully selected walking orbit, the satellite is always higher than and ahead of the on-station position and therefore will always drift toward the target through the second quadrant of the coordinate system shown.

It is possible to rewrite the equations of motion for a point, R, in an inverse-square gravitational force field in terms of a coordinate system fixed to another point, T, also moving in the field. The only restrictions of the analysis are that the points T and R be very close to each other compared to their distances from the center of the force field, and that the target, T, be in circular orbit. SCANNAR's rendezvous phase does not violate either of these restrictions.

The equations for rendezvous are functions of the initial X and Y positions and the initial X and Y velocities as seen from the coordinate system on the target as well as functions of the specified time, T, between TPI and final vehicle coincidence (that is, the total time for the rendezvous maneuver to take place). The equations for rendezvous are presented below:

$$\dot{x}_d(0) = \frac{14y(0)\,[\,1 - \cos\omega T] - [\,6y(0)\,\omega T - x(0)]\,\sin\omega T}{T\,[\,3\sin\omega T - \frac{8}{\omega T}\,(1 - \cos\omega T)]}$$

$$\dot{y}_d(0) = \frac{-y(0)(3\omega T\cos\omega T - 4\sin\omega T) - 2x(0)\,(1 - \cos\omega T)}{T\,[\,3\sin\omega T - \frac{8}{\omega T}\,(1 - \cos\omega T)]}$$

where x(0) and y(0) are position values before TPI begins
ω is angular rate of target

since $\dot{x}(0)$ and $\dot{y}(0)$ represent initial relative velocities:

$$\Delta V_{x_{TPI}} = \dot{x}_d(0) - \dot{x}(0)$$

$$\Delta V_{y_{TPI}} = \dot{y}_d(0) - \dot{y}(0)$$

and

$$\Delta V_{TPI} = \sqrt{\Delta V_{x_{TPI}}^2 + \Delta V_{y_{TPI}}^2}$$

The braking maneuver requires the following velocity changes:

$$\Delta V_{x_B} = [\,-3\,\dot{x}_d(0) - 6\,\omega y(0)] + [\,-2\dot{y}_d(0)]\,\sin\omega T + [\,4\,\dot{x}_d(0) + 6\,\omega y(0)]\,\cos\omega T$$

$$\Delta V_{y_B} = [\,2\dot{x}_d(0) + 3y(0)\omega]\,\sin\omega T + [\,\dot{y}_d(0)]\,\cos\omega T$$

so:

$$\Delta V_B = \sqrt{\Delta V_{x_B}^2 + \Delta V_{y_B}^2}$$

The total Delta V required for the entire rendezvous maneuver is the sum of the increments required at TPI and at braking:

$$\Delta V_T = \Delta V_{TPI} + \Delta V_B$$

H.5 ORBITAL STEADY-STATE RADIUS

Definition of symbols.

r_c - synchronous satellite orbital radius
r_o - Keplarian radius
J_2 - nondimensional correction factor

R_o - radius of earth
g_o - gravitational acceleration at earth's surface
$\dot{\theta}_E$ - angular rate of rotation of earth

$$r_o^3 = \frac{g_o R_o^2}{\dot{\theta}_E^2} \qquad \text{(Reference 9.1)}$$

$$r_o^3 = \frac{(32.174)\left[(3443.9)(60\ 76.1)\right]^2}{\left(\frac{2\pi}{86164}\right)^2}$$

$$r_o = 22,766.9 \text{ nm}$$

$$r_c = r_o \left(1 + \frac{1}{2} J_2 \frac{R_o^2}{r_o^2}\right)$$

$$r_c = 22,766.9 \left(1 + \frac{(1.08 \times 10^{-3})(3443.2)^2}{2\,(22,766.9)^2}\right)$$

$$r_c = 22767.1 \text{ nm}$$

The effect of the earth's triaxiality is to increase the steady-state radius of the synchronous satellite by 0.20 nm.

H.6 CALCULATION OF TIME TO DRIFT 1° LONGITUDE

Definition of symbols.

γ - satellite angular position relative to the minor axis of earth's equatorial section
γ_o - initial value of γ
$\Delta\gamma$ - variation of γ
K_2 - modified ellipticity coefficient
$\dot{\theta}_E$ - angular rate of rotation of earth
t - time

$$\Delta\gamma = (-9 K_2 \dot{\theta}_E^2 \sin 2\gamma_o) t^2 \qquad \text{(Reference 9.1)}$$

$$t = \sqrt{\Delta\gamma / (-9 K_2 \dot{\theta}_E^2 \sin 2\gamma_o)}$$

$$t = \sqrt{\frac{-1.74 \times 10^{-2}}{(-9)\left(\frac{2\pi}{86164}\right)^2 (-5.35 \times 10^{-6})\left(\frac{3443.2}{22,766.9}\right)(-0.19)}}$$

$$t = 43.2 \text{ days}$$

The time for a synchronous earth satellite nominally positioned at $27^{o}30'$ W longitude to drift 1^{o} longitude is 43.2 days.

H.7 CALCULATION OF VELOCITY CHANGE PER UNIT OPERATING TIME

Definition of symbols

K_2 - modified ellipticity coefficient
V_θ - velocity change per unit operating time
r_c - synchronous satellite orbital radius
$\dot{\theta}_E$ - angular rate of rotation of earth

$$V_\theta = 6 K_2 r_c \dot{\theta}_E^2 \sin 2\gamma_o \qquad \text{(Reference 9.1)}$$

$$V_\theta = 16.97 \sin 2\gamma_o$$

$$V_\theta = 3.23 \text{ ft/sec/yr}$$

The synchronous satellite nominally positioned at $27^{o}30'$ W longitude will drift eastward along the equator at the rate of 3.23 ft/sec/yr.

H.8 CALCULATION OF RADIAL DRIFT FOR 1^{o} DRIFT IN LONGITUDE

Definition of symbols

t - time to drift 1^{o} longitude
K_2 - modified ellipticity coefficient
$\dot{\theta}_E$ - angular rate of rotation of earth
r_c - synchronous satellite orbital radius
γ_o - initial value of γ

$$\Delta r = 12 (K_2 \dot{\theta}_E \sin 2\gamma_o)(t)(r_c) \qquad \text{(Reference 9.1)}$$

$$\Delta r = 12 \left(\frac{2\pi}{86164}\right) (22,766.9) \left(\frac{3443.2}{22,766.9}\right)^2 (-5.35 \times 10^{-6})$$

$$(-0.19)(3.72)10^{6}$$

$$\Delta r = 1.64 \text{ nm}$$

ACKNOWLEDGMENTS

We would like to thank those who have given up their time to us for detailed critique and recommendations.

Prof. William Anderson
The University of Michigan

Prof. W. E. Britton
The University of Michigan

Prof. Harm Buning
The University of Michigan

Mr. Robert Carlson
McDonnell Douglas Astronautics

Mr. Kenneth Case
Bendix Aerospace Systems Division

Mr. Duane F. Dunlap
The University of Michigan

Mr. Eugene Ehrlich
NASA-OSSA Washington, D.C.

Mr. John Engstrom
Bendix Aerospace Systems Division

Mr. Richard Gibson
Bendix Aerospace Systems Division

Mr. Hank Gorecki
Bendix Navigation and Control Division

Mr. Robert Hatch
Hamilton Standard

Mr. Charles Hunt
General Electric

Mr. R. E. Jorasch
Philco-Ford

Mr. E. S. Keats
Westinghouse Electric

Mr. Will Morrison
Bendix Navigation and Control Division

Prof. Wilbur C. Nelson
The University of Michigan

Mr. James O'Day
The University of Michigan

Prof. R. L. Phillips
The University of Michigan

Prof. W. F. Powers
The University of Michigan

Prof. L. L. Rauch
The University of Michigan

Prof. Thomas Sawyer
The University of Michigan

Mr. R. J. Simms
Bendix Aerospace Systems Division

Prof. N. X. Vinh
The University of Michigan

Mr. Alex B. Winick
FAA, Washington D. C.

We would like to give special thanks to Prof. Wilbur C. Nelson for his guidance throughout Project SCANNAR and also to Caroline Rehberg for typing this report. In addition we would like to thank Mr. W. James Lane for his assistance.

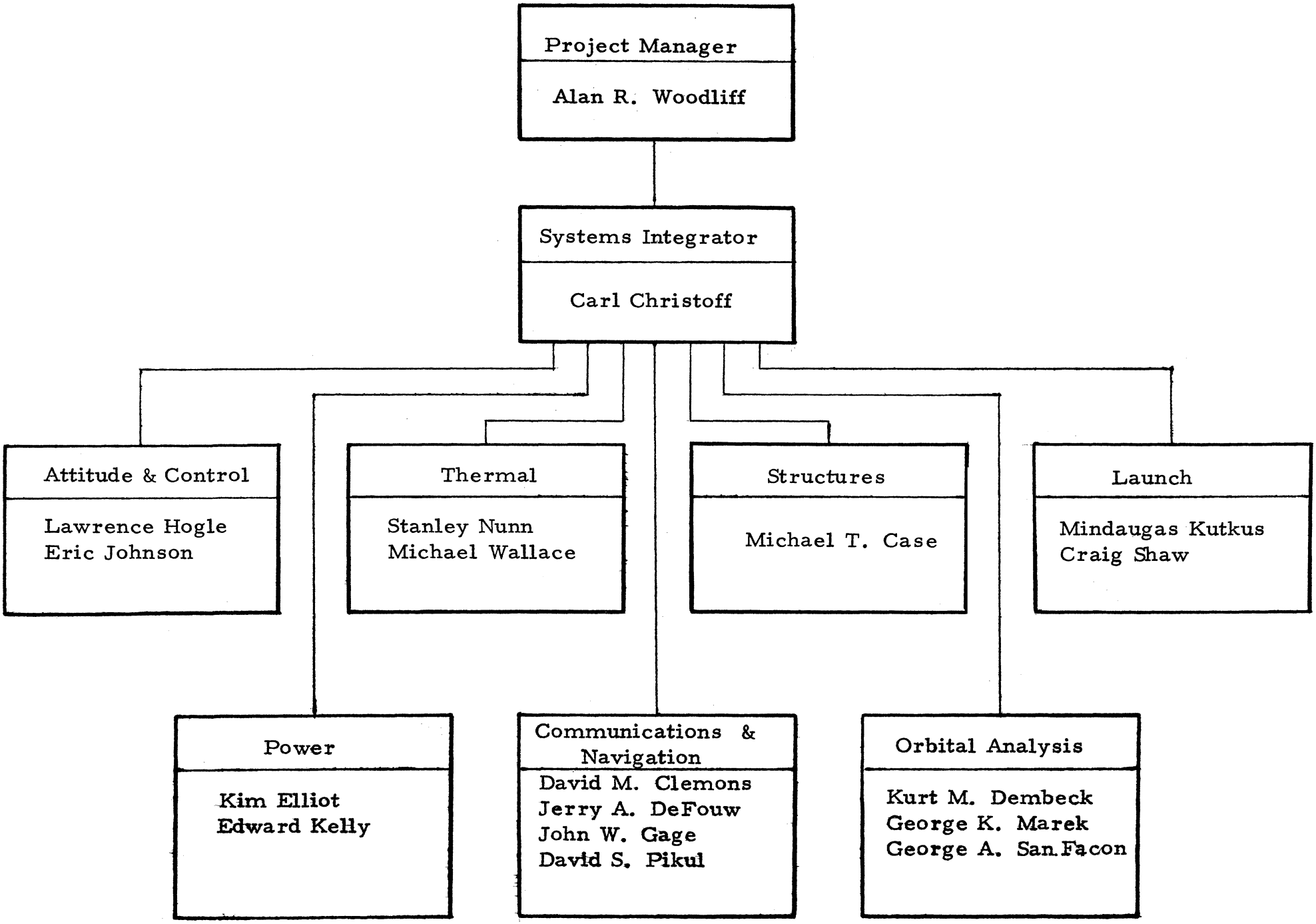

Project Personnel Chart